



City Research Online

City, University of London Institutional Repository

Citation: Zhang, Cheng (2013). Continuous and quad-graph integrable models with a boundary: Reflection maps and 3D-boundary consistency. (Unpublished Doctoral thesis, City University London)

This is the unspecified version of the paper.

This version of the publication may differ from the final published version.

Permanent repository link: <https://openaccess.city.ac.uk/id/eprint/3016/>

Link to published version:

Copyright: City Research Online aims to make research outputs of City, University of London available to a wider audience. Copyright and Moral Rights remain with the author(s) and/or copyright holders. URLs from City Research Online may be freely distributed and linked to.

Reuse: Copies of full items can be used for personal research or study, educational, or not-for-profit purposes without prior permission or charge. Provided that the authors, title and full bibliographic details are credited, a hyperlink and/or URL is given for the original metadata page and the content is not changed in any way.

City Research Online:

<http://openaccess.city.ac.uk/>

publications@city.ac.uk

Thesis

**Continuous and Quad-Graph
Integrable Models with a Boundary:
Reflection Maps and
 $3D$ -Boundary Consistency**

Cheng Zhang

Submitted in accordance with the requirements for the degree of
Doctor of Philosophy

**Department of Mathematical Sciences
City University, London
September 2013**

*The life was limited,
the knowledg was unlimited.
It wouldn't be wise,
if thee trying to conquer the unlimited with the limited.*

Chuang Tzu (c. 369-286 BC)

Acknowledgments

First of all, I would like to express my sincere gratitude to my supervisor Dr. Vincent Caudrelier, for his advice, guidance and encouragement throughout the course of this work. Special thanks to Dr. Nicolas Crampé for his valuable advice and discussion. Many thanks to the staff in the Department of Mathematical Sciences at City University London, in particular to Prof. Andreas Fring, Dr. Olalla Castro Alvaredo, Andrea Cavaglia and Emanuele Levi. Also, I would like to extend my appreciation to my internal examiner Prof. Joe Chuang and external examiner Prof. Alexander P. Veselov for their extremely careful reading and remarkably precious comments. Finally, thanks to my parents for their endless support.

Abstract

This thesis is focusing on *boundary problems* for various classical integrable schemes.

First, we consider the vector nonlinear Schrödinger (NLS) equation on the half-line. Using a Bäcklund transformation method which explores the *folding* symmetry of the system, classes of integrable boundary conditions (BCs) are derived. These BCs coincide with the *linearizable* BCs obtained using the *unified transform method* developed by Fokas. The notion of integrability is argued by constructing an explicit generating function for conserved quantities. Then, by adapting a *mirror image* technique, an inverse scattering method with an integrable boundary is constructed in order to obtain N -soliton solutions on the half-line, *i.e.* N -soliton reflections. An interesting phenomenon of transmission between different components of vector solitons before and after interacting with the boundary is demonstrated.

Next, in light of the fact that the soliton-soliton interactions give rise to Yang-Baxter maps, we realize that the soliton-boundary interactions that are extracted from the N -soliton reflections can be translated into maps satisfying the set-theoretical counterpart of the quantum reflection equation. Solutions of the *set-theoretical reflection equation* are referred to as *reflection maps*. Both the Yang-Baxter maps and the reflection maps guarantee the factorization of the soliton-soliton and soliton-boundary interactions for vector NLS solitons on the half-line.

Indeed, reflection maps represent a novel mathematical structure. Basic notions such as parametric reflection maps, their graphic representations and transfer maps are also introduced. As a natural extension, this object is studied in the context of quadrirational Yang-Baxter maps, and a classification of *quadrirational reflection maps* is obtained.

Finally, boundaries are added to discrete integrable systems on quad-graphs. Triangle configurations are used to discretize quad-graphs with boundaries. Relations involving vertices of the triangles give rise to *boundary equations* that are used to describe BCs. We introduce the notion of integrable BCs by giving a *three-dimensional boundary consistency* as a criterion for integrability. By exploring the correspondence between the quadrirational Yang-Baxter maps and the so-called ABS classification, we also show that quadrirational reflection maps can be used as a systematic tool to generate integrable boundary equations for the equations from the ABS classification.

Contents

1	Introduction	1
1.1	2D soliton theories	2
1.2	Yang-Baxter equation and reflection equation	5
1.3	Yang-Baxter maps	6
1.4	Discrete integrable systems	7
1.5	Outline of thesis	9
I	From the vector NLS equation on the half-line to reflection maps	10
2	ISM for the vector NLS equation	11
2.1	From Lax pair to RH problem	11
2.2	Dressing transformations	16
2.3	N -soliton solutions	20
3	The vector NLS equation on the half-line	25
3.1	Deriving integrable boundary conditions	26
3.2	Check of integrability	31
3.3	Mirror image construction	33
3.4	Example of one-soliton reflections	37
4	Factorization of soliton-soliton and soliton-boundary interactions	41
4.1	Factorization of N -soliton interactions	42
4.2	Factorization of N -soliton reflections	47
5	N-soliton solutions on the half-line using <i>space-evolution</i> method	54
5.1	Space-evolution formalism of the ISM	55

5.2	N -soliton reflections	59
II	Reflection maps: classification and applications	62
6	Set-theoretical reflection equation and reflection maps	63
6.1	Yang-Baxter maps	63
6.2	Reflection maps	66
7	Reflection maps for quadrirational Yang-Baxter maps	71
7.1	Quadrirational Yang-Baxter maps	71
7.2	Deriving reflection maps	75
7.3	Classification of reflection maps	79
8	Quad-graph integrable systems with boundary	82
8.1	$3D$ -consistent equations on quad-graphs	83
8.2	Boundary conditions for quad-graph systems	86
8.3	Integrability: the $3D$ -boundary consistency	88
8.4	From reflection maps to boundary equations	91
8.5	Boundary equations for $A1_{\delta=0}$ as an example	95
9	Conclusion	99
	Appendices	101
A	Unified transform method and linearizable boundary conditions	102
A.1	From Lax pair to global relation	103
A.2	Linearizable boundary conditions	107
B	Proof of Eq. (3.25)	109
C	Algorithm for constructing paired norming constants	113
D	Proof of Prop. 4.2.1	115
E	Reflection maps for H_{II}	118
F	Quad-graph equation-Yang-Baxter map correspondence	119
G	Boundary equations for the ABS classification	122
	Bibliography	127

Introduction

Since the birth of the modern theories of integrability dated back to the late 1960s, *integrable systems* have been extensively studied as one of the most attractive fields in mathematical physics. Probably, the most striking feature of integrable systems is that certain *nonlinear systems* can be exactly solved by mathematical methods and such systems exhibit *soliton solutions* that are particle-like objects interacting elastically with themselves. Nowadays, these nonlinear systems are qualified as integrable and believed to be widely involved in our understanding of natural phenomena. The appearance of integrable systems has been marked in almost every single branch of physics, and the impact has reached far to areas ranging from fiber optics, that engineers the transmissions of information and ensures our everyday communications, through the experiments in atomic physics, aiming to understand the utter properties of atoms and molecules, to the attempts of speculating some of the most fundamental problems in physics using concepts developed around string theory and conformal field theory. Numerous mathematical methods have also been developed and found to have deep connections to different areas of pure mathematics. So far, integrable systems have become a powerful tool to understand physics and develop new concepts and methods in mathematical physics.

Amongst the very rich topics in integrable systems, *boundary problems* arise as one of the fundamental problems in the discipline. Indeed, most of models are known to be integrable only in the presence of very special boundary conditions such as periodic boundary conditions. Adding more generic boundary conditions to integrable systems signifies a better description of physics, since real physical systems naturally involving boundaries. From the point of view of integrability, deriving *integrable boundary conditions*—boundary conditions that preserve the integrability property—consists of a highly non-trivial task.

The objectives of this thesis are to study boundary problems for certain classical

integrable models. We start, in this chapter, by giving a general introduction to the areas of study that are relevant to the thesis.

1.1 2D soliton theories

Two-dimensional (2D) soliton models, namely models possessing soliton solutions, are 2D—one dimensional space plus time—nonlinear partial differential equations that can be exactly solved by means of the *inverse scattering method*.

Historically, the development of soliton theories also marked the birth of the integrable theories. The story can be traced back to the late 19th century when the mathematicians in that epoch derived the *Korteweg-de Vries* (KdV) equation [30, 80] in the context of fluid dynamics. This equation is in the following simple form for a real field $u(x,t)$:

$$u_t + u_{xxx} + 6uu_x = 0, \quad (1.1)$$

where the subscripts mean the partial derivatives¹. After more than a half-century of its introduction, the KdV equation was revived in 1965 by Zabusky and Kruskal [120]. Using a numeric method, they discovered that Eq. (1.1) exhibits particle-like solutions that interact elastically with themselves. Apparently counter-intuitive, this particular type of solutions was named as solitons and gave an adequate explanation to the *Fermi-Pasta-Ulam problem* [49], a puzzle initiated in numeric experiments. Mathematical foundations for solitons were soon established notably following the inventions of the inverse scattering method [61] and the *Lax pair* [81] which created an elegant framework to solve the KdV equation. Gradually, soliton solutions were found in many other models such as the nonlinear Schrödinger equation [123], the modified KdV equation [116] and the sine-Gordon equation [7]. The notions of integrability such as infinite conservation laws [90, 81], Hamiltonian structure [60, 122] and Bäcklund transformations [117] were also clarified. Solitons have thus become a characteristic feature of integrable systems.

One-soliton solution of the KdV equation is the following traveling wave function:

$$u(x,t) = \frac{1}{2}c \operatorname{sech}^2 \left(\frac{\sqrt{c}}{2}(x - ct - a) \right), \quad c, a \in \mathbb{R}, \quad (1.2)$$

where c is a real parameter controlling both the velocity and the amplitude of $u(x,t)$. This wave maintains its shape while it travels at constant speed. To understand soliton phenomena, let us look back at the form of (1.1). There are two sources of force

¹This convention will be adopted for the rest of the thesis

coexisting: on one hand, the *dispersion*, coming from the linear term $u_t + u_{xxx}$ that physically tries to extend the wave envelope, and on the other, the *dissipation*, coming from the nonlinear term $6uu_x$ that basically tries to destroy the wave envelope. Then, the fact that (1.1) exhibits solutions like (1.2) can be understood as a "magic" balance between both the dispersion and the dissipation. In other word, to have wave functions such as (1.2), the nonlinearity is an essential ingredient! Indeed, observation of such waves had already been reported as "solitary waves" [102] in the mid-19th century by the Scottish engineer Russell when he studied the motion of water. Next, one can ask the following questions: first, do any other physical system governed by the KdV equation exist in nature? Second, does the "magic" balance between dispersion and dissipation exist for any other nonlinear system? The answers for both questions are yes. Nowadays, we know that the KdV equation appears in the context of acoustic waves traveling in crystals. Also, a wide range of soliton models exist. It is argued that soliton models are, in fact, of universal character and can be widely applied in describing Nature (see for instance [121]). A powerful method for solving soliton models, known as the inverse scattering method (ISM) (the ISM will be explained in depth in Chapter 2), exists.

Another universal integrable model is the nonlinear Schrödinger (NLS) equation:

$$iu_t + u_{xx} - 2\lambda|u|^2u = 0, \quad \lambda = \pm 1, \quad (1.3)$$

where u is a complex-valued field depending on x and t . In the case $\lambda = -1$, that is called *focusing* case for the nonlinear term $-2\lambda|u|^2u$ with $\lambda = -1$ arises as an attractive "force", the NLS equation (1.3) possesses soliton solutions. Its one-soliton solution can be written in the form

$$u(x,t) = ae^{-i(bx+(b^2-a^2)t+\phi_0)} \operatorname{sech}(a(x+2bt-\Delta c)), \quad (1.4)$$

where a, b are parameters controlling the velocity and amplitude of $u(x,t)$ and $\phi_0, \Delta c$ are parameters characterizing respectively the initial phase and space position. As a single integrable model, the NLS equation has a great impact in both mathematics and physics. In [123], Zakharov and Shabat first gave soliton solutions to the NLS equation by generalizing the Lax pair [81]. This just built up the basis for the later development in [7] in which a powerful framework of the ISM to generate and solve soliton models, known as the AKNS scheme, was derived. Also, Manakov generalized the NLS equation to a two-component coupled version [87], known as Manakov system or vector NLS model, aiming at simulating electro-magnetic field in a nonlinear medium. Thanks to its great relevance, the Manakov system has been

becoming the governing equation in the field of fiber optics—solitons were reportedly observed in experiments [68]—that is of great interest in engineering. The quantum version of the NLS equation, known as Lieb-Liniger model that is used to describe a gas of particles moving in one dimension and satisfying Bose-Einstein statistics, was solved in [84]. This result inspired Yang who gave his famous rational solution of the Yang-Baxter equation [119] by extending the spinless particles in [84] to particles with spin. Note that both Manakov and Yang’s ideas lie in adding internal degrees of freedom to a scalar quantity. In the context of soliton theories, this gives rise to the multi-component soliton models. The ISM for solving classes of multi-component soliton models was extensively studied, for instance in [110].

Initial-boundary value problems, initiated in the study of partial differential equations, appear naturally in soliton theories. Since an early attempt [4] in which the KdV equation on the half-line was considered, half-line problems for soliton models have attracted much attention from many researchers. An idea of using Bäcklund transformation to construct integrable boundary conditions was first proposed by Sklyanin in [103]. Later, in [25, 26, 66, 109], the Bäcklund transformation method was applied to the NLS and sine-Gordon equations for deriving integrable boundary conditions. In [50], the NLS model was again treated by using analysis of the linearized NLS equation. The common result of these two approaches consists in representing the half-line system by folding a full line system. The vector NLS equation on the half-line was studied in [67] using an algebraic approach. Recently, a nice mirror image construction was developed in [27] for the NLS equation, which led to N -soliton solutions on the half-line.

On the other hand, Fokas has recently developed a powerful method [51, 52, 54], referred to as *Fokas method* or *unified transform method* (this method will be discussed in more detail in Appendix A), for treating boundary value problems for soliton equations. Roughly speaking, this method is based on a simultaneous analysis of both parts of the Lax pair, which translates the initial-boundary conditions into spectral functions in Fourier space. Then the solutions of the original system can be obtained using certain inverse transforms from the spectral functions. The unified transform method can be applied to a large class of boundary problems for soliton equations ranging from half-line problems [52, 32, 57] and to systems defined on an finite interval [56, 33].

1.2 Yang-Baxter equation and reflection equation

The (quantum) Yang-Baxter equation, introduced separately by Yang [119] in the context of quantum field theory and by Baxter [17] in the context of statistical mechanics, is at the heart of understanding quantum integrable models. The equation can be written in the following form:

$$\mathcal{R}_{12}\mathcal{R}_{13}\mathcal{R}_{23} = \mathcal{R}_{23}\mathcal{R}_{13}\mathcal{R}_{12}, \quad (1.5)$$

where \mathcal{R} , commonly known as \mathcal{R} -matrix, is a matrix acting on $V \otimes V$ — V is a vector space—with the understanding that $\mathcal{R}_{12} = \mathcal{R} \otimes \mathbb{I}$, $\mathcal{R}_{23} = \mathbb{I} \otimes \mathcal{R}$ and so on. From a

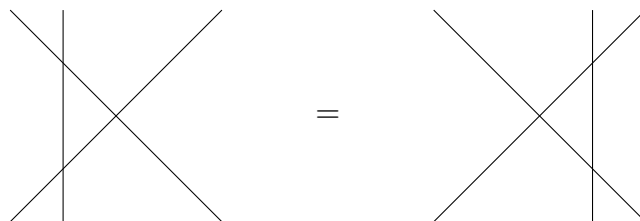


Fig. 1.1 : Yang-Baxter equation

physical point of view, as pointed out in [126], the Yang-Baxter equation describes the factorization of an N -particle scattering, which is a unique feature displayed by $2D$ integrable systems (see Fig. 1.1). On the other hand from a mathematical point of view, the algebraic structures underlying the Yang-Baxter equation can be seen as deformations of the usual Lie algebras or their infinite dimensional extensions: the Kac-Moody algebras [77]. Such deformed algebraic structures are known nowadays as quantum groups or quantum algebras [75, 76, 43].

In the context of quantum integrable systems with boundaries, there exists, in addition to the Yang-Baxter equation, a second equation: the reflection equation, also known as the boundary Yang-Baxter equation [42, 104], that is used to encode the interactions of quantum particles with boundaries. The equation is in the form

$$\mathcal{R}_{12}\mathcal{K}_1\mathcal{R}_{21}\mathcal{K}_2 = \mathcal{K}_2\mathcal{R}_{12}\mathcal{K}_1\mathcal{R}_{21}, \quad (1.6)$$

where \mathcal{K} , also known as \mathcal{K} -matrix, is a matrix acting on V . The appearance of \mathcal{K} in the reflection equation (1.6) can be seen as a certain consistency with the \mathcal{R} -matrix. Then, \mathcal{K} , that describes the particle-boundary scattering, along with \mathcal{R} , that describes the particle-particle scattering, ensure the integrability of the underlying quantum system with boundaries. This feature can be viewed in Fig. 1.2

as the factorization of both the particle-particle and particle-boundary scatterings.

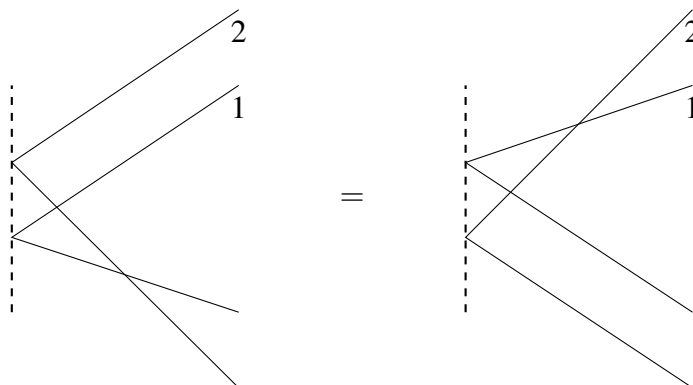


Fig. 1.2 : Reflection equation

1.3 Yang-Baxter maps

One aspect of the Yang-Baxter equation (1.5) is that the \mathcal{R} -matrix is an operator acting on tensor product of vector spaces, *i.e.* $V \otimes V$, which allows the equation itself to have rich algebraic structures. However, one can "relax" this property by replacing $V \otimes V$ by $S \times S$, where S is an arbitrary set and \times means Cartesian product. This gives rise to the *set-theoretical* version of the Yang-Baxter equation, first suggested as a subject of study by Drinfeld in [44] (a solution was already obtained earlier by Sklyanin [105]). Nowadays, solutions of the set-theoretical Yang-Baxter equation are commonly accepted as *Yang-Baxter maps*, originating from a suggestion of Veselov [113]. The name *rational set-theoretical \mathcal{R} -matrices* also exists in the literature. With the understanding that \mathcal{R} is a map acting on $S \times S$, the theoretical Yang-Baxter equation, which shares the same structure as the usual quantum Yang-Baxter equation (1.5), is now read as a compatibility condition of two different ways to do decompositions of maps.

Different aspects of Yang-Baxter maps have been developed and numerous connections have been established with, for example, Poisson-Lie groups and algebras [118, 70, 46, 86, 101], discrete Lax representation [106] and transfer maps [113]. Yang-Baxter maps also arise in different contexts in mathematical physics, such as geometric crystals [45], cellular automaton [107, 69, 58], factorization of multi-component solitons' scattering [111, 64, 9] and discrete integrable systems [98, 72, 79]. Note that, although the multi-component soliton theory is a well-established discipline, it has only been understood, rather recently in [111, 9] for the vector NLS equation and in [64] for the matrix KdV equation, that an N -soliton

scattering (or collision) factorizes into $\binom{N}{2}$ pairwise soliton scatterings, that can be expressed in terms of Yang-Baxter maps. In [14], effort was put into classifying Yang-Baxter maps in the case $\mathcal{S} = \mathbb{CP}^1$, which led to the important concept of *quadrirational maps*. Classifications of quadrirational Yang-Baxter maps were also exhausted in [14, 97].

1.4 Discrete integrable systems

Recently, there has been an increasing interest in two-dimensional discrete integrable systems. Practically, an important motivation comes from the use of computer and numeric analysis which is naturally involved with discrete variables—soliton solutions [120] of the KdV equations were first found by using numeric method! Moreover, all the concepts and methods developed in the continuous theories can be found to have their deep roots in discrete systems. Nowadays, it is believed that, in many aspects, discrete systems are more fundamental than their continuous counterpart (see for instance [92]).

Early developments of the discipline lie in discretizing one variable (usually the time variable) of certain known soliton systems [2, 3, 73, 74]. This corresponds to semi-discrete systems or differential-difference systems. Discrete equations that we are considering in this thesis are fully discrete systems or difference-difference systems, which discretize both the space and time variables. Mainly following [94, 99] by using the direct linearization method, a number of interesting discrete models were derived (see also [92]).

On the other hand, it is often possible to pass from a continuous equation to a discrete equation via Bäcklund transformations. Bäcklund transformations in soliton theories are transformations which map solutions of a soliton equation into new so-

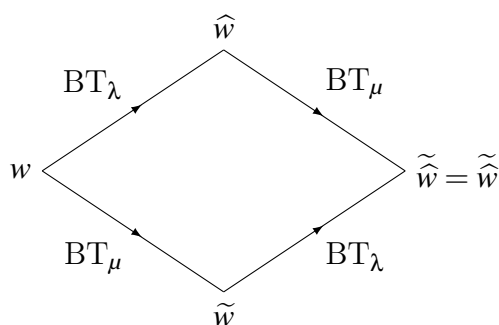


Fig. 1.3 : Bianchi diagram for Bäcklund transformations

lutions. They are known to satisfy the Bianchi permutability property (see Fig. 1.3). The most famous example is the discrete potential KdV (dpKdV) equation that can be obtained using Bäcklund transformations for the KdV equation [117]. The construction is illustrated in Fig. 1.3. The field w is defined as $w_x = u$ for u satisfying the KdV equation. Thanks to the permutability property, \tilde{w} and \hat{w} are compatible. Relation involving w , \tilde{w} , \hat{w} and $\tilde{\hat{w}}$ is in the form

$$(w - \tilde{w})(\hat{w} - \tilde{\hat{w}}) + 4(\lambda - \mu) = 0, \quad (1.7)$$

which is the dpKdV equation. In this way, discrete systems can be generated in a lattice following successive applications of Bäcklund transformation (see Fig. 1.4).

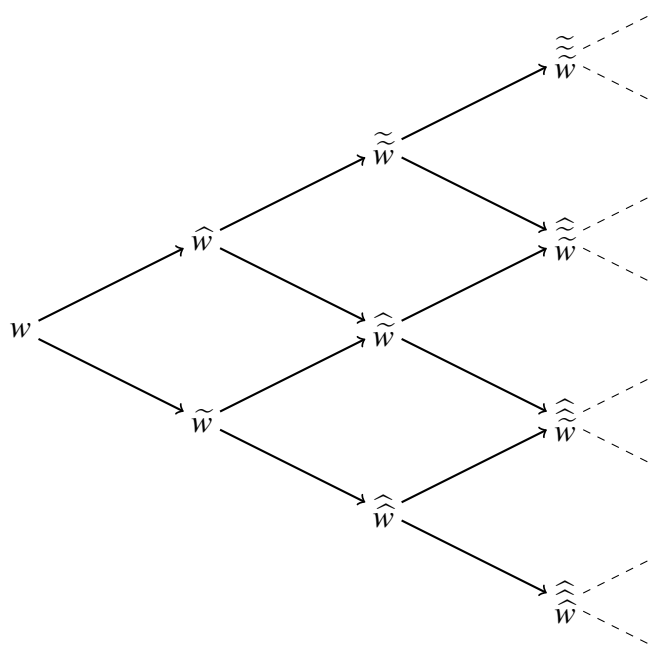


Fig. 1.4 : Lattice generated by Bäcklund transformations

There exist several notions and tests for integrability of discrete systems. Let us mention for instance *integrable mappings* [112], *algebraic entropy* [23], *singularity confinement* [65] and *three-dimensional consistency* [91, 29]. The latter will be discussed in Chapter 8. In [29, 13], discrete integrable systems were extended to *quad-graphs*, *i.e.* planar graph of cellular decompositions with quadrilateral faces (in contrast to the square lattice), and a classification of discrete integrable equations was accordingly given [13]. These laid the foundation for important developments in discrete integrable systems. Some important results have already been achieved, such as soliton generations [12, 93], Lagrangian structures [85] and discrete ISM [34], etc.

1.5 Outline of thesis

Following the two different types of the underlying integrable systems that we are considering in this thesis, namely continuous and discrete, this thesis is naturally divided into two parts. Motivations and notably notions of integrability will be clarified in each precise context of this presentation.

In Part I—Chapter 2 - Chapter 5—we study the vector NLS equation on the half-line. Chapter 2 reviews the ISM that is the basic instrument used throughout Part I. In Chapter 3, classes of integrable BCs are derived. Soliton solutions on the half-line are also constructed using a mirror image method. In Chapter 4, we introduce *reflection maps* that satisfy the set-theoretical counterpart of the reflection equation, in order to prove the factorization of soliton-soliton and soliton-boundary interactions. Another approach, called space-evolution method, to solve the vector NLS equation on the half-line, is proposed in Chapter 5. Part II—Chapter 6 - Chapter 8—deals with reflection maps and quad-graph systems with boundary. We study in detail the set-theoretical reflection equation and reflection maps in Chapter 6. Reflection maps in the context of quadrirational Yang-Baxter maps are considered in Chapter 7. In Chapter 8, boundaries are added to quad-graph systems. In particular, we propose a *three-dimensional boundary consistency* as a criterion for integrability for quad-graph integrable systems with boundary. Concluding remarks are reported in Chapter 9.

Part I

From the vector NLS equation on
the half-line to reflection maps

ISM for the vector NLS equation

In this chapter, we review the inverse scattering method (ISM) for the vector NLS equation, in order to collect results and notations needed in Part I of this thesis. The main technical complexity of the vector generalization of the NLS model lies in the computation of the N -soliton scattering data that are encoded in a matrix quantity $\mathbf{a}^+(k)$, in contrast to the scalar NLS case where $\mathbf{a}^+(k)$ is a scalar. To overcome this difficulty, we use the approach based on the *Riemann-Hilbert* (RH) formulation. This leads to a powerful framework, by virtue of the *dressing transformations*, to compute $\mathbf{a}^+(k)$ and the N -soliton solutions in a compact form. In particular, we put our emphasis on Theorem 2.2.7 which indeed reflects the *Bianchi permutativity property* in the context of dressing transformations. This theorem will play an important role when we study the factorization of an N -soliton interaction in the forthcoming chapters. We refer readers to [5, 47, 6, 8] for more detailed presentations of the ISM, and to [124, 125, 47, 16, 62] for the dressing transformations.

2.1 From Lax pair to RH problem

The traditional approach of the ISM consists of three steps: 1) *direct scattering* which transforms the soliton equation into a set of scattering data by using the x -part of the Lax pair; 2) *time-evolution* which makes the scattering data evolved in time by using the t -part of the Lax pair; 3) *inverse scattering* which reconstructs the solutions of the original soliton equation from the time-evolved scattering data. With the help of the RH formulation, these three steps can naturally be absorbed into the RH problem itself.

Let us first define the vector NLS equation. Given an n -component complex-

valued vector field

$$R(x, t) = \begin{pmatrix} r_1(x, t) \\ \vdots \\ r_n(x, t) \end{pmatrix}, \quad (2.1)$$

we require that the j th component $r_j(x, t)$, $j = 1, \dots, n$ is a smooth enough function that vanishes to zero as $x \rightarrow \pm\infty$ for all t . This requirement corresponds to the so-called *vanishing boundary conditions*¹. The vector NLS equation is defined as

$$iR_t(x, t) + R_{xx}(x, t) - 2\lambda(R^\dagger R)R(x, t) = 0, \quad (2.2)$$

where $R^\dagger(x, t)$ is the transpose conjugate of $R(x, t)$ and λ is the (real) coupling constant which can be normalized to $\lambda = \pm 1$. Define $Q(x, t)$ as the following $(n+1) \times (n+1)$ matrix-valued field:

$$Q(x, t) = \begin{pmatrix} 0 & R(x, t) \\ \lambda R^\dagger(x, t) & 0 \end{pmatrix}, \quad (2.3)$$

the vector NLS equation (2.2) can be written as the compatibility condition ($\Phi_{xt} = \Phi_{tx}$) of the two following linear problems, known as auxiliary problems or *Lax pair*, for an $(n+1) \times (n+1)$ matrix-valued function $\Phi(x, t, k)$ ²:

$$\Phi_x + ik[\Sigma_3, \Phi] = Q\Phi, \quad (2.4)$$

$$\Phi_t + 2ik^2[\Sigma_3, \Phi] = Q_T\Phi, \quad (2.5)$$

where

$$\Sigma_3 = \begin{pmatrix} I_n & 0 \\ 0 & -1 \end{pmatrix}, \quad Q_T = 2kQ - iQ_x\Sigma_3 - iQ^2\Sigma_3, \quad (2.6)$$

with I_n being the $n \times n$ identity matrix. Eq. (2.4) and (2.5) represent respectively the x -part and t -part of the Lax pair.

Remark 2.1.1 *The Lax pair for the vector NLS equation is also widely seen in the literature as two operators U and V satisfying the zero curvature condition:*

$$\left[U - \frac{\partial}{\partial x}, V - \frac{\partial}{\partial t} \right] = 0, \quad (2.7)$$

¹This requirement restricts the classes of solutions that we consider in this thesis, and detailed treatments can be seen for instance in [5, 47].

²From now on, we drop the x , t and k dependence for conciseness unless there is ambiguity.

where U, V are defined as

$$U = -ik\Sigma_3 + Q(x, t), \quad V = -2ik^2\Sigma_3 + Q_T(x, t, k). \quad (2.8)$$

The corresponding auxiliary problems turn out to be

$$U\Psi = \Psi_x, \quad V\Psi = \Psi_t. \quad (2.9)$$

For practical purposes, we work with the auxiliary problems (2.4, 2.5) that are simply related to (2.9) by specifying

$$\Psi(x, t, k) = \Phi(x, t, k) e^{-i(kx+2k^2t)\Sigma_3}. \quad (2.10)$$

From Eq. (2.3), one can observe that Q satisfies

$$WQW^{-1} = -Q^\dagger, \quad (2.11)$$

where

$$W = \begin{pmatrix} -\lambda I_n & 0 \\ 0 & 1 \end{pmatrix}. \quad (2.12)$$

This implies that, provided that $\Phi(x, t, k)$ is a solution of (2.4, 2.5), $W\Phi^\dagger(x, t, k^*)W^{-1}$ satisfies the same equations as $\Psi(x, t, k) \equiv \Phi^{-1}(x, t, k)$ does, *i.e.*

$$\Psi_x + ik[\Sigma_3, \Psi] = -\Psi Q, \quad (2.13)$$

$$\Psi_t + 2ik^2[\Sigma_3, \Psi] = -\Psi Q_T. \quad (2.14)$$

Following the vanishing boundary conditions, we are able to define two Jost solutions $X(x, t, k)$ and $Y(x, t, k)$ of (2.4, 2.5) satisfying

$$\lim_{x \rightarrow -\infty} e^{i\phi(x, t, k)\Sigma_3} X(x, t, k) e^{-i\phi(x, t, k)\Sigma_3} = I_{n+1}, \quad k \in \mathbb{R}, \quad (2.15)$$

$$\lim_{x \rightarrow \infty} e^{i\phi(x, t, k)\Sigma_3} Y(x, t, k) e^{-i\phi(x, t, k)\Sigma_3} = I_{n+1}, \quad k \in \mathbb{R}, \quad (2.16)$$

where

$$\phi(x, t, k) = kx + 2k^2t. \quad (2.17)$$

They enjoy the following properties:

- Volterra integral representations:

$$X(x, t, k) = I_{n+1} + \int_{-\infty}^x e^{-ik(x-y)\Sigma_3} Q(y, t) X(y, t, k) e^{ik(x-y)\Sigma_3} dy, \quad (2.18)$$

$$Y(x, t, k) = I_{n+1} + \int_{\infty}^x e^{-ik(x-y)\Sigma_3} Q(y, t) Y(y, t, k) e^{ik(x-y)\Sigma_3} dy. \quad (2.19)$$

- Due to the traceless property of $Q(x, t)$,

$$\det X(x, t, k) = \det Y(x, t, k) = 1. \quad (2.20)$$

- Since both $W\Phi^\dagger(x, t, k^*)W^{-1}$ and $\Phi^{-1}(x, t, k)$ satisfy (2.13, 2.14), one gets

$$WX^{-1}(x, t, k)W^{-1} = X^\dagger(x, t, k^*), \quad WY^{-1}(x, t, k)W^{-1} = Y^\dagger(x, t, k^*). \quad (2.21)$$

- X and Y can be split into the following "column" vectors³ forms:

$$X = (X^+, X^-), \quad Y = (Y^-, Y^+), \quad (2.22)$$

where X^+ , Y^+ (resp. X^- , Y^-) are analytic and bounded in the upper (resp. lower) half k -complex plane.

A straightforward calculation shows that if Ψ_1 and Ψ_2 are two solutions of (2.4, 2.5), then they satisfy

$$\Psi_1(x, t, k) = \Psi_2(x, t, k) e^{-i\phi(x, t, k)\Sigma_3} T(k) e^{i\phi(x, t, k)\Sigma_3}, \quad (2.23)$$

where the $(n+1) \times (n+1)$ matrix T depends on the spectral parameter k only. Therefore, we define the matrix $S(k)$ that relates the Jost solutions X and Y as

$$X(x, t, k) = Y(x, t, k) e^{-i\phi(x, t, k)\Sigma_3} S(k) e^{i\phi(x, t, k)\Sigma_3}, \quad k \in \mathbb{R}. \quad (2.24)$$

It follows from the properties of X and Y that $\det S(k) = 1$, and $S(k)$ can be split into block matrices of natural sizes⁴:

$$S(k) = \begin{pmatrix} \mathbf{a}^+(k) & \mathbf{b}^-(k) \\ \mathbf{b}^+(k) & \mathbf{a}^-(k) \end{pmatrix}. \quad (2.25)$$

³Here, the left "column" vector is made of the first left n columns and the right one is made of the remaining column. This column vector representation will be constantly used in the rest of this thesis.

⁴For instance, \mathbf{a}^+ is an $n \times n$ matrix and \mathbf{a}^- a scalar.

Again, $\mathbf{a}^\pm(k)$ are understood to be analytic in \mathbb{C}^\pm , where \mathbb{C}^+ and \mathbb{C}^- are used to denote the upper and lower half k -complex planes respectively. Moreover, one has

$$W S(k)^{-1} W^{-1} = S^\dagger(k^*). \quad (2.26)$$

Let $S(k)^{-1}$ be written in components as

$$S(k)^{-1} = \begin{pmatrix} \mathbf{c}^-(k) & \mathbf{d}^-(k) \\ \mathbf{d}^+(k) & \mathbf{c}^+(k) \end{pmatrix}, \quad (2.27)$$

where $\mathbf{c}^\mp(k)$ allow for analytic continuations into \mathbb{C}^\mp . The relation (2.26) can be explicitly translated into

$$(\mathbf{a}^\pm)^\dagger(k^*) = \mathbf{c}^\mp(k), \quad \mathbf{b}^\pm(k^*) = -\lambda(\mathbf{d}^\mp)^\dagger(k), \quad (2.28)$$

with the functions defined in the appropriate domains.

Remark 2.1.2 *For the scattering system (2.24), there are two equivalent sets: $\{\mathbf{a}^\pm, \mathbf{b}^\pm\}$ and $\{\mathbf{c}^\pm, \mathbf{d}^\pm\}$, known as the minimal set of scattering data [62], which are available to reconstruct $R(x, t)$ in the inverse part of the ISM. Without loss of generality, we choose to work with $\{\mathbf{a}^\pm, \mathbf{b}^\pm\}$ in the rest of this thesis.*

A crucial observation in the development of the ISM, originated from the work of Manakov [87] and Zakharov and Shabat [124], is that the scattering system (2.24) can be formulated as an RH problem and this RH problem is equivalent to the ISM associated with the Lax pair (2.4, 2.5). We state the following propositions which are well-known in the soliton theory. Proofs can be found, *e.g.*, in [47, 54].

Proposition 2.1.3 *The scattering system defined in (2.24) can be rewritten as the following RH problem*

$$J^+(x, t, k) J^-(x, t, k) = e^{-i\phi(x, t, k)\Sigma_3} J(k) e^{i\phi(x, t, k)\Sigma_3}, \quad k \in \mathbb{R}, \quad (2.29)$$

and

$$\lim_{|k| \rightarrow \infty} J^\pm(x, t, k) \rightarrow I_{n+1}. \quad (2.30)$$

Here $J^\pm(x, t, k)$ are analytic and bounded matrix-valued functions in \mathbb{C}^\pm , defined as

$$J^+(x, t, k) = \begin{pmatrix} \mathbf{a}^+(k) & 0 \\ 0 & \mathbf{c}^+(k) \end{pmatrix} (X^+, Y^+)^{-1}(x, t, k), \quad J^-(x, t, k) = (Y^-, X^-)(x, t, k), \quad (2.31)$$

and $J(k)$ is the jump matrix defined as

$$J(k) = \begin{pmatrix} I_n & \mathbf{b}^-(k) \\ \mathbf{d}^+(k) & 1 \end{pmatrix}, \quad k \in \mathbb{R}. \quad (2.32)$$

In particular, we have

$$\det J^+(x,t,k) = \det \mathbf{a}^+(k), \quad \det J^-(x,t,k) = \mathbf{a}^-(k). \quad (2.33)$$

Proposition 2.1.4 *Assume that the above RH problem (2.29, 2.30) has unique solutions $J^\pm(x,t,k)$ which are sufficiently smooth for all $(x,t) \in \mathbb{R}$. Then $J^+(x,t,k)$ (resp. $J^-(x,t,k)$) satisfies the Lax pair (2.13, 2.14) (resp. (2.4, 2.5)). In particular, $J^+(x,t,k)$ gives a uniquely defined $Q(x,t)$ in the form*

$$Q(x,t) = \lim_{|k| \rightarrow \infty} -ik[\Sigma_3, J^+(x,t,k)]. \quad (2.34)$$

Eq. (2.34) is called reconstruction formula.

Thanks to Prop. 2.1.3 and 2.1.4, the original problem of solving the vector NLS equation is now translated into the matrix RH problem (2.29, 2.30). Therefore, the ISM mainly consists of the following two steps: 1) to formulate an RH problem via the scattering system (2.24); 2) to solve the RH problem that will lead to the solutions of (2.2) via the reconstruction formula (2.34). Although in general one cannot solve a matrix RH problem explicitly, a powerful method exists inside such formalism for constructing its singular solutions which will correspond to soliton solutions. This method is precisely the dressing transformations that will be introduced in the following section.

2.2 Dressing transformations

In the context of soliton theory, dressing transformations were first introduced by Zakharov and Shabat in [124, 125]. Here, we present the dressing transformations and their connections to an RH problem in a general context. The application to the vector NLS case, which consists of a special reduction, will be treated in the next section. The main result lies in Theorem 2.2.7 which in fact reflects the Bianchi permutativity property. A system of notations, that captures this property is accordingly introduced. We refer readers to [16] for details and in particular for the proofs of Prop. 2.2.3 and 2.2.4. The study of matrix RH problems in a more general context is contained in [59, 1].

Consider the following matrix RH problem with canonical normalizations:

$$\mathcal{J}^+(k)\mathcal{J}^-(k) = \mathcal{J}(k), \quad k \in \mathbb{R}, \quad \lim_{|k| \rightarrow \infty} \mathcal{J}^\pm(k) \rightarrow I, \quad (2.35)$$

where $\mathcal{J}(k)$ is the jump matrix satisfying $\det \mathcal{J}(k) \neq 0$ for $k \in \mathbb{R}$. The matrix $\mathcal{J}^+(k)$ (resp. $\mathcal{J}^-(k)$) is analytic in \mathbb{C}^+ (resp. \mathbb{C}^-). This problem has unique regular solutions $\mathcal{J}_0^\pm(k)$, and the term "regular" means that $\det \mathcal{J}_0^\pm(k) \neq 0$ in the appropriate domain. By contrast, we specify the term "singular" in our context by the following definitions.

Definition 2.2.1 *A matrix function $M(k)$ is said to be singular at $k = k_0$ if $\det M(k_0) = 0$ and if in the neighborhood of k_0*

$$M(k) = M_0 + (k - k_0)M_1 + O(k - k_0)^2, \quad M^{-1}(k) = \frac{N_0}{k - k_0} + N_1 + O(k - k_0). \quad (2.36)$$

Definition 2.2.2 *An RH problem with zeros or poles at $k_j^\pm \in \mathbb{C}^\pm$, $j = 1, \dots, N$ is an RH problem as defined in (2.35) where $\mathcal{J}^\pm(k)$ are singular at k_j^\pm , $j = 1, \dots, N$.*

Given these two definitions, one can prove the following.

Proposition 2.2.3 *Fixing the subspaces $\mathcal{V}_j \equiv \text{Im } \mathcal{J}^+(k)|_{k=k_j^+}$ and $\mathcal{U}_j \equiv \text{Ker } \mathcal{J}^-(k)|_{k=k_j^-}$, $j = 1, \dots, N$ determines uniquely the solution of the RH problem with zeroes at $k_j^\pm \in \mathbb{C}^\pm$.*

In general, there is no known closed-form formula to solve a matrix RH problem. However, once the regular solutions are known, it is possible to construct singular solutions from them.

Proposition 2.2.4 *Let $\mathcal{J}^\pm(k)$ be the singular solutions at $k_0^\pm \in \mathbb{C}^\pm$ with*

$$\text{Im } \mathcal{J}^+(k)|_{k=k_0^+} = \mathcal{V}_0, \quad \text{Ker } \mathcal{J}^-(k)|_{k=k_0^-} = \mathcal{U}_0, \quad (2.37)$$

and let $\mathcal{J}_0^\pm(k)$ be the solution of the same RH problem regular at k_0^\pm . Then $\mathcal{J}^\pm(k)$ can be written as

$$\mathcal{J}^+(k) = \mathcal{J}_0^+(k) \left(I + \frac{k_0^- - k_0^+}{k - k_0^-} \Pi_0 \right), \quad \mathcal{J}^-(k) = \left(I + \frac{k_0^+ - k_0^-}{k - k_0^+} \Pi_0 \right) \mathcal{J}_0^-(k). \quad (2.38)$$

Here Π_0 is a projector defined as

$$\text{Ker } \Pi_0 = (\mathcal{J}_0^+(k_0^+))^{-1} \mathcal{V}_0, \quad \text{Im } \Pi_0 = \mathcal{J}_0^-(k_0^-) \mathcal{U}_0. \quad (2.39)$$

The form of singular solutions (2.38) introduces what are called dressing factors (of degree 1) which transform $\mathcal{J}_0^\pm(k)$ regular at k_0^\pm into $\mathcal{J}^\pm(k)$ singular at k_0^\pm . This gives an algorithm to construct singular solutions $\mathcal{J}^\pm(k)$ at *distinct* $k_j^\pm \in \mathbb{C}^\pm$, $j = 1, \dots, N$ from regular solutions $\mathcal{J}_0^\pm(k)$. Precisely, let $k_j^\pm \in \mathbb{C}^\pm$, $j = 1, \dots, N$ and the corresponding subspaces \mathcal{V}_j , \mathcal{U}_j be given, we can use Prop. 2.2.4 repeatedly to construct $\mathcal{J}^\pm(k)$ singular at k_j^\pm recursively from $\mathcal{J}_0^\pm(k)$ starting from k_1^\pm , k_2^\pm up to k_N^\pm . Consequently, $\mathcal{J}^\pm(k)$ can be written as

$$\mathcal{J}^+(k) = \mathcal{J}_0^+(k) \left(I + \frac{k_1^- - k_1^+}{k - k_1^-} \Pi_1 \right) \dots \left(I + \frac{k_N^- - k_N^+}{k - k_N^-} \Pi_N \right), \quad (2.40)$$

$$\mathcal{J}^-(k) = \left(I + \frac{k_N^+ - k_N^-}{k - k_N^+} \Pi_N \right) \dots \left(I + \frac{k_1^+ - k_1^-}{k - k_1^+} \Pi_1 \right) \mathcal{J}_0^-(k), \quad (2.41)$$

where, for $j = 1, \dots, N$

$$\text{Ker} \Pi_j = \left(\mathcal{J}_0^+(k_j^+) \left(I + \frac{k_1^- - k_1^+}{k_j^+ - k_1^-} \Pi_{j-1} \right) \dots \left(I + \frac{k_{j-1}^- - k_{j-1}^+}{k_j^+ - k_{j-1}^-} \Pi_1 \right) \right)^{-1} \mathcal{V}_j, \quad (2.42)$$

$$\text{Im} \Pi_j = \left(I + \frac{k_{j-1}^+ - k_{j-1}^-}{k_j^- - k_{j-1}^+} \Pi_{j-1} \right) \dots \left(I + \frac{k_1^+ - k_1^-}{k_j^- - k_1^+} \Pi_1 \right) \mathcal{J}_0^-(k_j^-) \mathcal{U}_j. \quad (2.43)$$

Now comes a fundamental observation: in the above construction, one can iterate the construction of $\mathcal{J}^\pm(k)$ by using a different order on the k_j^\pm . Let \mathcal{S}_N be the permutation group on the set $\{1, \dots, N\}$ and let $\sigma \in \mathcal{S}_N$. Denote the image of $(1, \dots, N)$ under σ by $(\sigma(1), \dots, \sigma(N))$ and introduce $\kappa_j^\pm = k_{\sigma(j)}^\pm$. Then, the subspaces corresponding to κ_j^\pm are $\mathcal{V}_{\sigma(j)}$, $\mathcal{U}_{\sigma(j)}$. Repeating the previous procedure, starting from κ_1^\pm up to κ_N^\pm , one gets

$$\tilde{\mathcal{J}}^+(k) = \mathcal{J}_0^+(k) \left(I + \frac{\kappa_1^- - \kappa_1^+}{k - \kappa_1^-} \Pi_1^\sigma \right) \dots \left(I + \frac{\kappa_N^- - \kappa_N^+}{k - \kappa_N^-} \Pi_N^\sigma \right), \quad (2.44)$$

$$\tilde{\mathcal{J}}^-(k) = \left(I + \frac{\kappa_N^+ - \kappa_N^-}{k - \kappa_N^+} \Pi_N^\sigma \right) \dots \left(I + \frac{\kappa_1^+ - \kappa_1^-}{k - \kappa_1^+} \Pi_1^\sigma \right) \mathcal{J}_0^-(k), \quad (2.45)$$

where, for $j = 1, \dots, N$,

$$\text{Ker} \Pi_j^\sigma = \left(\mathcal{J}_0^+(\kappa_j^+) \left(I + \frac{\kappa_1^- - \kappa_1^+}{\kappa_j^+ - \kappa_1^-} \Pi_{j-1}^\sigma \right) \dots \left(I + \frac{\kappa_{j-1}^- - \kappa_{j-1}^+}{\kappa_j^+ - \kappa_{j-1}^-} \Pi_1^\sigma \right) \right)^{-1} \mathcal{V}_{\sigma(j)}, \quad (2.46)$$

$$\text{Im} \Pi_j^\sigma = \left(I + \frac{\kappa_{j-1}^+ - \kappa_{j-1}^-}{\kappa_j^- - \kappa_{j-1}^+} \Pi_{j-1}^\sigma \right) \dots \left(I + \frac{\kappa_1^+ - \kappa_1^-}{\kappa_j^- - \kappa_1^+} \Pi_1^\sigma \right) \mathcal{J}_0^-(\kappa_j^-) \mathcal{U}_{\sigma(j)}. \quad (2.47)$$

It can be checked by direct calculation that

$$\mathcal{V}_j = \text{Im } \tilde{\mathcal{J}}^+(k)|_{k=k_j^+}, \quad \mathcal{U}_j = \text{Ker } \tilde{\mathcal{J}}^-(k)|_{k=k_j^-}, \quad (2.48)$$

$j = 1, \dots, N$, so that Prop. 2.2.3 implies that $\tilde{\mathcal{J}}^\pm(k) = \mathcal{J}^\pm(k)$. In turn, this implies that the product of dressing factors in (2.44, 2.45) is equal to the product of dressing factors in (2.40, 2.41). This construction introduces the notion of dressing factors of degree N which transform $\mathcal{J}_0^\pm(k)$ into $\mathcal{J}^\pm(k)$ singular at k_j^\pm , $j = 1, \dots, N$. Prop. 2.2.3 also ensures that a dressing factor of degree N factorizes into N dressing factors of degree 1 and that the order of the factorization is irrelevant. Note that this fact actually reflects the Bianchi permutativity property (see Fig. 2.1), as dressing transformations represent a special type of Darboux-Bäcklund transformations.

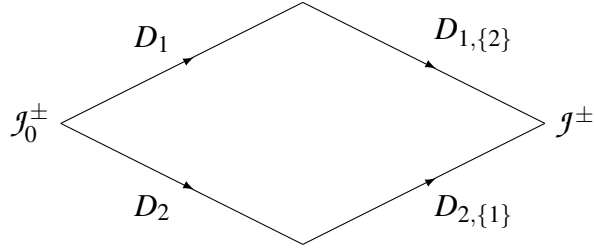


Fig. 2.1 : Bianchi diagram for dressing transformations

Remark 2.2.5 *It is important to realize that this does not mean that the individual dressing factors of degree 1 in a dressing factor of degree N commute. Indeed, in general $\Pi_j^\sigma \neq \Pi_{\sigma(j)}$. The message here is that, in the factorization of a dressing factor of degree N , the explicit forms of $\mathcal{J}^\pm(k)$ are obtained by using the equations governing the projectors as formulated in (2.46, 2.47), and in particular, the order of adding the singularities, in general, modifies the forms of the individual dressing factors. With this in mind, we introduce a notation that will help us to formulate the dressing factors.*

Definition 2.2.6 *Given $\mathcal{J}_0^\pm(k)$ regular solutions of the RH problem (2.35). Let $\sigma \in \mathcal{S}_N$ be given and write $(\sigma(1), \dots, \sigma(N)) = (i_1, \dots, i_N)$. Given k_j^\pm and $\mathcal{V}_j, \mathcal{U}_j$, $j = 1, \dots, N$, a general dressing factor of degree 1 is defined as, for $1 \leq \ell \leq N$,*

$$D_{i_\ell, \{i_1 \dots i_{\ell-1}\}}(k) = I + \frac{k_{i_\ell}^- - k_{i_\ell}^+}{k - k_{i_\ell}^-} \Pi_{i_\ell, \{i_1 \dots i_{\ell-1}\}} \quad (2.49)$$

where

$$\text{Ker}\Pi_{i_\ell, \{i_1 \dots i_{\ell-1}\}} = \left[D_{i_1}(k_{i_\ell}^+) \dots D_{i_{\ell-1}, \{i_1 \dots i_{\ell-2}\}}(k_{i_\ell}^+) \right]^{-1} \left(\mathcal{J}_0^+(k_{i_\ell}^+) \right)^{-1} \mathcal{V}_{i_\ell}, \quad (2.50)$$

$$\text{Im}\Pi_{i_\ell, \{i_1 \dots i_{\ell-1}\}} = \left[D_{i_1}(k_{i_\ell}^-) \dots D_{i_{\ell-1}, \{i_1 \dots i_{\ell-2}\}}(k_{i_\ell}^-) \right]^{-1} \mathcal{J}_0^-(k_{i_\ell}^-) \mathcal{U}_{i_\ell}. \quad (2.51)$$

Finally, the dressing factor of degree N is denoted as $D_{1\dots N}(k)$.

Note that in the case $\ell = 1$, we denote $D_{i_1, \{\}}(k) \equiv D_{i_1}(k)$. The indices in the subscript specify the order of adding the singularities, and thus determine the forms of dressing factors. This convention will be adopted in the rest of the thesis for any quantity involving sets of indices as subscripts. Along with this definition and the understanding from the above discussion, we have proved the following.

Theorem 2.2.7 *A dressing factor of degree N can be decomposed into $N!$ equivalent products of N dressing factors of degree 1*

$$D_{1\dots N}(k) = D_{i_1}(k) \dots D_{i_N, \{i_1 \dots i_{N-1}\}}(k), \quad (2.52)$$

where (i_1, \dots, i_N) is an arbitrary permutation of $(1, \dots, N)$.

2.3 *N*-soliton solutions

In this section, we consider only the *focusing* case of the vector NLS equation, which corresponds to $\lambda = -1$ in (2.2), for we are only concerned with soliton solutions.

Coming back to the Prop. 2.1.3 and 2.1.4 in which an RH problem and its relation to the Lax pair are clearly established, there are two more steps needed to make dressing transformations fully adapted to the vector NLS equation: 1) taking account of the (x, t) -dependence; 2) making the reduction, as the vector NLS equation consists of a special reduction of the ISM [89].

As to 1), dressing transformations are still valid for parameter-dependent RH problems [16]. Precisely, we work with (x, t) -dependent subspaces $\mathcal{V}_j(x, t)$, $\mathcal{U}_j(x, t)$, $j = 1, \dots, N$ which are simply related to \mathcal{V}_j , \mathcal{U}_j , $j = 1, \dots, N$ by

$$\mathcal{V}_j(x, t) = \Psi(x, t, k_j^+) \mathcal{V}_j, \quad \mathcal{U}_j(x, t) = \Psi(x, t, k_j^-) \mathcal{U}_j. \quad (2.53)$$

Here, Ψ , known as *undressed* Lax pair solution, is solution of (2.9) with U , V satisfying the zero curvature condition, for the solutions of the RH problem, constructed by the dressing transformations, obey the auxiliary problems (2.4, 2.5).

As to 2), consider the RH problem defined in Prop. 2.1.3 with zeros at $k_j \in \mathbb{C}^\pm$, $j = 1, \dots, N$. Because of (2.28), which is a consequence of the reduction symmetry (2.11), one can get the following relations concerning the singular points k_j^\pm and the corresponding subspaces $\mathcal{U}_j(x, t)$, $\mathcal{V}_j(x, t)$, $j = 1, \dots, N$:

$$k_j^+ = (k_j^-)^* \equiv k_j \in \mathbb{C}^+, \quad \mathcal{V}_j^\perp(x, t) = \mathcal{U}_j(x, t), \quad (2.54)$$

where \mathcal{V}_j^\perp represents the orthogonal complement of \mathcal{V}_j .

Then, by evaluating $J^\pm(x, t, k)$ defined in Prop. 2.1.3 at their singular points *i.e.* k_j and k_j^* according to (2.54), one gets

$$\mathcal{U}_j(x, t) = \text{span} \left\{ e^{-i\phi(x, t, k_j^*)\Sigma_3} \begin{pmatrix} \beta_j \\ -1 \end{pmatrix} \right\}, \quad (2.55)$$

where $\beta_j \in \mathbb{C}^n$ is a nonzero vector. Here, we adopt the following conventions: fixing $k_j \in \mathbb{C}^+$; choosing the nonzero vector $\beta_j \in \mathbb{C}^n$ as the *norming constant*⁵ associated to k_j . Note that Eq. (2.55) implies that the projectors involved in the dressing factors are rank-one orthogonal projectors, which is consistent with the vector nature of the underlying system.

Having specified these notions, we come to the construction of an *N*-soliton solution of the vector NLS equation. Information concerning soliton solutions lies in the zeros of $\det \mathbf{a}^+(k)$. This is translated into an RH problem with zeros, via Prop. 2.1.3. The usual assumption is that $\det \mathbf{a}^+(k)$ has a finite number of simple zeros located in \mathbb{C}^+ . Denote these points $k_j \in \mathbb{C}^+$, $j = 1, \dots, N$ as presented in (2.54). Consequently, $\mathbf{a}^-(k)$ has the same number of simple zeros in \mathbb{C}^- , located at k_j^* . We make a further assumption that the field $R(x, t)$ in the vector NLS equation (2.2) belongs to a certain functional space of exponentially fast decreasing functions⁶. Then $\mathbf{b}^+(k)$ can be analytically continued up to the strip $\{k \in \mathbb{C}; 0 \leq \text{Im } k \leq K\}$ where K controls the decrease of $R(x, t)$, with $K \geq \max\{\text{Im } k_j; j = 1, \dots, N\}$. This applies also to $\mathbf{b}^-(k)$, with $\mathbf{b}^-(k)$ being analytic in the strip $\{k \in \mathbb{C}; -K \leq \text{Im } k \leq 0\}$. This allows us to take the following definitions:

$$\beta_j \equiv \mathbf{b}^-(k_j^*), \quad \beta_j(x, t) \equiv \beta_j e^{-2i\phi(x, t, k_j^*)}, \quad (2.56)$$

where the vectors β_j are the norming constants as introduced in (2.55). Now the norming constants β_j of the system are associated to the scattering functions $\mathbf{b}^-(k)$,

⁵Norming constants are the proportionality coefficients between the bound states of the Jost solutions, and in general are only defined up to certain normalizations.

⁶Indeed, the soliton solutions belong to this functional space.

and the space-time evolution of the former is characterized by $\beta_j(x, t)$ as shown on the right-hand side of (2.56).

We call $\{k_j, \beta_j\}$, $j = 1, \dots, N$ a set of N -soliton scattering data. Therefore, N -soliton scattering data are obtained by specifying the quantities $\mathbf{a}^+(k)$ and $\mathbf{b}^-(k)$ at the singular points. In the pure soliton system *i.e.* $\mathbf{b}^\pm(k) = \mathbf{0}$, for $k \in \mathbb{R}$ (also known as *reflectionless conditions*), the unique regular solutions of the RH problem (2.29, 2.30) are $J_0^\pm(x, t, k) = I_{n+1}$, which correspond to $\mathcal{Q}(x, t) = \mathbf{0}$. Provided that the N -soliton scattering data $\{k_j; \beta_j\}$, $j = 1, \dots, N$ are given, one can completely determine singular solutions of the RH problem with zeroes at k_j^\pm , $j = 1, \dots, N$, thanks to dressing transformations. The resulting N -soliton solution is obtained by using the reconstruction formula (2.34).

More precisely, given $\{k_j; \beta_j\}$, $j = 1, \dots, N$, it follows directly from the construction of dressing factors (see Def. 2.2.6) that a dressing factor of degree 1 reads

$$D_{i_j, \{i_1 \dots i_{j-1}\}}(x, t, k) = I_{n+1} + \left(\frac{k_{i_j}^* - k_{i_j}}{k - k_{i_j}^*} \right) \Pi_{i_j, \{i_1 \dots i_{j-1}\}}(x, t), \quad (2.57)$$

and enjoys the property

$$D_{i_j, \{i_1 \dots i_{j-1}\}}^{-1}(x, t, k) = D_{i_j, \{i_1 \dots i_{j-1}\}}^\dagger(x, t, k^*). \quad (2.58)$$

Here the index set (i_1, \dots, i_N) is the image of $\sigma \in \mathcal{S}_N$ acting on $(1, \dots, N)$ as introduced in Def. 2.2.6. The projector $\Pi_{i_j, \{i_1 \dots i_{j-1}\}}$ is defined as

$$\Pi_{i_j, \{i_1 \dots i_{j-1}\}}(x, t) = \frac{\zeta_{i_j, \{i_1 \dots i_{j-1}\}} \zeta_{i_j, \{i_1 \dots i_{j-1}\}}^\dagger(x, t)}{\zeta_{i_j, \{i_1 \dots i_{j-1}\}}^\dagger \zeta_{i_j, \{i_1 \dots i_{j-1}\}}(x, t)}, \quad (2.59)$$

where

$$\zeta_{i_j, \{i_1 \dots i_{j-1}\}}(x, t) = D_{i_1 \dots i_{j-1}}^\dagger(x, t, k_j) e^{-i\phi(x, t, k_j^*) \Sigma_3} \begin{pmatrix} \beta_{i_j} \\ -1 \end{pmatrix}. \quad (2.60)$$

In particular, the reconstruction formula (2.34) turns out to be

$$\mathcal{Q}(x, t) = \sum_{j=1}^N i(k_j - k_j^*) [\Sigma_3, \Pi_{j, \{1, \dots, j-1\}}(x, t)]. \quad (2.61)$$

An N -soliton solution is thus completely determined by $\Pi_{i_j, \{i_1 \dots i_{j-1}\}}$, $j = 1, \dots, N$. Using an elegant method introduced in [47], one comes to the following proposition which gives the N -soliton solutions in a compact form.

Proposition 2.3.1 *Consider the pure soliton system, i.e. $\mathbf{b}^\pm(k) = \mathbf{0}$ for $k \in \mathbb{R}$.*

Given $\{k_j; \beta_j\}$, $j = 1, \dots, N$, and let $\beta_{j;\ell}$ be the ℓ th component of β_j . Define the following $(n+1) \times (n+1)$ matrix:

$$\mathcal{M}_\ell(x, t) = \begin{pmatrix} M(x, t) & \begin{pmatrix} \beta_{1;\ell}(x, t) \\ \vdots \\ \beta_{N;\ell}(x, t) \end{pmatrix} \\ \begin{pmatrix} 1 & \dots & 1 \end{pmatrix} & 0 \end{pmatrix}, \quad (2.62)$$

where $M(x, t)$ is an $n \times n$ matrix of entries $M_{kl}(x, t)$ defined as

$$M_{kl}(x, t) = \frac{\beta_l^\dagger(x, t)\beta_k(x, t) + 1}{k_k^* - k_l}. \quad (2.63)$$

Then, an N -soliton solution of the vector NLS equation (2.2) is of the form

$$r_\ell(x, t) = 2i \frac{\det \mathcal{M}_\ell}{\det M}(x, t), \quad (2.64)$$

where $r_\ell(x, t)$ is the ℓ th component of $R(x, t)$ as defined in (2.3).

As an illustration, we construct explicitly a one-soliton solution by taking $k_0 = \frac{1}{2}(u_0 + iv_0)$, $v_0 > 0$ and β_0 as scattering data. Applying Prop. 2.3.1 yields

$$R(x, t) = \mathbf{p}_0 v_0 \frac{e^{-i(u_0 x + (u_0^2 - v_0^2)t)}}{\cosh(v_0(x + 2u_0 t - \Delta x_0))} \equiv \mathbf{p}_0 q_0(x, t), \quad (2.65)$$

where

$$\Delta x_0 = \frac{\ln |\beta_0|}{v_0}, \quad \mathbf{p}_0 = \frac{\beta_0}{|\beta_0|}. \quad (2.66)$$

The main feature here is that a vector one-soliton is simply a vector \mathbf{p}_0 times a scalar one-soliton solution $q_0(x, t)$. The unit vector \mathbf{p}_0 is the *polarization* of the soliton, $-2u_0$ its velocity, v_0 its amplitude and Δx_0 is the position of the maximum of the envelope of the soliton at $t = 0$.

The final step aims at determining the matrix $\mathbf{a}^+(k)$ in the pure N -soliton case. This can be done by taking the limits $x \rightarrow \pm\infty$ of the dressing factor $D_{1, \dots, N}(x, t, k)$, and it turns out that $\mathbf{a}^+(k)$ is a dressing factor of degree N as well. Precisely, given $\{k_j; \beta_j\}$, $j = 1, \dots, N$, and let (i_1, \dots, i_N) be image of $\sigma \in \mathcal{S}_N$ on $(1, \dots, N)$. Define a dressing factor of degree N as

$$d_{i_1 \dots i_N}(k) = d_{i_1}(k) d_{i_2, \{i_1\}}(k) \dots d_{i_N, \{i_1 \dots i_{N-1}\}}(k), \quad (2.67)$$

where,

$$d_{i_j, \{i_1 \dots i_{j-1}\}}(k) = I_n + \left(\frac{k_{i_j}^* - k_{i_j}}{k - k_{i_j}^*} \right) \boldsymbol{\pi}_{i_j, \{i_1 \dots i_{j-1}\}}, \quad (2.68)$$

$$\boldsymbol{\pi}_{i_j, \{i_1 \dots i_{j-1}\}} = \frac{\boldsymbol{\xi}_{i_j, \{i_1 \dots i_{j-1}\}} \boldsymbol{\xi}_{i_j, \{i_1 \dots i_{j-1}\}}^\dagger}{\boldsymbol{\xi}_{i_j, \{i_1 \dots i_{j-1}\}}^\dagger \boldsymbol{\xi}_{i_j, \{i_1 \dots i_{j-1}\}}}, \quad \boldsymbol{\xi}_{i_j, \{i_1 \dots i_{j-1}\}} = d_{\{i_1 \dots i_{j-1}\}}^\dagger(k_{i_j}) \boldsymbol{\beta}_{i_j}. \quad (2.69)$$

Then, $\mathbf{a}^+(k)$ is in the form

$$\mathbf{a}^+(k) = d_{i_1 \dots i_N}(k), \quad \det \mathbf{a}^+(k) = \prod_{j=1}^N \left(\frac{k - k_j}{k - k_j^*} \right). \quad (2.70)$$

The left-hand side of (2.70) correspond to the *trace formulae* that is well-known in the scalar NLS case. In contrast, due to the matrix nature of $\mathbf{a}^+(k)$, it can only be constructed using both the singular points k_j and the associated norming constants $\boldsymbol{\beta}_j$. This reveals the complexity of vector solitons' interactions.

It is useful to introduce the matrix \mathcal{A}_j defined as

$$\frac{\mathcal{A}_j}{\det \mathbf{a}^+(k_j)'} = \lim_{k \rightarrow k_j} (k - k_j) (\mathbf{a}^+(k))^{-1}, \quad \det \mathbf{a}^+(k_j)' = \left. \frac{d \det \mathbf{a}^+(k)}{dk} \right|_{k=k_j}. \quad (2.71)$$

Indeed, the matrix \mathcal{A}_j contains the information of the residues of $(\mathbf{a}^+(k))^{-1}$ at k_j and comes only from the vector nature of the system. It will appear for instance when taking the transpose conjugate of the norming constants $\boldsymbol{\beta}_j$ as

$$\boldsymbol{\beta}_j^\dagger = -\mathbf{b}^+(k_j) \mathcal{A}_j. \quad (2.72)$$

We stress that both the form of $\mathbf{a}^+(k)$ and the matrix \mathcal{A}_j will play an important role in the forthcoming chapters in which soliton behaviors will be investigated in detail.

The vector NLS equation on the half-line

In this chapter, we study the vector NLS equation on the half-line, namely to restrict the system to $x \geq 0$ by adding a boundary at the origin. The main objectives are the following: 1) to derive integrable boundary conditions; 2) to formulate an ISM in the presence of such boundaries; 3) to obtain N -soliton solutions on the half-line. These will lay the foundations for a deeper understanding of interactions of vector solitons with an integrable boundary, which will be the topic of the forthcoming chapters.

As pointed out in Introduction, soliton models on the half-line have been investigated by various researchers over the years. Here, we generalize the notions and methods, developed in [50, 26, 27] for the (scalar) NLS case. First, we use a *folding technique* [26], which is based on a Bäcklund transformation, to derive two classes of boundary conditions. Integrability is argued by constructing an explicit generating function for the conserved quantities. Then, by extending the system to the full line [50], a (nonlinear) mirror image method [27] is used to put the ISM into use. Lastly, we construct the N -soliton solutions on the half-line. Again severe complexity appears due to the vector nature of the system, and such a construction is shown in Appendix C. Interestingly, a phenomenon of transmission between different modes of polarization is demonstrated.

These results are reported in [37] and partly in [38]. In addition, in Appendix A, we use the *unified transform method* developed by Fokas (see e.g. [54]) to construct the so-called *linearizable boundary conditions* for the vector NLS equation on the half-line. Remarkably, we see that this class of boundary conditions coincides with the integrable boundary conditions that we derived from the Bäcklund transformation method. In Appendix B, we provide a justification of the use of the mirror image method as the correct way to "build up" the integrable boundaries. To the best of the authors' knowledge, this argument is lacking in the literature.

Recall the vector NLS equation as defined in (2.2). The vector NLS equation on

the half-line is precisely the following initial-boundary value problem:

$$i\frac{\partial R}{\partial t} + \frac{\partial^2 R}{\partial x^2} - 2\lambda RR^\dagger R = 0, \quad x, t \in [0, \infty), \quad (3.1)$$

$$R(x, 0) = R_0(x) \quad , \quad R(0, t) = g_0(t), \quad R_x(0, t) = g_1(t). \quad (3.2)$$

Here, we assume that the functions R_0 , g_0 and g_1 live in appropriate functional spaces so as to ensure that the calculations are meaningful¹. In particular, we require that R decays at infinity.

3.1 Deriving integrable boundary conditions

We use the Bäcklund transformation method introduced in [66, 25, 26]. The idea lies in exploiting the folding transformation $R(x, t) \rightarrow R(-x, t)$ which is a (parity) symmetry of the NLS equation itself. Contrary to the scalar case [26], here it is important to study both the x -part and the t -part of the auxiliary problem (Lax pair).

Consider a Bäcklund matrix $L(x, t, k)$ relating the auxiliary problem (2.4, 2.5) for Φ to the same auxiliary problem for $\tilde{\Phi}$, with the potential Q replaced by a new potential \tilde{Q} , by the equation

$$\tilde{\Phi}(x, t, k) = L(x, t, k)\Phi(x, t, k). \quad (3.3)$$

It is well-known that L , also known as a gauge transformation of the auxiliary problem, satisfies the following equations:

$$L_x + ik[\Sigma_3, L] = \tilde{Q}L - LQ, \quad (3.4)$$

$$L_t + 2ik^2[\Sigma_3, L] = \tilde{Q}_T L - LQ_t, \quad (3.5)$$

where \tilde{Q}_T is the new potential written in terms of \tilde{Q} as Q_T (2.6). We look for a solution in the following form:

$$L(x, t, k) = kI_{n+1} + A(x, t), \quad (3.6)$$

under the symmetry constraint $\tilde{Q}(x, t) = Q(-x, t)$. Precisely, we write the matrix A

¹For details in the scalar case, see for instance the "rigorous considerations" section in [55]

in the natural block form²

$$\begin{pmatrix} A_1(x,t) & A_2(x,t) \\ A_3(x,t) & A_4(x,t) \end{pmatrix}. \quad (3.7)$$

To solve $A(x,t)$, first, we insert (3.6) in (3.4) which comes from the x -part of the auxiliary problem. This yields

$$2iA_2(x,t) = R(-x,t) - R(x,t), \quad (3.8a)$$

$$-2iA_3(x,t) = \lambda \left(R^\dagger(-x,t) - R^\dagger(x,t) \right), \quad (3.8b)$$

and

$$A_{1x}(x,t) = R(-x,t)A_3(x,t) - \lambda A_2(x,t)R^\dagger(x,t), \quad (3.9a)$$

$$A_{2x}(x,t) = R(-x,t)A_4(x,t) - A_1(x,t)R(x,t), \quad (3.9b)$$

$$A_{3x}(x,t) = \lambda \left[R^\dagger(-x,t)A_1(x,t) - A_4(x,t)R^\dagger(x,t) \right], \quad (3.9c)$$

$$A_{4x}(x,t) = \lambda R^\dagger(-x,t)A_2(x,t) - A_3(x,t)R(x,t). \quad (3.9d)$$

It follows from (3.8) that

$$A_3(x,t) = \lambda A_2^\dagger(x,t). \quad (3.10)$$

Combining (3.8) and (3.9b, 3.9c), and fixing $x = 0$, one gets the following boundary conditions:

$$R_x(0,t) = -i(A_4(0,t)I_n - A_1(0,t))R(0,t), \quad (3.11a)$$

$$R_x^\dagger(0,t) = iR^\dagger(0,t)(A_1(0,t) - A_4(0,t)I_n). \quad (3.11b)$$

The compatibility between (3.11a) and (3.11b) is ensured by

$$A_1(0,t) - A_4(0,t)I_n = -(A_1(0,t) - A_4(0,t)I_n)^\dagger. \quad (3.12)$$

Defining a matrix $H \equiv -i(A_1(0,t) - A_4(0,t)I_n)$, Eq. (3.12) imposes H to be a hermitian matrix. Now, the boundary condition reads

$$R_x(0,t) + HR(0,t) = 0. \quad (3.13)$$

Note that at this stage, we have boundary conditions that depend on time *a priori*. We remove this time dependence by requiring $A_1(0,t)$ and $A_4(0,t)$ to be time-

²It means that $A_1(x,t)$ is an $n \times n$ matrix and $A_4(x,t)$ a scalar quantity.

independent. Thus, H is time independent. It is apparent that Eq. (3.13) is the vector generalization of the usual *Robin boundary condition* in the scalar case ($r_x(0,t) + \alpha r(0,t) = 0$, $\alpha \in \mathbb{R}$). The fact that H is hermitian is the analog of α being real. Let us denote $A_4(0) = \beta$. What we have obtained so far reads

$$L(0,k) = kI_{n+1} + \begin{pmatrix} \beta I_n + iH & 0 \\ 0 & \beta \end{pmatrix}, \quad (3.14)$$

with L independent of t at $x = 0$.

The hermiticity property of H guarantees that H is diagonalizable by a unitary matrix V

$$H = VDV^\dagger, \quad (3.15)$$

where $D = \text{diag}\{d_1, \dots, d_n\}$ with $d_j \in \mathbb{R}$, $j = 1, \dots, n$. Note that the transformation $R(x,t) \mapsto V^\dagger R(x,t) = R'(x,t)$ leaves the vector NLS equation invariant and in the new basis the boundary condition takes the simple, diagonal form

$$R'_x(0,t) + DR'(0,t) = 0. \quad (3.16)$$

This shows that, in the presence of a boundary described by H , the vector NLS equation has a preferred polarization basis determined by the boundary. In the following, we work in this basis and drop the $'$. Then,

$$L(0,k) = kI_{n+1} + \begin{pmatrix} \beta I_n + iD & 0 \\ 0 & \beta \end{pmatrix}. \quad (3.17)$$

To complete the characterization of $L(0,k)$, we need to use the t -part of the auxiliary problem. Inserting (3.14) in (3.5), one gets

$$\tilde{Q}_T(0,k)L(0,k) - L(0,k)Q_T(0,k) = 0. \quad (3.18)$$

Due to $\tilde{Q}_T(0,k) = \Sigma_3 Q_T(0,-k)\Sigma_3$, this reads

$$Q_T(0,-k)\Sigma_3 L(0,k) = \Sigma_3 L(0,k)Q_T(0,k). \quad (3.19)$$

Combining Eq. (3.16) with (3.19) yields

$$(2i\beta I_n - D)DR(0,t) = 0, \quad (3.20a)$$

$$R^\dagger(0,t)(2i\beta I_n - D)D = 0, \quad (3.20b)$$

$$RR^\dagger(0,t)D = DRR^\dagger(0,t). \quad (3.20c)$$

The compatibility of the first two equations imposes that β is purely imaginary: $\beta \equiv i\alpha$, $\alpha \in \mathbb{R}$, unless $R(0,t) = 0$ —this Dirichlet boundary condition for all the components is formally obtained when all the d_j are infinite. Then, the first equation shows that either $d_j = 0$ or $d_j = -2\alpha$ or $R_j(0,t) = 0$. Finally, the last equation reads

$$d_j R_j R_k^*(0,t) = d_k R_j R_k^*(0,t), \quad j, k = 1, \dots, n. \quad (3.21)$$

In general, this means that $d_j = d_k \equiv d$, *i.e.* $D = dI_n$ is proportional to the identity matrix. The particular case $R_j(0,t) = 0$ for some j requires some attention. In this case, either $R_{jx}(0,t)$ is also zero and $d_j = d$ as before, or in general $R_{jx}(0,t) \neq 0$, meaning that $d_j = \infty$ is different from the common value d and we must have $d_j + 2\alpha = 0$. So this case occurs when formally $\alpha = -\infty$.

To summarize the results, we have the two following possible boundary conditions: (1) Robin boundary condition

$$R_x(0,t) - 2\alpha R(0,t) = 0, \quad \alpha \in \mathbb{R}; \quad (3.22)$$

(2) a mixture of Neumann and Dirichlet boundary conditions

$$R_j(0,t) = 0, \quad j \in M, \quad (3.23a)$$

$$R_{kx}(0,t) = 0, \quad k \in \{1, \dots, n\} \setminus M, \quad (3.23b)$$

where M is a nonempty subset of $\{1, \dots, n\}$. In fact, either the case that M is empty or $M = \{1, \dots, n\}$ just represents a subcase of the Robin boundary condition (3.22) as α can vary from 0 to $\pm\infty$. In terms of $L(0,k)$, this result is more conveniently written by considering

$$\mathcal{L}(x,t,k) = \frac{1}{k + i\alpha} L(x,t,k).$$

Note that \mathcal{L} is completely equivalent to L since a Bäcklund matrix is always defined up to a function of k , but it has the advantage of accommodating the $\alpha = -\infty$ case.

Then, the previous two cases correspond to

$$\mathcal{L}(0, k) = \begin{pmatrix} \frac{k-i\alpha}{k+i\alpha} I_n & & \\ & & \\ & & 1 \end{pmatrix}, \quad \text{or} \quad \mathcal{L}(0, k) = \begin{pmatrix} \sigma_1 & & & \\ & \ddots & & \\ & & \sigma_n & \\ & & & 1 \end{pmatrix}, \quad (3.24)$$

where $\sigma_j = -1$, $j \in M$ and $\sigma_j = 1$, $j \in \{1, \dots, n\} \setminus M$, M being a nonempty subset of $\{1, \dots, n\}$. The sign $+$ (resp. $-$) of σ_j corresponds to $R_{jx}(0, t) = 0$ (resp. $R_j(0, t) = 0$).

Remark 3.1.1 *Eq. (3.19) is precisely the relation that is imposed in the unified transform method to obtain the linearizable boundary conditions (with the identification $\Sigma_3 \mathcal{L}(0, k) \equiv N(k)$ (A.38) as presented in Appendix A). Thus, the class of linearizable boundary conditions in Fokas' language is directly connected, in our context, to the boundary conditions (3.22) and (3.23) via a special Bäcklund transformation.*

Having derived these boundary conditions, we now move on to clarify the following argument. Although the system that we are considering is restricted to $x \geq 0$, both the fields $Q(x, t)$ and $\tilde{Q}(x, t)$ are actually living on the full line. Provided that $\tilde{Q}(x, t) = Q(-x, t)$, the boundary is "astutely" built up at $x = 0$ by the presence of both $Q(x, t)$ and $\tilde{Q}(x, t)$, which are related by the Bäcklund matrix L . As shown in the previous chapter, such a system can be characterized by the scattering system (2.24) with the appearance of the matrix $S(k)$ relating Jost solutions. Let $\mathcal{B}(k) \equiv \Sigma_3 \mathcal{L}(0, k)$ where $\mathcal{L}(0, k)$ is defined in (3.24), then $S(k)$ satisfies the following relation:

$$W S^\dagger(k^*) W^{-1} = \mathcal{B}(k) S(-k) \mathcal{B}(-k), \quad (3.25)$$

where W is defined in (2.12). The proof of this relation is established in Appendix B.

Remark 3.1.2 *The proof of the relation (3.25) lies in the fact that $\mathcal{L}(0, k)$ can be regarded as a dressing factor of degree 1 with singular points $\pm i\alpha$, $\alpha \in \mathbb{R}$. Physically, such a dressing factor represents a static soliton located at $x = 0$ with amplitude proportional to α . Therefore, our system on the half-line in the presence of the boundary condition (3.22) or (3.23) can be nicely interpreted as a picture of two fields $R(x)$ and $\tilde{R}(x)$ ($\tilde{R}(x) = R(-x)$) living on the full line, plus a static soliton located at the origin with the amplitude controlled by the real parameter α . Restricting $x \geq 0$ by neglecting the part of $x < 0$ gives an exact description of a half-line system. The boundary effect precisely comes from the presence of the static soliton.*

3.2 Check of integrability

Before proceeding to implement the ISM for the vector NLS equation on the half-line, we comment in this section the use of the term "integrable boundary conditions". The fact that our boundary conditions is derived from a Bäcklund transformation ensures the existence of an infinite number of conserved quantities. This is what we mean by integrability in our context. In the following proposition, we construct explicitly a generating function of the conserved quantities.

Proposition 3.2.1 *A generating function for the conserved quantities of the vector NLS with integrable boundary conditions is given by*

$$i(I(k) - I^\dagger(k^*)), \quad (3.26)$$

where

$$I(k) = \text{tr} \left[\int_0^\infty [R(x,t)(\Gamma(x,t,k) - \Gamma(x,t,-k))] dx \right], \quad (3.27)$$

and $\Gamma(x,t,k)$ satisfies the following Riccati equation:

$$\Gamma_x = 2ik\Gamma + \lambda R^\dagger - \Gamma R \Gamma. \quad (3.28)$$

Proof: The proof follows the idea presented in [36], and is adapted to the present vector case with a boundary. Recall that we consider two copies of the auxiliary problem (2.4, 2.5) related by (3.3). Define $\Gamma(x,t,k) = \Phi_{21}\Phi_{11}^{-1}(x,t,k)$ and $\tilde{\Gamma}(x,t,k) = \tilde{\Phi}_{21}\tilde{\Phi}_{11}^{-1}(x,t,k)$, where the subscript indices indicate the entries of the 2×2 block matrix of natural form, *i.e.* Φ_{11} is an $n \times n$ matrix whilst Φ_{21} a $1 \times n$ (row) vector. Then, (2.4) yields (3.28) for Γ and the same equation for $\tilde{\Gamma}$ with R replaced by \tilde{R} . Also, we can write

$$\Phi_{11x}\Phi_{11}^{-1} = R\Gamma, \quad \Phi_{11t}\Phi_{11}^{-1} = Q_{T11} + Q_{T12}\Gamma, \quad (3.29)$$

so using $(\ln \Phi)_{xt} = (\ln \Phi)_{tx}$ we get $(R\Gamma)_t = (Q_{T11} + Q_{T12}\Gamma)_x$ where Q_{Tij} are the appropriate blocks of Q_T . A similar relation holds for $\tilde{\Gamma}$. Next, from (3.3) we have

$$\begin{aligned} \tilde{\Phi}_{11t} &= [(L_{11} + L_{12}\Gamma)\Phi_{11}]_t \\ &= [(L_{11} + L_{12}\Gamma)_t + (L_{11} + L_{12}\Gamma)(Q_{T11} + Q_{T12}\Gamma)](L_{11} + L_{12}\Gamma)^{-1}\tilde{\Phi}_{11}, \end{aligned} \quad (3.30)$$

which is used to compare with $\tilde{\Phi}_{11t} = (\tilde{Q}_{T11} + \tilde{Q}_{T12}\tilde{\Gamma})$ to get

$$\text{tr}(\tilde{Q}_{T11} + \tilde{Q}_{T12}\tilde{\Gamma}) = \text{tr}(Q_{T11} + Q_{T12}\Gamma) + \text{tr}\ln(L_{11} + L_{12}\Gamma)_t. \quad (3.31)$$

Swapping the roles of Φ and $\tilde{\Phi}$ and introducing $\tilde{L} = L^{-1}$ we can also obtain

$$\text{tr}(Q_{T11} + Q_{T12}\Gamma) = \text{tr}(\tilde{Q}_{T11} + \tilde{Q}_{T12}\tilde{\Gamma}) + \text{tr}\ln(\tilde{L}_{11} + \tilde{L}_{12}\tilde{\Gamma})_t. \quad (3.32)$$

This allows us to obtain a more symmetric form of the final result. Putting everything together, we get the general result

$$\begin{aligned} & \partial_t \text{tr} \left[\int_{-\infty}^0 \tilde{R}\tilde{\Gamma}(x,t,k) dx + \int_0^{\infty} R\Gamma(x,t,k) dx \right] \\ &= \frac{1}{2} \partial_t \text{tr} \left[\ln(L_{11}(0,k) + L_{12}(0,k)\Gamma(0,t,k)) - \ln(\tilde{L}_{11}(0,k) + \tilde{L}_{12}(0,k)\tilde{\Gamma}(0,t,k)) \right] \end{aligned} \quad (3.33)$$

Now, for the problem with boundary, note that under the reduction $\tilde{R}(x,t) = R(-x,t)$, we have

$$\tilde{\Gamma}(x,t,k) = -\Gamma(-x,t,-k), \quad \text{and} \quad \tilde{L}(x,t,k) = \frac{1}{k^2 + \alpha^2} \Sigma_3 L(-x,t,-k) \Sigma_3. \quad (3.34)$$

Finally, at $x=0$, $L(0,k)$ does not depend on t for the class of boundary conditions we have derived and $L_{12}(0,k) = 0$, so that the right-hand side in (3.33) vanishes. Therefore, we have shown

$$\partial_t I(k) = 0. \quad (3.35)$$

The special form (3.26) is used to get real conserved quantities. ■

In practice, the conserved quantities are determined recursively by inserting the following expansion

$$\Gamma(x,t,k) = \sum_{n=1}^{\infty} \frac{\Gamma_n(x,t)}{(2ik)^n}, \quad (3.36)$$

into the Riccati equation to obtain

$$\Gamma_1 = -\lambda R^\dagger, \quad \Gamma_{n+1} = \Gamma_{nx} + \sum_{k=1}^{n-1} \Gamma_k R \Gamma_{n-k}, \quad n \geq 1. \quad (3.37)$$

As expected from the presence of the boundary, we see that the conserved quantities corresponding to even powers of $1/k$ do not appear. In particular, the momentum is not conserved.

3.3 Mirror image construction

Following the arguments of Remark 3.1.2, we turn now to use the formalism of the ISM on the line to describe a half-line problem. It can be done by introducing the following extended potential [50, 27]:

$$P(x, t, k) = \theta(x)Q(x, t) + \theta(-x)\mathcal{B}(k)Q(-x, t)\mathcal{B}(-k), \quad (3.38)$$

where θ is the Heaviside function— $\theta(x) = 1$ for $x \geq 0$ and $\theta(x) = 0$ for $x < 0$ —and

$$\mathcal{B}(k) \equiv \begin{pmatrix} B(k) & 0 \\ 0 & -1 \end{pmatrix} = \Sigma_3 \mathcal{L}(0, k). \quad (3.39)$$

From the form of $\mathcal{L}(0, k)$ defined in (3.24), the matrix $B(k)$ is in either of the forms

$$B(k) = \frac{k - i\alpha}{k + i\alpha}I, \quad \alpha \in \mathbb{R}, \quad \text{or} \quad B(k) = \begin{pmatrix} \sigma_1 & & \\ & \ddots & \\ & & \sigma_n \end{pmatrix}, \quad (3.40)$$

where $\sigma_j = -1$, $j \in M$ and $\sigma_j = 1$, $j \in \{1, \dots, n\} \setminus M$. It satisfies

$$B^\dagger(k^*)B(k) = I_n = B(-k)B(k), \quad k \in \mathbb{C}. \quad (3.41)$$

We call the matrix $B(k)$ *boundary matrix*, for it will be used below in the ISM scheme to represent either the Robin boundary condition (3.22) or the mixed Neumann and Dirichlet boundary condition (3.23) that we deduced previously. Now, we state the following proposition which justifies the use of P as an accurate way to describe the half-line problem we are considering.

Proposition 3.3.1 *Let P be the potential defined in (3.38), and perform the ISM for P . Then the restriction of the solutions for $x \geq 0$ are solutions of the half-line system (3.1, 3.2) in the presence of either of the boundary conditions (3.22) or (3.23).*

Proof: Half of the proof has already been established following arguments of Sec. 3.1. Precisely, in light of the "picture" depicted in Remark 3.1.2, in the ISM scheme, what we only need to access is that the extended potential P gives the same symmetry

relation as (3.25). Indeed, such relation exercises a constraint to the scattering data which are used to reconstruct soliton solutions the half-line system.

It follows from the form of $P(x, t, k)$ and $\mathcal{B}(k)$ that

$$P(-x, t, -k) = -\mathcal{B}(-k)P(x, t, k)\mathcal{B}(k). \quad (3.42)$$

Recall the Jost solutions $X(x, t, k)$ and $Y(x, t, k)$ defined in (2.15) and (2.16) respectively. Using Eq. (3.42), we obtain that $Y(x, t, k)$ and $\mathcal{B}(k)X(-x, t, -k)\mathcal{B}(-k)$ satisfy the same Volterra integral equation. Noting that they have the same asymptotic behaviors as $x \rightarrow \infty$, one gets

$$Y(x, t, k) = \mathcal{B}(k)X(-x, t, -k)\mathcal{B}(-k). \quad (3.43)$$

From this relation together with Eq. (2.24) and (2.26), we come to

$$S^{-1}(k) = WS^\dagger(k^*)W^{-1} = \mathcal{B}(k)S(-k)\mathcal{B}(-k), \quad (3.44)$$

which is the same relation as given in (3.25). The fact that both the Bäcklund matrix L and the extended potential P lead to the same relation for the scattering data ensures the equivalence of these two constructions. ■

Through the use of the extended potential P , a half-line system is nicely interpreted as a full line system with the help of the relation (3.25), which we call *mirror symmetry relation*. The boundary condition at $x = 0$ is precisely represented by the boundary matrix $B(k)$. The subtle point now is to clarify the effects of this relation on the scattering data. Since our focus is on soliton solutions, only the soliton scattering data are considered so that the restriction $\lambda = -1$ (corresponding to the focusing case) is understood. In components, Eq. (3.25) reads

$$(\mathbf{a}^+)^\dagger(k^*) = B(k)\mathbf{a}^+(-k)B(-k), \quad (\mathbf{a}^-)^*(k^*) = \mathbf{a}^-(-k), \quad (3.45)$$

$$(\mathbf{b}^-)^\dagger(k^*) = -\mathbf{b}^+(-k)B(-k), \quad (\mathbf{b}^+)^\dagger(k^*) = -B(k)\mathbf{b}^-(-k). \quad (3.46)$$

Due to the property $B^\dagger(k^*) = B(-k)$, the last two relations are consistent (by the transpose conjugate). The first relation implies that if k_j is a zero of $\det \mathbf{a}^+(k)$ then $-k_j^*$ is also a zero. The same holds true for $\mathbf{a}^-(k)$. Therefore, we find that the main observation of [27], that the relevant zeros of $\det \mathbf{a}^+(k)$ to formulate the inverse problem come in pairs, $(k_j, -k_j^*)$ is also valid in the vector case. The total number J of the zeros of $\mathbf{a}^+(k)$ in \mathbb{C}^+ is even: $J = 2N$ and there are N zeros in both quadrants of the upper half k -complex plane.

Recall the definition of scattering data introduced in Sec. 2.3, a J -soliton solution can be obtained, provided $\{k_l, \beta_l\}$, $l = 1, \dots, J$ where β_l is the norming constant associated to k_l . For convenience, the following convention (see Fig 3.1) for k_l , $l = 1, \dots, J$ as zero of $\mathbf{deta}^+(k)$ is imposed: let k_j , $j = 1, \dots, N$ be in the first quadrant of the k -complex plane *i.e.* $\text{Re}k_j \geq 0$ and $\text{Im}k_j > 0$, then the paired zero $-k_j^*$ is labelled as k_{j+N} , *i.e.*

$$k_{j+N} = -k_j^*, \quad j = 1, \dots, N. \quad (3.47)$$

Along with this convention, the following proposition specifies a relation between the corresponding norming constants.

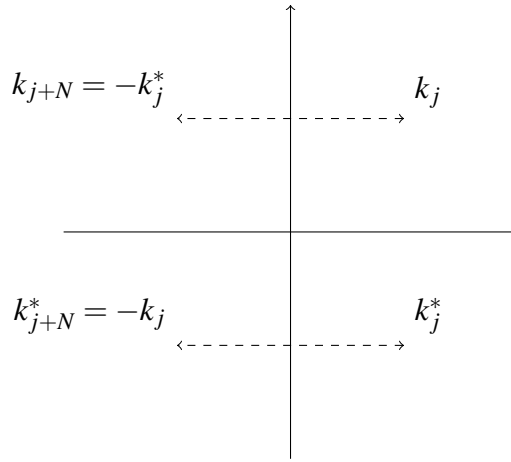


Fig. 3.1 : $2N$ zeros on the k -complex plane with $k_{j+N} = -k_j^*$, $j = 1, \dots, N$

Proposition 3.3.2 Consider the pure soliton solution for P ($\lambda = -1$, $\mathbf{b}^\pm(k) = 0$) with the scattering data $\{k_l; \beta_l\}$, $l = 1, \dots, J$ where $J = 2N$. Without loss of generality, assume that for k_j , $j = 1, \dots, N$, $\text{Re}k_j \geq 0$ and $\text{Im}k_j > 0$, and its paired zero k_{j+N} is related to k_j by Eq. (3.47). Then, the corresponding paired norming constants (β_j, β_{j+N}) , $j = 1, \dots, N$ satisfy the following relation:

$$\beta_j \beta_{j+N}^\dagger = B(k_j^*) \mathcal{A}_{j+N}, \quad j = 1, \dots, N, \quad (3.48)$$

where the matrix \mathcal{A}_{j+N} is defined in Eq. (2.71).

Proof: Taking the forms of the Jost solutions defined in (2.22) and inserting them into (2.24) and (3.43), letting $x = t = 0$ for simplicity, one gets

$$X^+(k) = Y^-(k) \mathbf{a}^+(k) + Y^+(k) \mathbf{b}^+(k), \quad (3.49)$$

$$X^-(k) = Y^+(k) \mathbf{a}^-(k) + Y^-(k) \mathbf{b}^-(k), \quad (3.50)$$

and

$$(Y^-(k), Y^+(k)) = \mathcal{B}(k) (X^+(-k)B(-k), -X^-(-k)). \quad (3.51)$$

Evaluating (3.50) and (3.51) at $k = k_j^*$ give

$$X^-(k_j^*) = Y^-(k_j^*) \mathbf{b}^-(k_j^*), \quad X^+(k_j^*) = -\mathcal{B}^{-1}(-k_j^*) Y^+(-k_j^*). \quad (3.52)$$

It follows from (3.47) and (3.49) and also the definition of the matrix \mathcal{A}_{j+N} in (2.71) that

$$X^+(-k_j^*) \mathcal{A}_{j+N} = Y^+(-k_j^*) \mathbf{b}^+(k_{j+N}) \mathcal{A}_{j+N}. \quad (3.53)$$

In addition from (3.51), one has

$$Y^-(k_j^*) = \mathcal{B}(k_j^*) X^+(-k_j^*) B(-k_j^*). \quad (3.54)$$

Reminding the definition of the norming constant β_j in (2.56) and the relation (2.72) that is: $\beta_{j+N}^\dagger = -\mathbf{b}^+(k_{j+N}) \mathcal{A}_{j+N}$, then the compatibility of (3.52 - 3.54) yields the relation (3.48). Note that there is another relation in the form

$$\beta_{j+N} \beta_j^\dagger = B(-k_j) \mathcal{A}_j, \quad j = 1, \dots, N, \quad (3.55)$$

that could be derived by evaluating (3.49 - 3.51) at $k = k_j$ and $k = -k_j$. This relation is compatible (in the sense of transpose conjugate) with (3.48). \blacksquare

The relations (3.47) and (3.48) give a complete characterization of the $2N$ -soliton scattering data $\{k_l, \beta_l\}$, $l = 1, \dots, J$, where $J = 2N$. They are indeed the consequences of the mirror symmetry relation (3.25). It is worth noting that the appearance of the matrix \mathcal{A}_{j+N} in Eq. (3.48) between the paired norming constants (β_j, β_{j+N}) , $j = 1, \dots, N$, is a consequence of the vector nature of the system. As defined in Eq. (2.71) (using dressing transformations), this matrix can be expressed in terms of all the $2N$ norming constants *i.e.* β_l , $l = 1, \dots, 2N$, involved in the system. Hence, Eq. (3.48) consists of a system of nonlinearly coupled matrix equations that one has to solve in order to completely characterize the N -soliton solutions on the half-line. This is technically more challenging in contrast to the scalar case in which (β_j, β_{j+N}) and \mathcal{A}_{j+N} are just scalar quantities [27]. In Appendix C, we show an algorithm to solve *recursively* (3.47, 3.48), provided that $\{k_j, \beta_j\}$, $j = 1, \dots, N$, are given. Therefore, N -soliton solutions on the half-line can be obtained.

3.4 Example of one-soliton reflections

We consider the pure soliton case on the half-line with $N = 1$, *i.e.*, one soliton bounces off the boundary. The scattering data are $\{k_1, k_2; \beta_1, \beta_2\}$, and according to Prop. 3.3.2 obey

$$k_2 = -k_1^*, \quad \beta_1 \beta_2^\dagger = B(k_1^*) \mathcal{A}_2. \quad (3.56)$$

Here the matrix \mathcal{A}_2 according to Eq. (2.71) is in the following form:

$$\mathcal{A}_2 = \begin{pmatrix} k_2 - k_1 \\ k_2 - k_1^* \end{pmatrix} \pi_{2,\{1\}} d_1^{-1}(k_2), \quad (3.57)$$

where

$$d_1(k) = I_n + \begin{pmatrix} k_1^* - k_1 \\ k - k_1^* \end{pmatrix} \frac{\beta_1 \beta_1^\dagger}{\beta_1^\dagger \beta_1}, \quad \pi_{2,\{1\}} = \frac{\xi_{2,\{1\}} \xi_{2,\{1\}}^\dagger}{\xi_{2,\{1\}}^\dagger \xi_{2,\{1\}}}, \quad \xi_{2,\{1\}} = d_1^\dagger(k_2) \beta_2. \quad (3.58)$$

Given $\{k_1; \beta_1\}$, it follows from direct computations (see Appendix C) that the previous relations determine uniquely $\{k_2; \beta_2\}$ as

$$k_2 = -k_1^*, \quad \beta_2 = \frac{\mathbf{v}_2}{|\mathbf{v}_2|^2}, \quad (3.59)$$

where

$$\mathbf{v}_2 = \frac{k_2 - k_1^*}{k_2 - k_1} B^\dagger(k_1) \beta_1. \quad (3.60)$$

Therefore, a one-soliton system on the half-line can be solved using the reconstruction formula (2.34) for the two-soliton scattering data $\{k_1, k_2; \beta_1, \beta_2\}$.

In the following, we present some numeric results of a two-component ($n = 2$) vector soliton on the half-line. The Robin boundary condition does not bring anything new in the vector case as compared to the scalar case in the sense that in any polarization basis, each component of \mathbf{R} always satisfies a scalar Robin boundary condition. However, in the mixed Neumann and Dirichlet case, if the polarization basis is different from the preferred boundary basis *i.e.* if we restore the unitary V matrix in (3.15), then an interesting phenomenon of reflection-transmission between the modes appears: the amplitude of the soliton envelope $|r_j(x, t)|$ is different before and after its interaction with the boundary!

As an example, we take

$$V = \begin{pmatrix} \cos \theta e^{i\zeta} & \sin \theta e^{i\zeta} \\ -\sin \theta e^{-i\zeta} & \cos \theta e^{-i\zeta} \end{pmatrix}, \quad (3.61)$$

with $\theta, \xi, \zeta \in \mathbb{R}$ and consider the boundary matrix B_V parametrized by V as

$$B_\theta = V \begin{pmatrix} 1 & 0 \\ 0 & -1 \end{pmatrix} V^{-1}. \quad (3.62)$$

The parameters θ, ζ, ξ measure the "deviation" from the natural boundary basis corresponding to $\theta = \zeta = \xi = 0$. Below are plots of $|r_1|$ and $|r_2|$ in (x, t) -space for $k_1 = 1 + \frac{i}{2}$ and $\beta_1 = \begin{pmatrix} 2 & 1 \end{pmatrix}^T$.

First, take $\theta = \zeta = \xi = 0$. Fig. 3.2 is a realization of our mirror image construction as explained in Remark 3.1.2. In Fig 3.2, the real system is defined on the positive part $x \geq 0$ of the axis whilst the negative part $x < 0$ plays the virtual role which is in a mirror symmetry to the real system. The boundary conditions are satisfied by the vector soliton field at $x = 0$ that are results of both the real and virtual systems.

In Fig. 3.3, by restricting Fig. 3.2 to $x \geq 0$, we can see that, as expected, the first mode satisfies a Neumann boundary condition while the second mode satisfies a Dirichlet boundary condition. These plots are very similar to those of [27] in each case. Each mode behaves like a scalar solution seeing its own boundary condition.

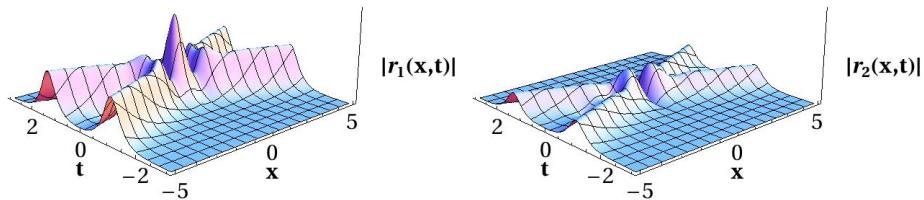


Fig. 3.2 : A two-soliton system on the line with its scattering data satisfying the mirror symmetry relations (3.47, 3.48). The mirror symmetry can be clearly seen as the positive part ($x \geq 0$) mirrors the negative part ($x \leq 0$) for both of the components r_1 and r_2 .

Then, for $\theta = \frac{\pi}{6}$ and $\zeta = \xi = 0$ (see Fig. 3.4), we clearly see that the amplitude of each mode before and after the interaction with the boundary is different. Both modes are reflected but part of mode 1 is transmitted to mode 2.

This shows that the boundary acts as some sort of polarization filter. We emphasize though that there is no loss in the transmission process in the sense that the quantity $|r_1|^2 + |r_2|^2$ is indeed a conserved density. This can be checked using the formalism developed in the next chapter in which both the incoming ($t \rightarrow -\infty$) and outgoing ($t \rightarrow \infty$) soliton solutions are explicitly computed. One may also wonder whether the boundary could be used to control the amplitudes of the modes by changing the values of the boundary parameters. This is shown in Fig. 3.5, in which

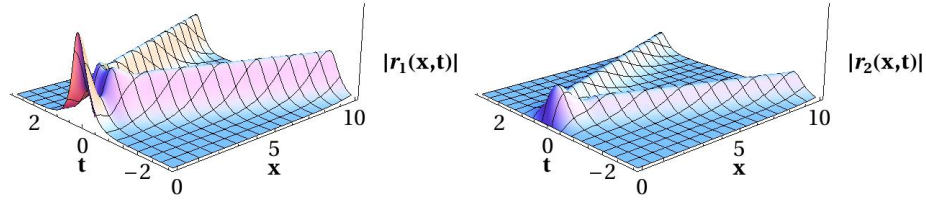


Fig. 3.3 : One soliton reflection on the half-line by restricting $x \geq 0$: the first component of the soliton on the boundary satisfies Neumann boundary condition, the second component satisfies Dirichlet boundary condition.

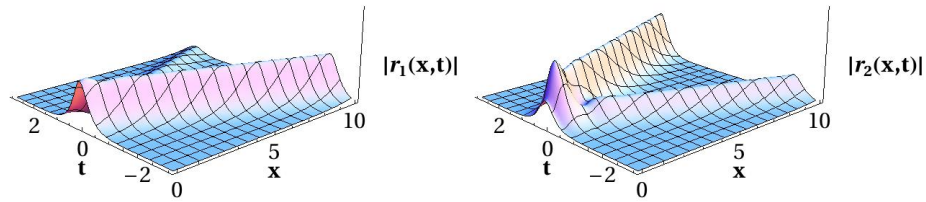


Fig. 3.4 : One soliton reflection on the half-line with $\theta = \frac{\pi}{6}$, $\zeta = \xi = 0$: the outgoing mode of the first component of the soliton has a smaller amplitude than the incoming one, while for the second component, part of the first mode has been transmitted to the outgoing mode.

we keep $k_1 = 1 + \frac{i}{2}$ and $\beta_1 = \begin{pmatrix} 2 & 1 \end{pmatrix}^T$ and vary θ from 0 to $\frac{\pi}{2}$ by fixing $\zeta = 1.11$ and $\xi = 0$.

In our example, we see that the second mode (in blue) can be made vanishingly small for $\theta \approx 1.15$. However, the total outgoing amplitude is constant (black line) and is equal to the total incoming amplitude as expected. This feature is shown in Fig. 3.6.

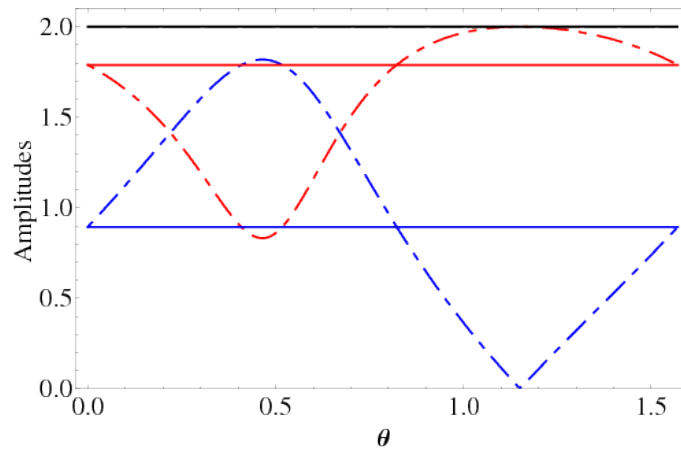


Fig. 3.5 : Amplitudes of the soliton frame as functions of θ in the reference of the maximal amplitude. The red line is the incoming $|r_1|$ amplitude. The blue line is incoming $|r_2|$. Dashed curves are the corresponding outgoing amplitudes. The black line is the total amplitude $|r_1|^2 + |r_2|^2$.

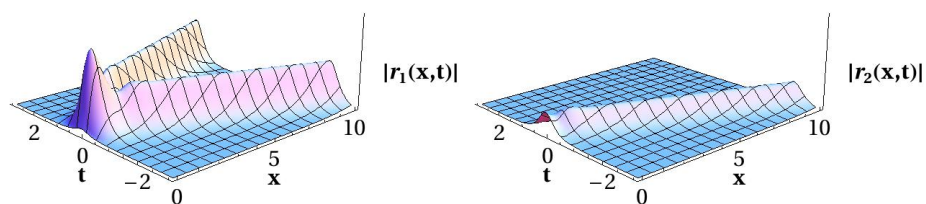


Fig. 3.6 : One soliton reflection on the half-line with $\theta \approx 1.15$, $\zeta = 1.11$ and $\xi = 0$: the first component of the soliton is maximally enhanced after interacting with the boundary, while the second component becomes vanishingly small.

Factorization of soliton-soliton and soliton-boundary interactions

Factorization property is at the heart of understanding integrable system, and it is widely believed that integrability reveals factorization, and vice versa (see *e.g.* [126] for the factorization involving in quantum integrable theories). In the context of soliton models, however, the factorization of a multi-component solitons' interaction was fully clarified only recently in [63, 64, 35] for the matrix KdV equation and in [111, 9] for the vector NLS equation, despite the fact that the ISM for the multi-component soliton models has been well developed since the early work by Manakov [87]. As mentioned in the Introduction, such factorization is understood by virtue of Yang-Baxter maps that are solutions of the set-theoretical Yang-Baxter equation.

In this chapter we study the behaviors of the vector NLS solutions both on the line and on the half-line, in order to track the factorization of both the soliton-soliton and soliton-boundary interactions. By considering only soliton solutions, the focusing case of the vector NLS equation ($\lambda = -1$ in Eq. (2.2)) is understood. First, we discuss the factorization of an N -soliton system. This is followed by representing soliton-soliton interactions as Yang-Baxter maps as pointed out in [111, 64, 9]. In addition, in the previous chapter we have completely characterized the vector NLS solitons on the half-line with an integrable boundary. This strongly suggests that the factorization property is underlying the half-line soliton system as well. Indeed, following our (mirror image) construction (see Remark 3.1.2), a soliton-boundary interaction can be "unsurprisingly" described as a map, which together with the Yang-Baxter maps, satisfy the set-theoretical reflection equation that we briefly introduced in Introduction. These topics comprise the content of the second section in this chapter. Note that these results are reported in [38].

4.1 Factorization of N -soliton interactions

Collecting results of Chapter 2, we are ready here to analyze the factorization of the interactions of vector solitons. This question has already been addressed in [111, 9] through two different angles: in [111], such factorization is shown by means of an involved direct computation from the N -soliton solution; in [9], two-soliton collisions are characterized by means of a Yang-Baxter map [113]. However, we stress that our approach differs from [111, 9] in a number of important respects. Indeed, dressing transformations and, in particular, Theorem 2.2.7 are used in our case to extract directly soliton interactions from an N -soliton configuration. Such interactions can be formulated as Yang-Baxter maps and the factorization can be seen as an "a priori" consequence of the N -soliton construction itself. This is in contrast with [9] in which the Yang-Baxter map was only established from a two-soliton solution and the factorization was then discussed based on the Yang-Baxter property. The alternative approach of [111] took the N -soliton configuration into account, but the discussions about factorization can be only seen as "a posteriori" checks that the asymptotic N -soliton solutions as $t \rightarrow \pm\infty$ obtained with the ISM are consistent.

To make the discussion more concrete, recall the general form of a one-soliton solution as characterized in (2.65). Now, consider the N -soliton solution corresponding to

$$k_j = \frac{1}{2}(u_j + iv_j), v_j > 0 \quad , \quad j = 1, \dots, N, \quad (4.1)$$

with the associated norming constants β_j . Let $w_j \equiv -2u_j$ representing the j th soliton, then the following proposition shows that as $t \rightarrow \pm\infty$, an N -soliton solution looks like the sum of N one-soliton solutions up to exponentially vanishing terms.

Proposition 4.1.1 *Suppose without loss of generality that $u_1 < u_2 < \dots < u_N$. Denote $R^{in}(x, t)$ (resp. $R^{out}(x, t)$) the asymptotic solution $R(x, t)$ corresponding to $t \rightarrow -\infty$ (resp. $t \rightarrow \infty$). Then,*

$$R^{in/out}(x, t) = \sum_{j=1}^N \mathbf{p}_j^{in/out} v_j \frac{e^{-i(u_j x + (u_j^2 - v_j^2)t)}}{\cosh(v_j(x - w_j t - \Delta x_j^{in/out}))} + \mathcal{O}(e^{-v\tilde{w}|t|}). \quad (4.2)$$

Here $v = \min_j v_j$, $\tilde{w} = \min_{l \neq j} |w_l - w_j|$, $\Delta x_j^{in/out} = \frac{\ln |\beta_j^{in/out}|}{v_j}$ and $\mathbf{p}_j^{in/out} = \frac{\beta_j^{in/out}}{|\beta_j^{in/out}|}$ with p

$$\beta_j^{in} = \left(\prod_{\ell=1}^{j-1} \frac{k_j^* - k_\ell}{k_j^* - k_\ell^*} \right) d_{j+1 \dots N}^\dagger(k_j) \beta_j, \quad \beta_j^{out} = \left(\prod_{\ell=j+1}^N \frac{k_j^* - k_\ell}{k_j^* - k_\ell^*} \right) d_{1 \dots j-1}^\dagger(k_j) \beta_j, \quad (4.3)$$

where $d_{i_1 \dots i_\ell}(k)$ are defined in Chapter 2.

Proof: We follow the idea of the scalar case [47] which is based on the evaluation of the projectors $\Pi_{j,\{1\dots j-1\}}(x,t)$ as $t \rightarrow \pm\infty$. To get the result, it is enough to show that $R(x,t)$ approaches the one-soliton solution following the trajectory of a particular soliton l i.e. $x - w_\ell t = \text{constant}$, and that it vanishes exponentially for all other directions in the (x,t) -plane. But here in the vector case, Theorem 2.2.7 is crucial and allows us to write the dressing factor in the following form

$$D_{1\dots N} = D_1 \dots D_{\ell-1, \{1\dots\ell-2\}} D_{\ell+1, \{1\dots\ell-1\}} \dots D_{N, \{1\dots\ell\dots N-1\}} D_{\ell, \{1\dots\ell\dots N\}}, \quad (4.4)$$

where the notation $\{1\dots\hat{\ell}\dots j\}$ means that ℓ is not listed in $\{1\dots j\}$. This means that $D_{\ell, \{1\dots\hat{\ell}\dots N\}}$ is the last dressing factor added. Then, recalling (2.59, 2.60), one obtains for $x - w_\ell t = \text{constant}$ as $t \rightarrow -\infty$

$$D_1 \dots D_{N, \{1\dots\hat{\ell}\dots N-1\}}(x, t, k) = \begin{pmatrix} d_{\ell+1\dots N}(k) & 0 \\ 0 & \prod_{j=1}^{\ell-1} \begin{pmatrix} k-k_j \\ k-k_j^* \end{pmatrix} \end{pmatrix} + O(e^{-v\tilde{w}|t|}), \quad (4.5)$$

whereas for all other directions, the same calculation yields $O(e^{-v\tilde{w}|t|})$. Consequently,

$$\zeta_{\ell, \{1\dots\hat{\ell}\dots N\}}(x, t) = \begin{pmatrix} d_{\ell+1\dots N}^\dagger(k_\ell) & 0 \\ 0 & \prod_{j=1}^{\ell-1} \begin{pmatrix} k_\ell^* - k_j^* \\ k_\ell^* - k_j \end{pmatrix} \end{pmatrix} e^{-i\phi(x, t, k_\ell^*)\Sigma_3} \begin{pmatrix} \beta_\ell \\ -1 \end{pmatrix} + O(e^{-v\tilde{w}|t|}), \quad (4.6)$$

and the reconstruction formula (2.61) implies

$$Q(x, t) = i(k_\ell - k_\ell^*) \left[\Sigma_3, \frac{\zeta_{\ell, \{1\dots\hat{\ell}\dots N\}}^\dagger \zeta_{\ell, \{1\dots\hat{\ell}\dots N\}}(x, t)}{\zeta_{\ell, \{1\dots\hat{\ell}\dots N\}}^\dagger \zeta_{\ell, \{1\dots\hat{\ell}\dots N\}}(x, t)} \right]. \quad (4.7)$$

Direct calculation then gives for $x - w_\ell t = \text{constant}$ as $t \rightarrow -\infty$

$$R(x, t) = \mathbf{p}_\ell^{in} v_\ell \frac{e^{-i(u_\ell x + (u_\ell^2 - v_\ell^2)t)}}{\cosh(v_\ell(x - w_\ell t - \Delta x_\ell^{in}))} + O(e^{-v\tilde{w}|t|}), \quad (4.8)$$

with the various parameters being defined in the proposition. The same technique can be applied as $t \rightarrow \infty$ to obtain $R^{out}(x, t)$. \blacksquare

In Prop. 4.1.1, the quantity $\Delta x_j^{out} - \Delta x_j^{in}$ represents the total position shift incurred by soliton j through its collisions with the other solitons. The unit vector $\mathbf{p}_j^{in/out}$ represents the asymptotic polarization vector of soliton j before and after all its collisions with the other solitons. These quantities are independent of the order of soliton collisions, and this fact is indeed the factorization property.

Remark 4.1.2 *The order $u_1 < \dots < u_N$ means that the relative velocity $w_j - w_{j+1}$ of two consecutive solitons is always positive. Consequently, as $t \rightarrow -\infty$, the solitons are distributed along the x -axis in the order $1, 2, \dots, N$. The picture is reversed as $t \rightarrow \infty$. The relative positions of the solitons are therefore completely determined as $t \rightarrow \pm\infty$.*

Remark 4.1.3 *Using Theorem 2.2.7, we could have performed the proof analogously but choosing any permutation placing i_ℓ at position N hence giving*

$$D_{i_1} \cdots D_{i_{\ell-1}, \{i_1 \dots i_{\ell-2}\}} D_{i_\ell, \{i_1 \dots i_{\ell-1}\}} \cdots D_{i_{N-1}, \{i_1 \dots i_{N-2}\}} D_{i_\ell, \{i_1 \dots i_{N-1}\}}$$

instead of (4.4). This corresponds to the possibility that the soliton collisions can occur in a different order since we do not know their relative positions at an arbitrary time t . However, the final result for $\beta_j^{in/out}$ would be the same. This is the essence of the factorization property. It turns out that this can be made precise by assigning an intermediate time polarization vector to each soliton and by considering the effect of a two-soliton collision within an N -soliton solution on the assigned polarization vectors. The map between the polarization vectors before and after the two-soliton collision is a Yang-Baxter map satisfying the set-theoretical Yang-Baxter equation. The mathematical translation of the factorization property of collisions is therefore an associativity property of the operation on polarization vectors given by the Yang-Baxter map.

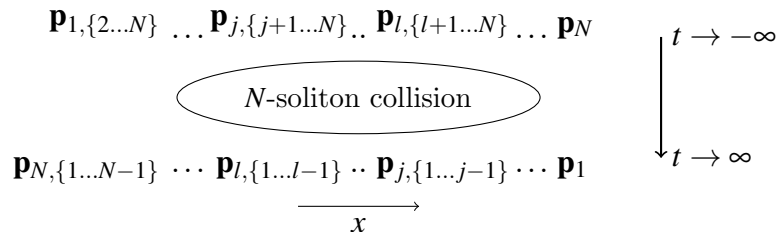
To complete the argument and finish the proof of the claims in the previous remarks, we define the following intermediate time polarization vectors. Let

$$\mathcal{Y}_{i_j, \{i_{j+1} \dots i_N\}} = \left(\prod_{\ell=i_1}^{i_{j-1}} \frac{k_{i_j}^* - k_\ell}{k_{i_j}^* - k_\ell^*} \right) d_{i_{j+1} \dots i_N}^\dagger(k_{i_j}) \beta_{i_j}, \quad (4.9)$$

and

$$\mathbf{p}_{i_j, \{i_{j+1} \dots i_N\}} = \frac{\mathcal{Y}_{i_j, \{i_{j+1} \dots i_N\}}}{|\mathcal{Y}_{i_j, \{i_{j+1} \dots i_N\}}|}. \quad (4.10)$$

So in particular, $\mathbf{p}_j^{in} = \mathbf{p}_{j, \{j+1 \dots N\}}$ and $\mathbf{p}_j^{out} = \mathbf{p}_{j, \{1 \dots j-1\}}$ and they can be pictorially represented as



We can now formulate the following important lemma.

Lemma 4.1.4 *Choose k_j and k_l and assume $u_j < u_l$. Write for convenience $i_\rho = i_1 \dots i_q$ for some $q \in \{1, \dots, N\}$ such that j and l are not in $\{i_1, \dots, i_q\}$. Then*

$$\mathbf{p}_{l, \{j i_\rho\}} = \Xi_{lj}^{-1} \left(\frac{k_l - k_j^*}{k_l - k_j} \right) \left(I_n + \left(\frac{k_j - k_j^*}{k_l - k_j} \right) \mathbf{p}_{j, \{l i_\rho\}} (\mathbf{p}_{j, \{l i_\rho\}})^\dagger \right) \mathbf{p}_{l, \{i_\rho\}}, \quad (4.11)$$

$$\mathbf{p}_{j, \{i_\rho\}} = \Xi_{lj}^{-1} \left(\frac{k_j^* - k_l^*}{k_j^* - k_l^*} \right) \left(I_n + \left(\frac{k_j^* - k_l}{k_j^* - k_l^*} \right) \mathbf{p}_{l, \{i_\rho\}} (\mathbf{p}_{l, \{i_\rho\}})^\dagger \right) \mathbf{p}_{j, \{l i_\rho\}}, \quad (4.12)$$

where

$$\Xi_{lj}^2 = \left| \left(\frac{k_l^* - k_j}{k_l^* - k_j^*} \right) \right|^2 \left(1 + \left(\frac{(k_j^* - k_j)(k_l - k_l^*)}{|k_l - k_j|^2} \right) |p_{jl, \{i_\rho\}}|^2 \right), \quad p_{jl, \{i_\rho\}} = \mathbf{p}_{l, \{i_\rho\}}^\dagger \mathbf{p}_{j, \{l i_\rho\}}. \quad (4.13)$$

Proof: From (4.9), we have

$$\gamma_{j, \{i_\rho\}} = \prod_{p \in \{1 \dots N\} \setminus \{j, i_\rho\}} \left(\frac{k_j^* - k_p}{k_j^* - k_p^*} \right) d_{i_\rho}^\dagger(k_j) \beta_j, \quad \gamma_{j, \{l i_\rho\}} = \prod_{p \in \{1 \dots N\} \setminus \{j, l, i_\rho\}} \left(\frac{k_j^* - k_p}{k_j^* - k_p^*} \right) d_{l i_\rho}^\dagger(k_j) \beta_j, \quad (4.14)$$

$$\gamma_{l, \{i_\rho\}} = \prod_{p \in \{1 \dots N\} \setminus \{l, i_\rho\}} \left(\frac{k_l^* - k_p}{k_l^* - k_p^*} \right) d_{i_\rho}^\dagger(k_l) \beta_l, \quad \gamma_{l, \{j i_\rho\}} = \prod_{p \in \{1 \dots N\} \setminus \{l, j, i_\rho\}} \left(\frac{k_l^* - k_p}{k_l^* - k_p^*} \right) d_{j i_\rho}^\dagger(k_l) \beta_l. \quad (4.15)$$

The relation between $d_{i_\rho}^\dagger$ and $d_{j i_\rho}^\dagger$ implies that

$$\gamma_{j, \{l i_\rho\}} = \left(\frac{k_j^* - k_l^*}{k_j^* - k_l} \right) \left(I_n + \left(\frac{k_l - k_l^*}{k_j^* - k_l} \right) \mathbf{p}_{l, \{i_\rho\}} \mathbf{p}_{l, \{i_\rho\}}^\dagger \right) \gamma_{j, \{i_\rho\}}, \quad (4.16)$$

$$\gamma_{l, \{j i_\rho\}} = \left(\frac{k_l^* - k_j^*}{k_l^* - k_j} \right) \left(I_n + \left(\frac{k_j - k_j^*}{k_l^* - k_j} \right) \mathbf{p}_{j, \{i_\rho\}} \mathbf{p}_{j, \{i_\rho\}}^\dagger \right) \gamma_{l, \{i_\rho\}}. \quad (4.17)$$

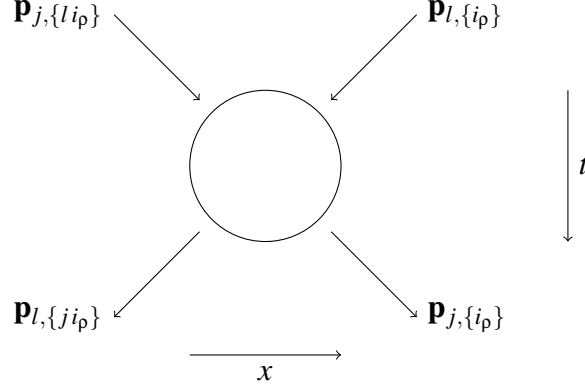
Introduce

$$\Xi_{lj} = \frac{|\gamma_{j, \{i_\rho\}}|}{|\gamma_{j, \{l i_\rho\}}|}. \quad (4.18)$$

Inserting this into (4.16, 4.17) yields (4.11, 4.12) by direct calculations. \blacksquare

Remark 4.1.5 *The relations defined in Lemma 4.1.4 have a natural interpretation as an intermediate time pairwise collision between soliton j and soliton l . Since $w_j > w_l$ ($u_j < u_l$), after a certain number of collisions with other solitons (related to*

the set $\{i_\rho\}$), soliton j with polarization $\mathbf{p}_{j,\{i_\rho\}}$ overtakes soliton l with polarization $\mathbf{p}_{l,\{i_\rho\}}$ and acquires polarization $\mathbf{p}_{j,\{i_\rho\}}$ while soliton l has then polarization $\mathbf{p}_{l,\{j_\rho\}}$. Pictorially, this can be represented as



We complete the discussion by rewriting the relations in Lemma 4.1.4 in terms of the following map acting on $\mathbb{C}\mathbb{P}^{n-1} \times \mathbb{C}\mathbb{P}^{n-1}$ onto itself (so that the normalizations in (4.11), (4.12) are irrelevant)

$$\mathcal{R}(k_1, k_2) : (\mathbf{p}_1^{(i)}, \mathbf{p}_2^{(i)}) \mapsto (\mathbf{p}_1^{(ii)}, \mathbf{p}_2^{(ii)}), \quad (4.19)$$

$$\mathbf{p}_1^{(ii)} = \left(I_n + \left(\frac{k_2^* - k_2}{k_1^* - k_2^*} \right) \frac{\mathbf{p}_2^{(i)} (\mathbf{p}_2^{(i)})^\dagger}{(\mathbf{p}_2^{(i)})^\dagger \mathbf{p}_2^{(i)}} \right) \mathbf{p}_1^{(i)}, \quad (4.20)$$

$$\mathbf{p}_2^{(ii)} = \left(I_n + \left(\frac{k_1 - k_1^*}{k_2 - k_1} \right) \frac{\mathbf{p}_1^{(i)} (\mathbf{p}_1^{(i)})^\dagger}{(\mathbf{p}_1^{(i)})^\dagger \mathbf{p}_1^{(i)}} \right) \mathbf{p}_2^{(i)}. \quad (4.21)$$

Then, one finds that the map $\mathcal{R}(k_1, k_2)$ is a reversible (parametric) Yang-Baxter map [113] i.e. it satisfies

$$\mathcal{R}_{12}(k_1, k_2) \mathcal{R}_{13}(k_1, k_3) \mathcal{R}_{23}(k_2, k_3) = \mathcal{R}_{23}(k_2, k_3) \mathcal{R}_{13}(k_1, k_3) \mathcal{R}_{12}(k_1, k_2), \quad (4.22)$$

and

$$\mathcal{R}_{21}(k_2, k_1) \mathcal{R}(k_1, k_2) = Id. \quad (4.23)$$

The rewriting of relations between polarization vectors as a Yang-Baxter map is the basis of the argument in [9]. However, we obtained the Yang-Baxter maps in complete generality for arbitrary polarization vectors within a full N -soliton solution and not just from the two-soliton solution. This is similar in spirit to the approach by Tsuchida in [111] but again with the importance difference that here, this was made possible by our a priori derivation of Theorem 2.2.7 about dressing factors,

instead of an a posteriori derivation from the explicit N -soliton solution. We then recover the following result originally formulated in [111]

Theorem 4.1.6 *An N -soliton collision in the Manakov model can be factorized into a nonlinear superposition of $\binom{N}{2}$ pairwise collisions in arbitrary order.*

4.2 Factorization of N -soliton reflections

We are now ready to discuss the factorization of an N -soliton reflection on the half-line using the arguments of the previous section. Recall our construction of N -soliton reflections: an N -soliton solution on the half-line can be obtained as the restriction $x \geq 0$ of a $2N$ -soliton solution of the vector NLS equation on the full line provided that the norming constants β_j and the singular points k_j obey the mirror symmetry relations (3.47, 3.48) depending on the boundary matrix $B(k)$ defined in (3.40, 3.41).

To fix ideas, consider $k_j = \frac{1}{2}(u_j + iv_j)$, $v_j > 0$, $j = 1, \dots, 2N$ and assume that

$$u_j > 0, \quad j = 1, \dots, N \quad \text{and} \quad u_1 < u_2 < \dots < u_N. \quad (4.24)$$

This corresponds to the situation where solitons 1 to N are the *real* solitons (on $x \geq 0$) and the solitons $N+1$ to $2N$ are the *mirror* solitons (on $x < 0$) as $t \rightarrow -\infty$. The real solitons have negative velocities so they evolve towards the boundary where they meet their "mirrored" solitons which then become the real solitons. The net result when restricted to $x \geq 0$ is that N solitons interact with the boundary and bounce back. This looks like

$$\begin{array}{l} 2N, 2N-1, \dots, N+1 \mid 1, 2, \dots, N, \quad t \rightarrow -\infty, \\ N, N-1, \dots, 1 \mid N+1, N+2, \dots, 2N, \quad t \rightarrow \infty, \end{array}$$

where the vertical bar represents the boundary.

Proposition 4.2.1 *Consider $2N$ polarization vectors as defined in (4.9, 4.10). Let $\{i_1 \dots i_N\}$ be a permutation of $\{1 \dots N\}$ and $\{k_{i_j}, k_{i_j+N}; \beta_{i_j}, \beta_{i_j+N}\}_{j \in \{1 \dots N\}}$ be the paired scattering data satisfying the following mirror symmetry relations:*

$$k_{i_j+N} = -k_{i_j}^*, \quad \beta_{i_j} \beta_{i_j+N}^\dagger = B(k_{i_j}^*) \mathcal{A}_{i_j+N}. \quad (4.25)$$

Then the following relations hold

$$\mathbf{p}_{i_j+N, \{i_1 \dots i_N i_1+N \dots i_{j-1}+N\}} = \bar{B}(k_{i_j}) \mathbf{p}_{i_j, \{i_{j+1} \dots i_N\}}, \quad (4.26)$$

with the $n \times n$ matrix function $\bar{B}(k)$ defined as

$$\bar{B}(k) = \left(\frac{(k - i\alpha)|k + i\alpha|}{|k - i\alpha|(k + i\alpha)} \right) I_n, \quad \alpha \in \mathbb{R}, \quad \text{or} \quad \bar{B}(k) = \begin{pmatrix} \sigma_1 & & \\ & \ddots & \\ & & \sigma_n \end{pmatrix}, \quad (4.27)$$

where $\sigma_p = 1$, $p \in M$ and $\sigma_q = -1$, $q \in \{1 \dots n\} \setminus M$ with M being a nonempty subset of $\{1, \dots, n\}$. In particular,

$$\mathbf{p}_{j+N, \{1 \dots N\}} = \bar{B}(k_j) \mathbf{p}_{j, \{1 \dots \hat{j} \dots N\}}. \quad (4.28)$$

Here the matrix $\bar{B}(k)$ is the normalized boundary matrix. The proof is long and is given in Appendix D. Let us look at these relations from the soliton collision viewpoint. As $t \rightarrow -\infty$, the polarization vectors are ordered as follows along the x -axis

$$\mathbf{p}_{2N, \{1 \dots 2N-1\}}, \mathbf{p}_{2N-1, \{1 \dots 2N-2\}}, \dots, \mathbf{p}_{N+1, \{1 \dots N\}} \left| \mathbf{p}_{1, \{2 \dots N\}}, \mathbf{p}_{2, \{3 \dots N\}}, \dots, \mathbf{p}_N, \quad t \rightarrow -\infty.$$

By applying (4.26), this becomes

$$\bar{B}(k_N) \mathbf{p}_N, \dots, \bar{B}(k_2) \mathbf{p}_{2, \{3 \dots N\}}, \bar{B}(k_1) \mathbf{p}_{1, \{2 \dots N\}} \left| \mathbf{p}_{1, \{2 \dots N\}}, \mathbf{p}_{2, \{3 \dots N\}}, \dots, \mathbf{p}_N, \quad t \rightarrow -\infty.$$

In fact, (4.26) shows that this picture extends to all intermediate-time polarization vectors. Therefore, any pairwise collision between soliton i_l and i_j , described by the Yang-Baxter map $\mathcal{R}_{i_l i_j}(k_{i_l}, k_{i_j})$, is accompanied by a simultaneous pairwise collision between solitons $i_j + N$ and $i_l + N$ described by $\mathcal{R}_{i_j+N i_l+N}(k_{i_j+N}, k_{i_l+N})$, and vice versa.

Consider now the situation evolving from $t \rightarrow -\infty$. After a certain number of pairwise collisions, soliton j is next to the boundary and the pairwise collision that is to take place is given by $\mathcal{R}_{j+N j}(k_{j+N}, k_j)$. The map $\mathcal{R}_{j+N j}(k_{j+N}, k_j)$, which means the interaction between solitons j and its "mirrored" counterpart $j + N$, can be naturally interpreted as a map of soliton j interacting with the boundary. After this interaction, soliton $j + N$, now playing the role of the reflected soliton j , undergoes general pairwise collisions of the form $\mathcal{R}_{j+N l}(k_{j+N}, k_l)$ with the remaining real solitons and $\mathcal{R}_{q+N j+N}(k_{q+N}, k_{j+N})$ for certain solitons $q + N$ that travel faster than itself.

Having the picture of how the $2N$ -soliton system evolving in time as discussed previously, we are now in the position to characterize the soliton-boundary interactions. They are precisely described by the map $\mathcal{R}_{j+N j}(k_{j+N}, k_j)$, $j = 1, \dots, N$, which,

according to (4.20, 4.21), is in the form

$$\mathbf{p}_{j+N}^{(ii)} = \left(I_n + \left(\frac{k_j^* - k_j}{k_{j+N}^* - k_j^*} \right) \frac{\mathbf{p}_j^{(i)} (\mathbf{p}_j^{(i)})^\dagger}{(\mathbf{p}_j^{(i)})^\dagger \mathbf{p}_j^{(i)}} \right) \mathbf{p}_{j+N}^{(i)}, \quad (4.29)$$

$$\mathbf{p}_j^{(ii)} = \left(I_n + \left(\frac{k_{j+N} - k_{j+N}^*}{k_j - k_{j+N}} \right) \frac{\mathbf{p}_{j+N}^{(i)} (\mathbf{p}_{j+N}^{(i)})^\dagger}{(\mathbf{p}_{j+N}^{(i)})^\dagger \mathbf{p}_{j+N}^{(i)}} \right) \mathbf{p}_j^{(i)}, \quad (4.30)$$

where the states (i) and (ii) are respectively the states before and after the interaction between the solitons j and $j+N$. For the sake of simplicity, we drop the complicated soliton-dependence that is represented by a certain subscript $\{\dots\}$. Thanks to the mirror symmetry (4.25) and its consequence (4.28), one has $(\mathbf{p}_{j+N}^{(ii)}, k_{j+N})$, that is the outgoing soliton bouncing off from the boundary, in the form

$$\mathbf{p}_{j+N}^{(ii)} = \left(I_n + \left(\frac{k_j - k_j^*}{k_j + k_j^*} \right) \frac{\mathbf{p}_j^{(i)} (\mathbf{p}_j^{(i)})^\dagger}{(\mathbf{p}_j^{(i)})^\dagger \mathbf{p}_j^{(i)}} \right) \bar{B}(k) \mathbf{p}_j^{(i)}, \quad k_{j+N} = -k_j^*. \quad (4.31)$$

This relation is in terms of k_j and $\mathbf{p}_j^{(i)}$, that represent the incoming soliton before hitting the boundary with the boundary matrix $\bar{B}(k)$ being involved. This is the map of soliton-boundary interactions.

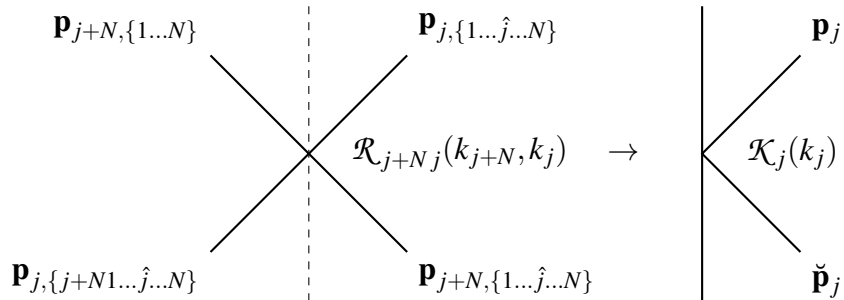
We can now define the following map from $\mathbb{C}\mathbb{P}^{n-1} \times (\mathbb{C} \setminus i\mathbb{R})$ to itself that describes the change of the polarization vector of a soliton when it interacts with the boundary:

$$\mathcal{K}: (\mathbf{p}, k) \mapsto (\check{\mathbf{p}}, -k^*), \quad (4.32)$$

where

$$\check{\mathbf{p}} = \left(I_n + \left(\frac{k - k^*}{k + k^*} \right) \frac{\mathbf{p}\mathbf{p}^\dagger}{\mathbf{p}^\dagger \mathbf{p}} \right) \bar{B}(k) \mathbf{p}. \quad (4.33)$$

Clearly, this relation is in a similar form to (4.31). Pictorially, this correspond to



We have (\mathbf{p}, k) and $(\check{\mathbf{p}}, -k^*)$ representing the soliton before and after interacting with the boundary respectively. For convenience, we introduce a parametric notation for

such map: $\mathcal{K}(k)$ acting only on vector \mathbf{p} . Its action on a multiplet of vectors can be seen as

$$\mathcal{K}_j(k_j) : (\mathbf{p}_1, \dots, \mathbf{p}_j, \dots, \mathbf{p}_N) \mapsto (\mathbf{p}_1, \dots, \check{\mathbf{p}}_j, \dots, \mathbf{p}_N). \quad (4.34)$$

We are now ready to state the following theorem that guarantees the factorization property of the soliton interactions with a boundary by virtue of the set-theoretical reflection equation. We call its solutions *reflection maps* and such object will be the focus of Part II of this thesis.

Theorem 4.2.2 *Consider the Yang-Baxter map $\mathcal{R}_j(k_l, k_j)$ defined in (4.19 - 4.21) and $\mathcal{K}_j(k_j)$ in (4.32 - 4.34). Then the following (parametric) set theoretical reflection equation holds as an identity of maps on $\mathbb{C}\mathbb{P}^{n-1} \times \mathbb{C}\mathbb{P}^{n-1}$*

$$\begin{aligned} \mathcal{K}_1(k_1) \mathcal{R}_{21}(-k_2^*, k_1) \mathcal{K}_2(k_2) \mathcal{R}_{12}(k_1, k_2) = \\ \mathcal{R}_{21}(-k_2^*, -k_1^*) \mathcal{K}_2(k_2) \mathcal{R}_{12}(-k_1^*, k_2) \mathcal{K}_1(k_1). \end{aligned} \quad (4.35)$$

We call $\mathcal{K}(k)$ (parametric) reflection map. It satisfies the following involutive property:

$$\mathcal{K}(-k^*) \mathcal{K}(k) = Id. \quad (4.36)$$

Proof: The involutive property can be found by direct calculation from the definition of the reflection map. For the set-theoretical reflection equation, we use the set theoretical Yang-Baxter equation together with our mirror image construction. Take k_j and $k_{j+2} = -k_j^*$, $j = 1, 2$. Since pairwise collision occurs simultaneously on each side of the boundary, there are only 2 possible configurations of collisions and they are identical using the Yang-Baxter equation

$$\begin{aligned} \mathcal{R}_{31}(k_1, k_3) \mathcal{R}_{32}(k_3, k_2) \mathcal{R}_{41}(k_4, k_1) \mathcal{R}_{42}(k_4, k_2) \mathcal{R}_{43}(k_4, k_3) \mathcal{R}_{12}(k_1, k_2) = \\ \mathcal{R}_{43}(k_4, k_3) \mathcal{R}_{12}(k_1, k_2) \mathcal{R}_{42}(k_4, k_2) \mathcal{R}_{32}(k_4, k_2) \mathcal{R}_{41}(k_4, k_1) \mathcal{R}_{31}(k_3, k_1). \end{aligned} \quad (4.37)$$

Consider now the following sequence of pairwise collisions

$$\begin{aligned} & \mathcal{R}_{31}(k_3, k_1) \mathcal{R}_{32}(k_3, k_2) \mathcal{R}_{41}(k_4, k_1) \mathcal{R}_{42}(k_4, k_2) \mathcal{R}_{43}(k_4, k_3) \mathcal{R}_{12}(k_1, k_2) (\mathbf{p}_1^{(i)}, \mathbf{p}_2^{(i)}, \mathbf{p}_3^{(i)}, \mathbf{p}_4^{(i)}) \\ &= \mathcal{R}_{31}(k_3, k_1) \mathcal{R}_{32}(k_3, k_2) \mathcal{R}_{41}(k_4, k_1) \mathcal{R}_{42}(k_4, k_2) (\mathbf{p}_1^{(ii)}, \mathbf{p}_2^{(ii)}, \mathbf{p}_3^{(ii)}, \mathbf{p}_4^{(ii)}) \\ &= \mathcal{R}_{31}(k_3, k_1) \mathcal{R}_{32}(k_3, k_2) \mathcal{R}_{41}(k_4, k_1) (\mathbf{p}_1^{(iii)}, \mathbf{p}_2^{(iii)}, \mathbf{p}_3^{(iii)}, \mathbf{p}_4^{(iii)}) \\ &= \mathcal{R}_{31}(k_3, k_1) (\mathbf{p}_1^{(iv)}, \mathbf{p}_2^{(iv)}, \mathbf{p}_3^{(iv)}, \mathbf{p}_4^{(iv)}) \\ &= (\mathbf{p}_1^{(v)}, \mathbf{p}_2^{(v)}, \mathbf{p}_3^{(v)}, \mathbf{p}_4^{(v)}), \end{aligned} \quad (4.38)$$

with $(\mathbf{p}_1^{(i)}, \mathbf{p}_2^{(i)}, \mathbf{p}_3^{(i)}, \mathbf{p}_4^{(i)})$ being the initial polarization vectors and $(\mathbf{p}_1^{(v)}, \mathbf{p}_2^{(v)}, \mathbf{p}_3^{(v)}, \mathbf{p}_4^{(v)})$ the final polarization vectors. Similarly, consider the following sequence of soliton-soliton and soliton-boundary collisions

$$\begin{aligned}
& \mathcal{K}_1(k_1) \mathcal{R}_{21}(-k_2^*, k_1) \mathcal{K}_2(k_2) \mathcal{R}_{12}(k_1, k_2) (\mathbf{q}_1^{(i)}, \mathbf{q}_2^{(i)}) \\
&= \mathcal{K}_1(k_1) \mathcal{R}_{21}(-k_2^*, k_1) \mathcal{K}_2(k_2) (\mathbf{q}_1^{(ii)}, \mathbf{q}_2^{(ii)}) \\
&= \mathcal{K}_1(k_1) \mathcal{R}_{21}(-k_2^*, k_1) (\mathbf{q}_1^{(iii)}, \mathbf{q}_2^{(iii)}) \\
&= \mathcal{K}_1(k_1) (\mathbf{q}_1^{(iv)}, \mathbf{q}_2^{(iv)}) \\
&= (\mathbf{q}_1^{(v)}, \mathbf{q}_2^{(v)}). \tag{4.39}
\end{aligned}$$

We claim now that if $(\mathbf{q}_1^{(i)}, \mathbf{q}_2^{(i)}) = (\mathbf{p}_1^{(i)}, \mathbf{p}_2^{(i)})$, then $(\mathbf{q}_1^{(v)}, \mathbf{q}_2^{(v)}) = (\mathbf{p}_3^{(v)}, \mathbf{p}_4^{(v)})$. From (4.38) and (4.39), we have

$$\mathbf{p}_1^{(ii)} = \left(I_n + \left(\frac{k_2^* - k_2}{k_1^* - k_2^*} \right) \frac{\mathbf{p}_2^{(i)} (\mathbf{p}_2^{(i)})^\dagger}{(\mathbf{p}_2^{(i)})^\dagger \mathbf{p}_2^{(i)}} \right) \mathbf{p}_1^{(i)}, \tag{4.40}$$

$$\mathbf{q}_1^{(ii)} = \left(I_n + \left(\frac{k_2^* - k_2}{k_1^* - k_2^*} \right) \frac{\mathbf{q}_2^{(i)} (\mathbf{q}_2^{(i)})^\dagger}{(\mathbf{q}_2^{(i)})^\dagger \mathbf{q}_2^{(i)}} \right) \mathbf{q}_1^{(i)}, \tag{4.41}$$

$$\mathbf{p}_1^{(iv)} = \left(I_n + \left(\frac{k_4 - k_4^*}{k_1 - k_4} \right) \frac{\mathbf{p}_4^{(iii)} (\mathbf{p}_4^{(iii)})^\dagger}{(\mathbf{p}_4^{(iii)})^\dagger \mathbf{p}_4^{(iii)}} \right) \mathbf{p}_1^{(iii)}, \tag{4.42}$$

$$\mathbf{q}_1^{(iv)} = \left(I_n + \left(\frac{k_2 - k_2^*}{k_1 + k_2^*} \right) \frac{\mathbf{q}_2^{(iii)} (\mathbf{q}_2^{(iii)})^\dagger}{(\mathbf{q}_2^{(iii)})^\dagger \mathbf{q}_2^{(iii)}} \right) \mathbf{q}_1^{(iii)}, \tag{4.43}$$

$$\mathbf{p}_3^{(v)} = \left(I_n + \left(\frac{k_1^* - k_1}{k_3^* - k_1^*} \right) \frac{\mathbf{p}_1^{(iv)} (\mathbf{p}_1^{(iv)})^\dagger}{(\mathbf{p}_1^{(iv)})^\dagger \mathbf{p}_1^{(iv)}} \right) \mathbf{p}_3^{(iv)}, \tag{4.44}$$

$$\mathbf{q}_1^{(v)} = \left(I_n + \left(\frac{k_1 - k_1^*}{k_1 + k_1^*} \right) \frac{\mathbf{q}_1^{(iv)} (\mathbf{q}_1^{(iv)})^\dagger}{(\mathbf{q}_1^{(iv)})^\dagger \mathbf{q}_1^{(iv)}} \right) \mathbf{q}_1^{(iv)}. \tag{4.45}$$

First, from (4.40, 4.41) we have $\mathbf{p}_1^{(ii)} = \mathbf{q}_1^{(ii)}$, since $\mathbf{p}_j^{(i)} = \mathbf{q}_j^{(i)}$, $j = 1, 2$. Then, we have $\mathbf{p}_1^{(iii)} = \mathbf{p}_1^{(ii)}$ and $\mathbf{q}_1^{(iii)} = \mathbf{q}_1^{(ii)}$. Next, recall that $k_4 = -k_2^*$ and $\mathbf{p}_4^{(ii)} = \bar{B}(k_2) \mathbf{p}_2^{(ii)}$, it follows from the forms of $\mathcal{R}_{42}(k_4, k_2)$ and $\mathcal{K}_2(k_2)$ that $\mathbf{p}_4^{(iii)} = \mathbf{q}_2^{(iii)}$. Then, Eq. (4.42, 4.43) give $\mathbf{p}_1^{(iv)} = \mathbf{q}_1^{(iv)}$. Finally, since $k_3 = -k_1^*$ and $\mathbf{p}_3^{(iv)} = \bar{B}(k_1) \mathbf{p}_1^{(iv)}$, Eq. (4.44, 4.45) imply $\mathbf{p}_3^{(v)} = \mathbf{q}_1^{(v)}$. In the same way, $\mathbf{p}_4^{(v)} = \mathbf{q}_2^{(v)}$ can be checked as well. The same argument holds for

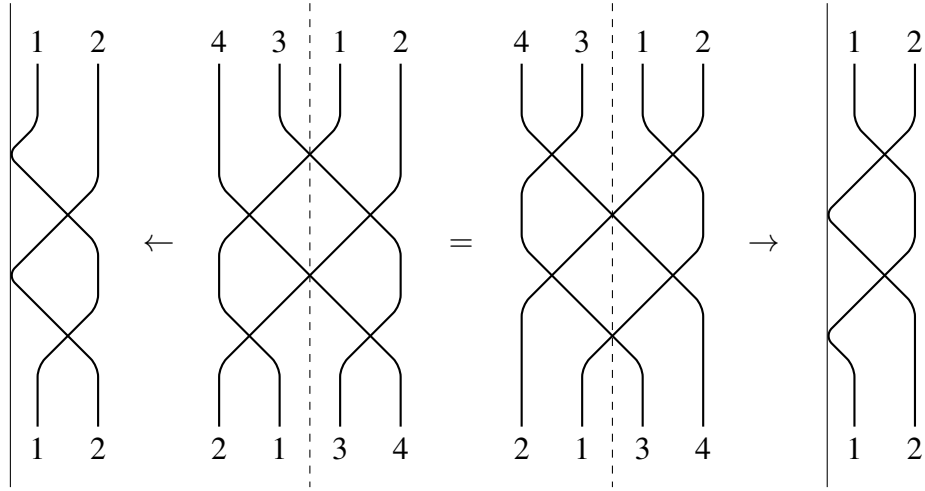
$$\mathcal{R}_{12}(k_1, k_2) \mathcal{R}_{43}(k_4, k_3) \mathcal{R}_{42}(k_4, k_2) \mathcal{R}_{32}(k_3, k_2) \mathcal{R}_{41}(k_4, k_1) \mathcal{R}_{13}(k_1, k_3) (\mathbf{p}_1^{(i)}, \mathbf{p}_2^{(i)}, \mathbf{p}_3^{(i)}, \mathbf{p}_4^{(i)}), \tag{4.46}$$

and

$$\mathcal{R}_{21}(-k_2^*, -k_1^*) \mathcal{K}_2(k_2) \mathcal{R}_{12}(-k_1^*, k_2) \mathcal{K}_1(k_1) (\mathbf{q}_1^{(i)}, \mathbf{q}_2^{(i)}). \quad (4.47)$$

Since (4.38) is equal to (4.46) by (4.37), then (4.39) is equal to (4.47). Note that (4.36) can be proceed in the same way by considering the unitary property of $\mathcal{R}_{12}(k_1, k_2)$ defined in (4.23) and the proof is complete. \blacksquare

The previous proof can amount to the following diagram:



Note that the Yang-Baxter map (4.19) is invariant under the diagonal action of \mathcal{W} , the set of $n \times n$ unitary matrices, on $\mathbb{C}\mathbb{P}^{n-1} \times \mathbb{C}\mathbb{P}^{n-1}$ and could therefore be defined on $\mathbb{C}\mathbb{P}^{n-1} \times \mathbb{C}\mathbb{P}^{n-1} / \mathcal{W}$. However, this is not the case in general for the reflection map defined in (4.32) except when $\bar{\mathbf{B}}$ is proportional to I_n . In this case, the reflection map is proportional to I_n when acting on the polarization vectors and thus reduces to the identity map in $\mathbb{C}\mathbb{P}^{n-1}$. Otherwise, in the right-hand side of Eq. (4.27) in which $\bar{\mathbf{B}}$ is composed of ± 1 on its diagonal, the action of \mathcal{W} results in a different reflection map. This is the mathematical translation of the physical effects on the polarizations when the so-called boundary basis does not coincide with the polarization basis (see Sec. 3.4). Therefore, we have found two classes of reflection maps on $\mathbb{C}\mathbb{P}^{n-1}$: the identity map and a family parametrized by \mathcal{W} as

$$\mathcal{K}_{\mathcal{W}}(k): \mathbf{p} \mapsto \left(I_n + \left(\frac{k - k^*}{k + k^*} \right) \frac{\mathbf{p}\mathbf{p}^\dagger}{\mathbf{p}^\dagger \mathbf{p}} \right) \mathcal{W}^\dagger \bar{\mathbf{B}} \mathcal{W} \mathbf{p}, \quad (4.48)$$

where

$$\bar{B}(k) = \begin{pmatrix} \sigma_1 & & \\ & \ddots & \\ & & \sigma_n \end{pmatrix}, \quad (4.49)$$

where $\sigma_p = 1$, $p \in M$ and $\sigma_q = -1$, $q \in \{1 \dots n\} \setminus M$ with M being a nonempty subset of $\{1, \dots, n\}$.

N -soliton solutions on the half-line using *space-evolution* method

So far, the previous chapters have completely characterized N -soliton (vector NLS solitons) behaviors on the half-line with an integrable boundary. In this chapter, we demonstrate a conceptually *novel approach* to treat the same problem, namely the vector NLS equation on the half-line. For purposes that will be clarified following the presentation, this new formalism is called *space-evolution* formalism. Apparently, it is in contrast to the time-evolution process of the ISM. Indeed, it will be argued that the space-evolution formalism represents an alternative way to formulate the ISM, and also provides a natural and powerful framework to study boundary value problems. Before proceeding to the details, it is necessary to address the following motivations.

- In [41, 21], an inverse scattering transform for an $n \times n$ linear differential system in the form

$$\frac{\partial \Phi}{\partial x} = (A(k) + B(x, k)) \Phi, \quad (5.1)$$

is considered. Here the matrix $B(x, k)$ playing the role of potential is to be reconstructed from scattering data. This lays the foundation of an inverse scattering transform for a generic potential. Recall that the traditional ISM is based on a time-evolution formalism *i.e.* one first obtains the scattering data from the analysis of the x -part of the Lax pair, then makes them evolve in time through the use of the t -part of the Lax pair. It is clear that both parts of the Lax pair are of the form (5.1), but differ in the potentials. Therefore, the understanding of [41, 21] suggests that, provided a Lax pair is given, the traditional ISM that first considers the x -part of the Lax pair is just of conventional purpose! A formalism in which one first obtains the scattering data

from the t -part of the Lax pair, then makes them evolve in space using the x -part is technically conceivable.

- As pointed out in Introduction, Fokas (see *e.g.* [54]) developed a powerful method to solve partial differential equations with generic boundary conditions. This method is referred to as the *unified transform method*, and a number of soliton models on the half-line have been investigated using this method [52, 31, 53, 32, 57] (in Appendix A the vector NLS equation on the half-line is treated using this method). Its main idea lies in the simultaneous treatments of both the x -part and t -part of the Lax pair. Precisely, it is understood that the information of boundary is encoded by the scattering data using the t -part of the Lax pair evaluated at $x = 0$.
- Following Fokas' method, it is hard (almost impossible) to address a rather simple situation such as N -soliton reflection on the half-line. This is mainly because a half-line problem using such method is strictly restricted to $x \geq 0$, $t \geq 0$, whilst an extended potential in the form of Eq. (3.38) allowing $x \in \mathbb{R}$ seems to be more appropriate to track the problem. Therefore, this suggests that an extension of the space-time domain inside the unified transform method might be necessary.

In light of the previous discussions, we first attempt to introduce the space-evolution method as an alternative to the usual ISM for the vector NLS equation. Then, it will be applied to the space-time domain in which $x \geq 0$, $t \in \mathbb{R}$ using the linearizable (integrable) boundary conditions at $x = 0$. It turns out that this leads naturally to an N -soliton reflection solution and a great simplification at the level of calculation also takes place. Note that the content of this chapter, to the best of the authors' knowledge (and surprise), has not been addressed in the literature and is not available anywhere else.

5.1 Space-evolution formalism of the ISM

Briefly speaking, the space-evolution formalism of the ISM consists of the following three steps: 1) *direct scattering* which transforms the soliton equation into a set of scattering data by using the t -part of the Lax pair; 2) *space-evolution* which makes the scattering data evolve in space by using the x -part of the Lax pair; 3) *inverse scattering* which reconstructs the solutions of the original soliton equation from the scattering data.

Consider the focusing ($\lambda = -1$) vector NLS equation defined in (2.1, 2.2). We assume that the j th component $r_j(x, t)$, $j = 1, \dots, n$ is a smooth enough function that vanishes to zero as $t \rightarrow \pm\infty$ for all x . This requirement characterizes indeed a vanishing condition as $t \rightarrow \pm\infty$ that is relevant to the class of (soliton) solutions we are considering.

Following the t -part of the Lax pair defined in (2.5), two Jost solutions $X(x, t, k)$ and $Y(x, t, k)$ as $t \rightarrow \pm\infty$ can be defined as

$$\lim_{t \rightarrow \infty} e^{i\phi(x, t, k)\Sigma_3} X(x, t, k) e^{-i\phi(x, t, k)\Sigma_3} = I_{n+1}, \quad k \in \mathbb{R}, \quad (5.2)$$

$$\lim_{t \rightarrow -\infty} e^{i\phi(x, t, k)\Sigma_3} Y(x, t, k) e^{-i\phi(x, t, k)\Sigma_3} = I_{n+1}, \quad k \in \mathbb{R}, \quad (5.3)$$

where $\phi(x, t, k) = kx + 2k^2t$. Taking the Volterra integral representations evaluated at $x = 0$, one gets

$$X(0, t, k) = I_{n+1} + \int_{\infty}^t e^{-2ik^2(t-\tau)\Sigma_3} (Q_T X)(0, \tau, k) e^{2ik^2(t-\tau)\Sigma_3} d\tau, \quad (5.4)$$

$$Y(0, t, k) = I_{n+1} + \int_{-\infty}^t e^{-2ik^2(t-\tau)\Sigma_3} (Q_T Y)(0, \tau, k) e^{2ik^2(t-\tau)\Sigma_3} d\tau. \quad (5.5)$$

Since Q_T depends linearly on k , the domains of analyticity of the block components of X and Y defined in (5.4, 5.5) can be completely determined by their associated exponential (see *e.g.* [54] for similar treatments in the scalar NLS case). Let $k \equiv a + ib$, then

$$\phi(0, t, k) = 2i(a^2 - b^2)t - 4abt. \quad (5.6)$$

The real part of this term *i.e.* $-4abt$ suggests that X and Y can be split into the block-column vector forms of natural size as

$$X = (X^{(24)}, X^{(13)}), \quad Y = (Y^{(13)}, Y^{(24)}) \quad (5.7)$$

where $X^{(24)}$, $Y^{(24)}$ (resp. $X^{(13)}$, $Y^{(13)}$) are analytic and bounded in the union of the quadrants (2) and (4) or equivalently $ab < 0$ (resp. in the union of the quadrants (1) and (3) or $ab > 0$). The four quadrant of the k -complex plane is defined in Fig. 5.1. Then according to (2.23), X and Y can be related by a matrix $T(k)$ as

$$X(0, t, k) = Y(0, t, k) e^{-2ik^2t\Sigma_3} T(k) e^{2ik^2t\Sigma_3}, \quad (5.8)$$

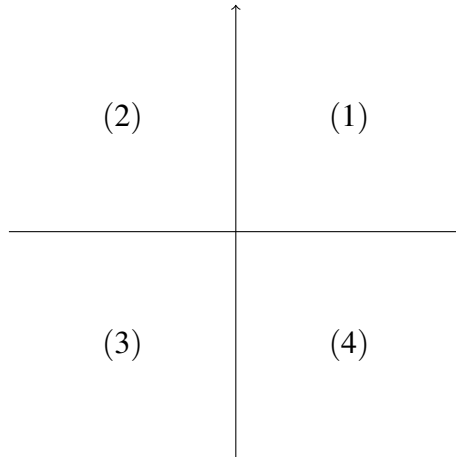


Fig. 5.1 : Four quadrants of the k -complex plane

where $T(k)$ can be written in the following 2×2 block-matrix form:

$$T(k) = \begin{pmatrix} \mathbf{A}^{(24)}(k) & \mathbf{B}^{(13)}(k) \\ \mathbf{B}^{(24)}(k) & \mathbf{A}^{(13)}(k) \end{pmatrix}. \quad (5.9)$$

Again the superscripts (24) and (13) are understood to indicate the domain of analyticity. Its inverse can be written as

$$T(k)^{-1} = \begin{pmatrix} \mathbf{C}^{(13)}(k) & \mathbf{D}^{(13)}(k) \\ \mathbf{D}^{(24)}(k) & \mathbf{C}^{(24)}(k) \end{pmatrix}. \quad (5.10)$$

Due to the traceless property of \mathcal{Q}_T , one has $\det T(k) = 1$, and due to the reduction symmetry (2.11), one has $T(k)^{-1} = T^\dagger(k^*)$. The latter relation specifies in components as

$$(\mathbf{A}^{(24)}(k^*))^\dagger = \mathbf{C}^{(13)}(k), \quad (\mathbf{B}^{(24)}(k^*))^\dagger = \mathbf{D}^{(13)}(k). \quad (5.11)$$

$$(\mathbf{A}^{(13)}(k^*))^\dagger = \mathbf{C}^{(24)}(k), \quad (\mathbf{B}^{(13)}(k^*))^\dagger = \mathbf{D}^{(24)}(k). \quad (5.12)$$

Remark 5.1.1 *As far as we perform direct scattering using the linear Lax pair equations (2.4, 2.5), similar steps take place both here and in Sec. 2.1. Apparently, these two approaches differ only in the use of potentials, as \mathcal{Q}_T is the potential applied here. According to [41, 21], the use of \mathcal{Q}_T as the potential to perform the direct scattering, and later the inverse scattering, is technically acceptable. Conceptually, it switches the role of initial condition to boundary condition, i.e. instead of characterizing initial condition data and making them evolve in time, boundary condition data now are encoded in $T(k)$, for $T(k)$ is obtained at $x=0$, and will evolve in space.*

A priori, the matrix $T(k)$ defined in (5.8) is space-dependent, for both the Jost solutions X and Y depend on x . Its x -dependence can be obtained by inserting (5.8) into the x -part of the Lax pair (2.4):

$$\frac{\partial T(x, k)}{\partial x} = -ik[\Sigma_3, T(x, k)]. \quad (5.13)$$

This relation precisely characterizes the evolution of scattering data in space. In the following, we absorb the x -dependence of the scattering system (5.8) into an (x, t) -dependent RH problem.

Define the following RH problem as

$$G^{(13)} G^{(24)}(x, t, k) = e^{-i\phi(x, t, k)\Sigma_3} G(k) e^{i\phi(x, t, k)\Sigma_3}, \quad k \in \mathbb{R} \cup i\mathbb{R}, \quad (5.14)$$

where

$$G^{(13)} = \begin{pmatrix} \mathbf{C}^{(13)}(k) & 0 \\ 0 & \mathbf{A}^{(13)}(k) \end{pmatrix} (Y^{(13)}, X^{(13)}), \quad G^{(24)} = (X^{(24)}, Y^{(24)}), \quad (5.15)$$

and the jump matrix $G(k)$ is defined as

$$G(k) = \begin{pmatrix} I_n & \mathbf{D}^{(13)}(k) \\ \mathbf{B}^{(13)}(k) & 1 \end{pmatrix}. \quad (5.16)$$

Here $G^{(13)}$ and $G^{(24)}$ are matrix functions living in (13) and (24) of the k -complex plane respectively with the jump condition (5.14) being defined on the union of the real and imaginary axes *i.e.* $\mathbb{R} \cup i\mathbb{R}$. This is in contrast to RH problem defined in (2.29) for the time-evolution ISM in which the contour only lies on \mathbb{R} . One can also show that

$$\det G^{(13)}(x, t, k) = \mathbf{A}^{(13)}(k), \quad \det G^{(24)}(x, t, k) = \mathbf{A}^{(24)}(k). \quad (5.17)$$

Provided that the $G^{(13)}(x, t, k)$ and $G^{(24)}(x, t, k)$ are solutions of such RH problem (5.14), $G^{(24)}(x, t, k)$ satisfies the Lax pair (2.4, 2.5). As a result, the reconstruction formula is written as

$$Q(x, t) = \lim_{|k| \rightarrow \infty} ik[\Sigma_3, G^{(24)}(x, t, k)]. \quad (5.18)$$

Finally, we are ready to collect N -soliton scattering data in order to construct N -soliton solutions. As usual, this step is under the assumption that $\det \mathbf{A}^{(24)}(k)$ and

$\mathbf{C}^{(24)}(k)$ have a finite number of simple zeros located in the domain (24). Denote them κ_j , $j = 1, \dots, N$, $\kappa_j \in (24)$. Consequently, $\mathbf{A}^{(13)}(k)$ and $\det \mathbf{C}^{(13)}(k)$ have the same number N of simple zeros κ_j^* , $j = 1, \dots, N$. We make a further assumption that we restrict ourselves only to soliton solutions, so that the scattering functions $\mathbf{B}^{(13)}(k)$ and $\mathbf{D}^{(24)}(k)$ (resp. $\mathbf{B}^{(24)}(k)$ and $\mathbf{D}^{(13)}(k)$) can be analytically defined at κ_j , $\kappa_j \in (24)$ (resp. $\kappa_j^* \in (13)$). This allows us to specify the norming constant $\bar{\beta}_j$ associated to κ_j as

$$\bar{\beta}_j \equiv D^{(13)}(\kappa_j^*). \quad (5.19)$$

Consider the pure soliton system *i.e.*

$$\mathbf{B}^{(24)}(k) = \mathbf{D}^{(24)}(k) = \mathbf{B}^{(13)}(k) = \mathbf{D}^{(13)}(k) = 0, \quad k \in \mathbb{R} \cup i\mathbb{R}. \quad (5.20)$$

Given the N -soliton scattering data $\{\kappa_j; \bar{\beta}_j\}$, $j = 1, \dots, N$, $\kappa_j \in (24)$. Let $\bar{\beta}_{j;i}$ be the i -th component of $\bar{\beta}_j$ and $\bar{\beta}_j(x, t) \equiv \bar{\beta}_j e^{-2i\phi(x, t; \kappa_j^*)}$. Then, the N -soliton solutions of the vector NLS equation defined in $x, t \in \mathbb{R}$ can be expressed as the same form as that presented in (2.62 - 2.64), with k_j being substituted by κ_j and β_j substituted by $\bar{\beta}_j$. Therefore, an N -soliton solution using the space-evolution method is obtained.

5.2 N -soliton reflections

Having introduced the space-evolution method, we turn now to implement the linearizable (integrable) boundary conditions obtained in Appendix A (see also Sec. 3.1) to the vector NLS equation on the half-line. Note the system is restricted to $x \geq 0$, so that the domain of using the space-evolution method is $x \geq 0$, $t \in \mathbb{R}$.

At the level of the Lax pair, the linearizable boundary conditions are encoded into the following relation (see Appendix A for details):

$$V(t, -k)N(k) = N(k)V(t, k), \quad (5.21)$$

where $V(t, k) = -i2k^2\Sigma_3 + Q_T(0, t, k)$ and

$$N(k) = \begin{pmatrix} \frac{k-i\alpha}{k+i\alpha}I_n & & & \\ & & & \\ & & & -1 \end{pmatrix}, \quad \text{or } N(k) = \begin{pmatrix} \sigma_1 & & & \\ & \ddots & & \\ & & \sigma_n & \\ (13) & & & -1 \end{pmatrix}, \quad (5.22)$$

where $\sigma_j = -1$, $j \in M$ and $\sigma_j = 1$, $j \in \{1, \dots, n\} \setminus M$, M being a nonempty subset of $\{1, \dots, n\}$. Inserting the constraint (5.21) into the scattering system (5.8), one can

show¹ that the matrix $T(k)$ satisfies the following symmetry relation:

$$T(-k) = N(k)T(k)N^{-1}(k). \quad (5.23)$$

Taking the form of the boundary matrix $B(k)$ defined in (3.40), it is clear that $B(k)$ is precisely the first $n \times n$ block matrix of $N(k)$. Then, in components, Eq. (5.23) reads as

$$\mathbf{A}^{(24)}(-k) = B(k)\mathbf{A}^{(24)}(k)B^{-1}(k), \quad \mathbf{A}^{(13)}(-k) = \mathbf{A}^{(13)}(k), \quad (5.24)$$

$$\mathbf{B}^{(13)}(-k) = -B(k)\mathbf{B}^{(13)}(k), \quad \mathbf{B}^{(24)}(-k) = -\mathbf{B}^{(13)}(k)B^{-1}(k). \quad (5.25)$$

Similar observation to that of Sec. 3.3 can be found using the first relation: the relevant zeros of $\det \mathbf{A}^{(24)}(k)$ to formulate the inverse problem come in pairs $(\kappa_j, -\kappa_j)$ where $\kappa_j \in (24)$. The total number J of the zeros of $\mathbf{A}^{(24)}(k)$ in (24) is even: $J = 2N$ and there are N zeros in both the domains (13) and (24) (see Fig. 5.2). In addition,

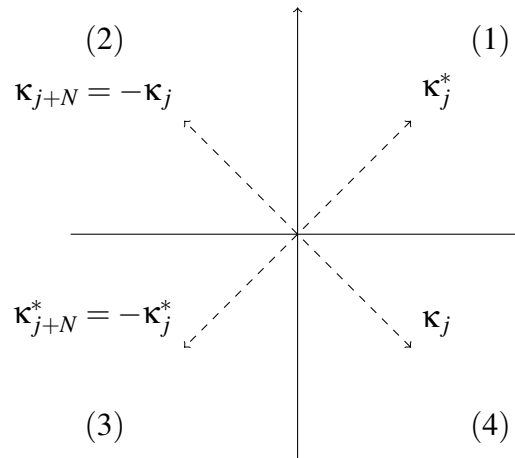


Fig. 5.2 : $2N$ zeros on the k -complex plane with $\kappa_{j+N} = -\kappa_j$, $j = 1, \dots, N$, $\kappa_j \in -$

from the definition of the norming constant (5.19), the relation between the paired norming constants $(\bar{\beta}_j, \bar{\beta}_{j+N})$ can be read directly from (5.25) as

$$\kappa_{j+N} = -\kappa_j, \quad \bar{\beta}_{j+N} = -B(k_j^*)\bar{\beta}_j. \quad (5.26)$$

The relation (5.26) constitutes the main result of this chapter. First, an N -soliton reflexion solution $R(x, t)$ on the half-line can be obtained using the ISM by evolving the space variable of the $2N$ -soliton scattering data satisfying (5.26) from 0 to x . For instance, in the case of the mixed Neumann and Dirichlet boundary condition

¹The proof is very similar to that of Prop. 3.3.1 in which the mirror symmetry relation (3.25) is obtained.

(3.23), numeric simulations give similar results to what is presented in Sec. 3.4 *i.e.* different components of the polarization satisfy either the Neumann ($R_x(\mathbf{0}, t) = \mathbf{0}$) or the Dirichlet ($R(\mathbf{0}, t) = \mathbf{0}$) boundary conditions. This confirms that the use of the space-evolution method with a linearizable (integrable) boundary solves the vector NLS half-line problem. Then, what is highly interesting is the comparison between (5.26) and the mirror symmetry relation (3.55). The observation that the scattering data appear in paired forms holds true for both features. The paired zeros in (5.26) are conjugated by a minus sign *i.e.* $\kappa_{j+N} = -\kappa_j$ whilst in (3.55) they are conjugated by a reflection along the real axis *i.e.* $k_{j+N} = -k_j^*$. As to norming constants, in (5.26) the paired norming constants $(\bar{\beta}_j, \bar{\beta}_{j+N})$ are *linearly coupled* by the boundary matrix $B(k)$. This is in sharp contrast to the mirror symmetry relation (3.55) in which the paired norming constants (β_j, β_{j+N}) are *nonlinearly coupled*. Instead of performing the rather complicated computations to solve the nonlinear system (3.55) as presented in Appendix C, a great simplification takes place here! This suggests that the space-evolution formalism represents a more natural framework to study half-line problems. Indeed, by restricting the space-time domain to $x \geq 0, t \in \mathbb{R}$, there is no need to introduce an extended potential on the full line as performed in Eq. (3.38). The boundary effect comes from the linearizable boundary conditions through the analysis of the unified transform method. In another word, the space-evolution method for studying half-line problems with linearizable boundary conditions can be regarded as a modification of the unified transform method by extending the time variable from $t \geq 0$ to $t \in \mathbb{R}$.

Part II

Reflection maps: classification and applications

Set-theoretical reflection equation and reflection maps

In the study of N -soliton reflections on the half-line in Part I of this thesis, the set-theoretical reflection equation is introduced, along with the set-theoretical Yang-Baxter equation, to guarantee the factorization property of the soliton-soliton and soliton-boundary interactions. This completes the *set-theoretical* counterpart of the *quantum reflection equation* [42, 104]. In particular, we call its solutions *reflection maps* following the use of "Yang-Baxter maps" proposed by Veselov in [113]. The purpose of this chapter is to introduce some basic notions of the set-theoretical reflection equation and reflection maps. This will lay the foundation for the understanding of the forthcoming chapters.

6.1 Yang-Baxter maps

In this section, we mainly follow the presentation of the review [114] to collect some well-known facts of the set-theoretical Yang-Baxter equation and Yang-Baxter maps.

Let S be a set and $\mathcal{R} : S \times S \rightarrow S \times S$ a map from the Cartesian product of S onto itself represented as

$$\mathcal{R}(X, Y) = (U, V) \equiv (f(X, Y), g(X, Y)). \quad (6.1)$$

Let $S^N = S \times \cdots \times S$ be the N -fold Cartesian product of S . Then, \mathcal{R} can be extended to S^N by defining $\mathcal{R}_{ij} : S^N \rightarrow S^N$ as the map acting as \mathcal{R} on the i th and j th copies of

S in S^N and identically on the others. Precisely, for $i < j$,

$$\mathcal{R}_{ij}(X_1, \dots, X_n) = (X_1, \dots, X_{i-1}, f(X_i, X_j), \dots, g(X_i, X_j), X_{j+1}, \dots, X_n), \quad (6.2)$$

$$\mathcal{R}_{ji}(X_1, \dots, X_n) = (X_1, \dots, X_{i-1}, g(X_j, X_i), \dots, f(X_j, X_i), X_{j+1}, \dots, X_n). \quad (6.3)$$

In other words, \mathcal{R}_{ij} and \mathcal{R}_{ji} are related by

$$\mathcal{R}_{ji} = P_{ij} \mathcal{R}_{ij} P_{ij}, \quad (6.4)$$

where P_{ij} is the permutation operator acting on the i th and j th copies of S in S^N . Note that for $N = 2$, one has $\mathcal{R}_{12} \equiv \mathcal{R}$. If \mathcal{R} satisfies the following Yang-Baxter relation

$$\mathcal{R}_{12} \mathcal{R}_{13} \mathcal{R}_{23} = \mathcal{R}_{23} \mathcal{R}_{13} \mathcal{R}_{12}, \quad (6.5)$$

as an identity on $S \times S \times S$, then \mathcal{R} is called a *Yang-Baxter map*. We call the arguments of Yang-Baxter maps *i.e.* the variable X, Y, U, V in (6.1) *Yang-Baxter variables*. In addition, if \mathcal{R} satisfies

$$\mathcal{R}_{21} \mathcal{R}_{12} = Id, \quad (6.6)$$

then \mathcal{R} is called a *reversible Yang-Baxter map*.

The class of parameter-dependent Yang-Baxter maps turns out to be of special importance as the Yang-Baxter maps arising from the study of multi-component soliton models [64, 9, 111] (see also Sec. 4.1) and the quadrirational Yang-Baxter maps [14, 97] belong to this class. It is obtained by considering an extension of the set S to $S \times \Sigma$ where Σ is some parameter set (usually \mathbb{C}). The corresponding map is now defined as

$$\mathcal{R} : (X, a; Y, b) \mapsto (f(X, a; Y, b), a; g(X, a; Y, b), b) \equiv (f_{ab}(X, Y), a; g_{ab}(X, Y), b). \quad (6.7)$$

This map is usually written as $\mathcal{R}(a, b)$ and seen as acting only on $S \times S$:

$$\mathcal{R}(a, b) : (X, Y) \mapsto (f_{ab}(X, Y), g_{ab}(X, Y)). \quad (6.8)$$

It satisfies the parametric Yang-Baxter equation

$$\mathcal{R}_{12}(a, b) \mathcal{R}_{13}(a, c) \mathcal{R}_{23}(b, c) = \mathcal{R}_{23}(b, c) \mathcal{R}_{13}(a, c) \mathcal{R}_{12}(a, b), \quad (6.9)$$

and the corresponding reversibility condition reads

$$\mathcal{R}_{21}(b,a)\mathcal{R}_{12}(a,b) = Id. \quad (6.10)$$

There is a well-known pictorial representation of Yang-Baxter maps (see *e.g.* [14]). Indeed, a Yang-Baxter map \mathcal{R} can be associated to a quadrilateral (see Fig. 6.1) with the Yang-Baxter variables and parameters assigned to the edges. The parameters remain constant on opposite edges. Then, the parametric set-theoretical Yang-Baxter

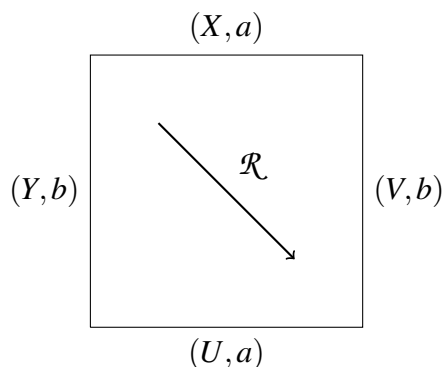


Fig. 6.1 : A parametric Yang-Baxter map $\mathcal{R}(a,b) : (X,Y) \mapsto (U,V)$

equation (6.9) can be understood as the consistency condition ensuring that the two possible orders of the action of the map \mathcal{R} on $(X,a;Y,b;Z,c)$, described by both sides of the equation (6.9), provide the same result. This feature is shown in Fig. 6.2. Note that the two configurations of Fig. 6.2 can also be regarded as the *front* and *back* sides of a cube respectively, which is specified as the cubic representation.

In [113], Veselov also introduced the notion of *transfer maps* for reversible Yang-Baxter maps, by analogy to the transfer matrix that is a central concept in quantum integrable theories [108, 18]. It is defined as the following. Fix $N \geq 2$, and defined the following maps of S^N :

$$T_j = \mathcal{R}_{jj+N-1}\mathcal{R}_{jj+N-2} \cdots \mathcal{R}_{jj+1}. \quad (6.11)$$

where the indices are considered modulo N . Then, as proved in [113], T_j commutes with T_k :

$$T_i T_k = T_k T_j, \quad (6.12)$$

and satisfy the property

$$T_1 T_2 \cdots T_N = Id. \quad (6.13)$$

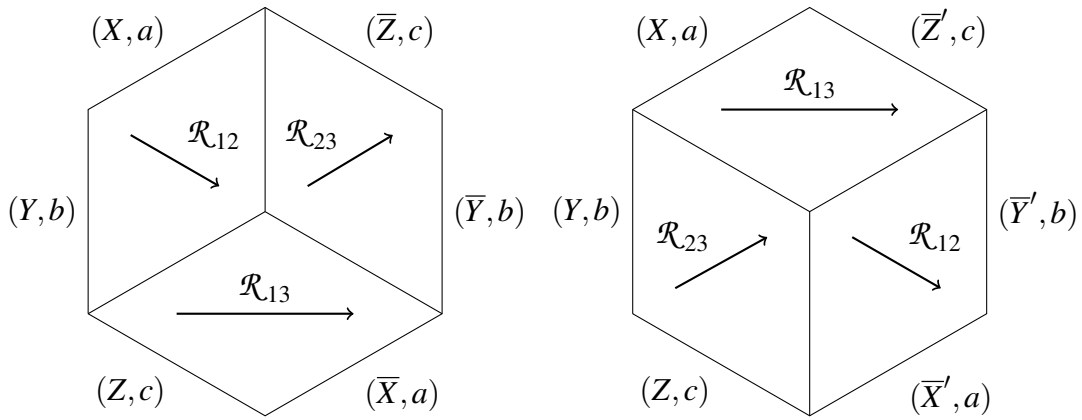


Fig. 6.2 : Pictorial representation of the set-theoretical Yang-Baxter equation

6.2 Reflection maps

Based on the form of the quantum reflection equation [42] and the example that was studied in Sec. 4.2, we are now accessing to the following general definition of reflection maps, that is also reported in [38, 40].

Definition 6.2.1 *Given a Yang-Baxter map \mathcal{R} , a reflection map \mathcal{K} is a solution of the set-theoretical reflection equation*

$$\mathcal{K}_1 \mathcal{R}_{21} \mathcal{K}_2 \mathcal{R}_{12} = \mathcal{R}_{21} \mathcal{K}_2 \mathcal{R}_{12} \mathcal{K}_1, \quad (6.14)$$

as an identity on $S \times S$. The reflection map is called involutive if

$$\mathcal{K} \mathcal{K} = Id. \quad (6.15)$$

Here \mathcal{K}_j is understood to act as \mathcal{K} on the j th copy of S in S^N and identically on the others. To introduce the notion of parametric reflection map, we need some extension of the above discussion for parametric Yang-Baxter maps. Indeed, a parametric Yang-Baxter map has a trivial action on the parameter set Σ . However, it is shown in Sec. 4.2 from the example found for reflection maps that a parametric reflection map can in general have a nontrivial action on the parameter set. This feature suggests the following form of a reflection map:

$$\mathcal{K} : (X, a) \mapsto (h_a(X), \sigma(a)), \quad X \in S, \quad a \in \Sigma. \quad (6.16)$$

The maps h_a and σ together constitute a reflection map. One can then use the convenient notation $\mathcal{K}(a)$ for a parametric reflection map but keep in mind of the

nontrivial action of σ when composing a reflection map with other maps. This is illustrated in the following definition of parametric reflection maps.

Definition 6.2.2 *Given a parametric Yang-Baxter map $\mathcal{R}_{12}(a,b)$, $a,b \in \Sigma$, a parametric reflection map $\mathcal{K}(a)$, composed of h_a and σ as presented in (6.16), is a solution of the parametric set-theoretical reflection equation*

$$\mathcal{K}_1(a)\mathcal{R}_{21}(\sigma(b),a)\mathcal{K}_2(b)\mathcal{R}_{12}(a,b) = \mathcal{R}_{21}(\sigma(b),\sigma(a))\mathcal{K}_2(b)\mathcal{R}_{12}(\sigma(a),b)\mathcal{K}_1(a), \quad (6.17)$$

as an identity on $S \times S$. The reflection map is called involutive if σ is an involution in Σ and

$$\mathcal{K}(\sigma(a))\mathcal{K}(a) = Id. \quad (6.18)$$

Analogous to the quadrilateral description of a Yang-Baxter map, we introduce a pictorial description of a reflection map as a half-quadrilateral or a triangle shown in Fig. 6.3. Then, the (parametric) set-theoretical reflection equation can be depicted

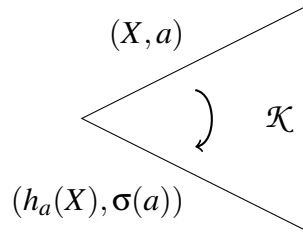


Fig. 6.3 : A parametric reflection map $\mathcal{K}(a)$

in Fig. 6.4 with the quadrilaterals representing Yang-Baxter maps.

Note that there are similarities between Fig. 6.4 and half of the figure representing the tetrahedron equation for interaction round-a-cube [19, 20]. Similar figures also appeared in [15, 48, 22] as the face representation of the quantum reflection equation. Indeed, one can glue the two sides of Fig. 6.4 together and make them prolonged into a *three-dimensional* configuration. This gives exactly the half of a *rhombic dodecahedron* as represented in Fig. 6.5. Then the reflection equation is regarded as the consistency condition that the quadrilaterals on Fig. 6.5 represent the same Yang-Baxter map \mathcal{R} whilst the triangles the same reflection map \mathcal{K} .

Returning back to Fig. 6.4, it can be explicitly put into the following: the left-hand side represents the following chain of maps

$$(X, a; Y, b) \xrightarrow{\mathcal{R}_{12}} (X_1, a; Y_1, b) \xrightarrow{\mathcal{K}_2} (X_1, a; Y_2, \sigma(b)) \xrightarrow{\mathcal{R}_{21}} (X_2, a; Y_3, \sigma(b)) \xrightarrow{\mathcal{K}_1} (X_3, \sigma(a); Y_3, \sigma(b))$$

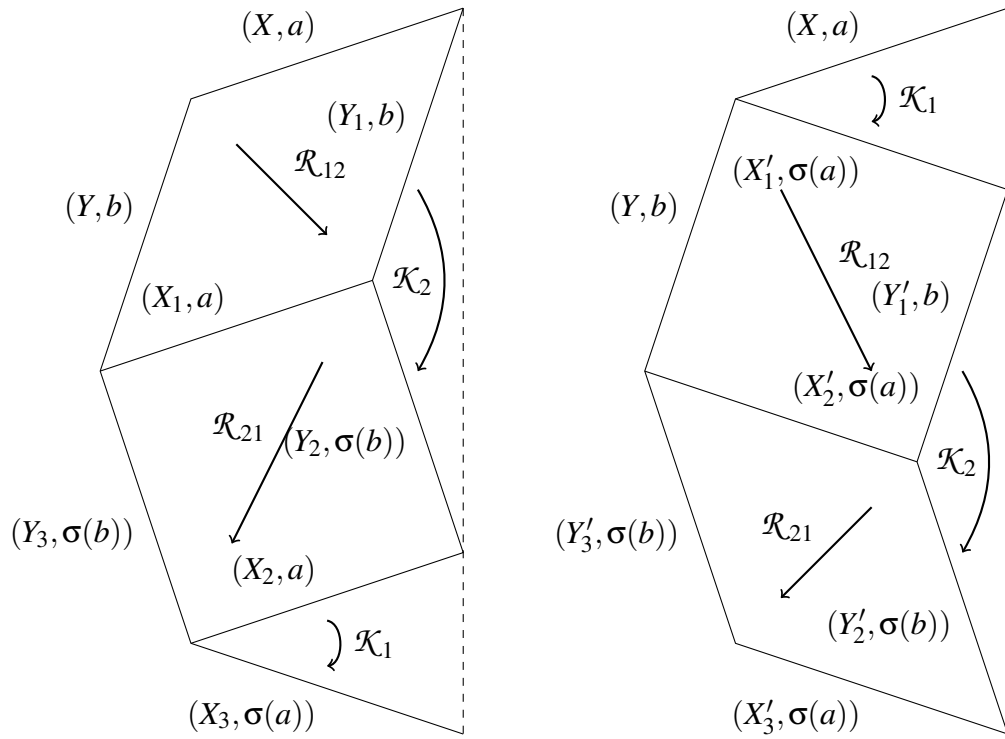


Fig. 6.4 : Pictorial representation of the reflection equation

with

$$\begin{aligned} X_1 &= f_{ab}(X, Y) , \quad Y_1 = g_{ab}(X, Y) , \quad Y_2 = h_b(Y_1) , \\ X_2 &= g_{\sigma(b)a}(Y_2, X_1) , \quad Y_3 = f_{\sigma(b)a}(Y_2, X_1) , \quad X_3 = h_a(X_2) . \end{aligned}$$

Similarly, for the right-hand side, one gets

$$(X, a; Y, b) \xrightarrow{\mathcal{K}_1} (X'_1, \sigma(a); Y, b) \xrightarrow{\mathcal{R}_{12}} (X'_2, \sigma(a); Y'_1, b) \xrightarrow{\mathcal{K}_2} (X'_2, \sigma(a); Y'_2, \sigma(b)) \xrightarrow{\mathcal{R}_{21}} (X'_3, \sigma(a); Y'_3, \sigma(b))$$

with

$$\begin{aligned} X'_1 &= h_a(X) , \quad X'_2 = f_{\sigma(a)b}(X'_1, Y) , \quad Y'_1 = g_{\sigma(a)b}(X'_1, Y) , \\ Y'_2 &= h_b(Y'_1) , \quad X'_3 = g_{\sigma(b)\sigma(a)}(Y'_2, X'_2) , \quad Y'_3 = f_{\sigma(b)\sigma(a)}(Y'_2, X'_2) . \end{aligned}$$

Therefore, given the same $(X, a; Y, b)$ for the both sides, Eq. (6.17) ensures the equality of the final results:

$$(X_3, \sigma(a); Y_3, \sigma(b)) = (X'_3, \sigma(a); Y'_3, \sigma(b)) . \quad (6.19)$$

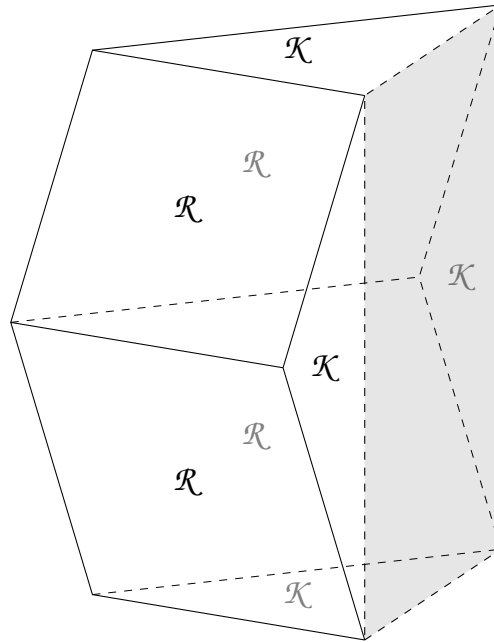


Fig. 6.5 : Three-dimensional consistency for the reflection equation

Following the discussion of the transfer maps for reversible Yang-Baxter maps [113], we can define similar objects for reflection maps. This is by analogy to the construction of transfer matrix in the study of the quantum reflection equation [104]. Fix $N \geq 2$ and define for $j = 1, \dots, N$ the following maps of S^N into itself,

$$\mathcal{T}_j = \mathcal{R}_{j+1j} \dots \mathcal{R}_{Nj} \mathcal{K}_j^- \mathcal{R}_{jN} \dots \mathcal{R}_{jj+1} \mathcal{R}_{jj-1} \dots \mathcal{R}_{j1} \mathcal{K}_j^+ \mathcal{R}_{1j} \dots \mathcal{R}_{j-1j}, \quad (6.20)$$

where \mathcal{K}^+ is a solution of

$$\mathcal{K}_1 \mathcal{R}_{21} \mathcal{K}_2 \mathcal{R}_{12} = \mathcal{R}_{21} \mathcal{K}_2 \mathcal{R}_{12} \mathcal{K}_1, \quad (6.21)$$

and \mathcal{K}^- a solution of

$$\mathcal{K}_1 \mathcal{R}_{12} \mathcal{K}_2 \mathcal{R}_{21} = \mathcal{R}_{12} \mathcal{K}_2 \mathcal{R}_{21} \mathcal{K}_1. \quad (6.22)$$

Then one proves by direct (but long) calculations the following result.

Proposition 6.2.3 *For any reversible Yang-Baxter map \mathcal{R} , the transfer maps (6.20) commute with each other:*

$$\mathcal{T}_j \mathcal{T}_\ell = \mathcal{T}_\ell \mathcal{T}_j, \quad (6.23)$$

This result can be easily extended to the parametric case.

We conclude this chapter with a reminder of the reflection maps that were found in Chapter 4. We stress that this is the first concrete example of reflection maps. Precisely, according to the definition of Yang-Baxter maps in Sec. 6.1, one has $\mathcal{S} \equiv \mathbb{C}\mathbb{P}^{n-1}$ and $\Sigma \equiv \mathbb{C}$. The parametric Yang-Baxter map, extracted from the vector NLS solitons' interactions, is in the form

$$\mathcal{R}_{j,k}(k_j, k_k) : (\mathbf{p}_1, \dots, \mathbf{p}_j, \dots, \mathbf{p}_k, \dots, \mathbf{p}_N) \mapsto (\mathbf{p}_1, \dots, \tilde{\mathbf{p}}_j, \dots, \tilde{\mathbf{p}}_k, \dots, \mathbf{p}_N), \quad (6.24)$$

where

$$\tilde{\mathbf{p}}_j = \left(I + \left(\frac{k_k^* - k_k}{k_j^* - k_k^*} \right) \frac{\mathbf{p}_k \mathbf{p}_k^\dagger}{\mathbf{p}_k^\dagger \mathbf{p}_k} \right) \mathbf{p}_j, \quad \tilde{\mathbf{p}}_k = \left(I + \left(\frac{k_j - k_j^*}{k_k - k_j} \right) \frac{\mathbf{p}_j \mathbf{p}_j^\dagger}{\mathbf{p}_j^\dagger \mathbf{p}_j} \right) \mathbf{p}_k. \quad (6.25)$$

The Yang-Baxter variables \mathbf{p}_j , \mathbf{p}_k , $\tilde{\mathbf{p}}_j$, $\tilde{\mathbf{p}}_k$ are in their homogeneous coordinates. Then, the parametric reflection maps are found in the following form:

$$\mathcal{K}(k) : (\mathbf{p}, k) \mapsto (\mathbf{p}', \sigma(k)), \quad (6.26)$$

where $\sigma(k) = -k^*$ is clearly an involution and

$$\mathbf{p}' = \left(I + \left(\frac{k - k^*}{k + k^*} \right) \frac{\mathbf{p} \mathbf{p}^\dagger}{\mathbf{p}^\dagger \mathbf{p}} \right) B(k) \mathbf{p}, \quad (6.27)$$

with the matrix $B(k)$ being the boundary matrix defined in (3.40).

Reflection maps for quadrirational Yang-Baxter maps

Classification of Yang-Baxter maps in the case where $S = \mathbb{CP}^1$ was recently investigated by Adler, Bobenko and Suris [14]. This led to an important class of maps that was called *quadrirational maps*, and also a corresponding classification that shares a beautiful geometric interpretation in terms of *pencil of conics*. Later, in [97], quadrirational maps that satisfy the set-theoretical Yang-Baxter equation were studied, which resulted in an additional classification. Remarkably, the quadrirational maps classified in both [14] and [97] are Yang-Baxter maps. This represents a natural field of applications for reflection maps. In this chapter, we present the results originally reported in [40] where a classification of reflection maps for quadrirational Yang-Baxter maps was constructed.

7.1 Quadrirational Yang-Baxter maps

This section reviews the important results obtained in [14, 97] regarding the classification of quadrirational Yang-Baxter maps.

Let a nondegenerate map \mathcal{R} be in the form

$$\mathcal{R} : (X, Y) \mapsto (U, V) \equiv (f(X, Y), g(X, Y)), \quad (7.1)$$

where the variables $X, Y, U, V \in \mathbb{CP}^1$. Then \mathcal{R} is called quadrirational if both \mathcal{R} and the so-called *companion map* $\overline{\mathcal{R}}$, defined as

$$\overline{\mathcal{R}} : (X, V) \mapsto (U, Y) \equiv (\bar{f}(X, V), \bar{g}(X, V)), \quad (7.2)$$

are birational maps of $\mathbb{CP}^1 \times \mathbb{CP}^1$ into itself. It was concluded in [14] that the quadrirational maps are in the form

$$f(X, Y) = \frac{a(Y)X + b(Y)}{c(Y)X + d(Y)}, \quad g(X, Y) = \frac{A(X)Y + B(X)}{C(X)Y + D(X)}, \quad (7.3)$$

where $a(Y), \dots, d(Y)$ and $A(X), \dots, D(X)$ are polynomials of degree at most 2. There are three subclasses of such maps, denoted as $[1 : 1]$, $[1 : 2]$ and $[2 : 2]$ corresponding to the highest degrees of the coefficients of the both fractions in (7.3). For the most interesting subclass $[2 : 2]$, the authors also proved that any quadrirational map is $(\mathcal{M}\ddot{o}b)^4$ -equivalent to one of five families, named as $F_I - F_V$, whose explicit forms are listed in Table 7.1. The action of $\mathcal{M}\ddot{o}b$ is precisely the Möbius transformation:

$$\mathcal{M}\ddot{o}b: \quad z \mapsto \frac{\alpha z + \beta}{\gamma z + \tau}, \quad \alpha, \beta, \gamma, \tau \in \mathbb{C}. \quad (7.4)$$

It is remarkable that the maps $F_I - F_V$ in their canonical forms in Table 7.1 are parametric Yang-Baxter maps depending on $a, b \in \mathbb{C}$. Moreover, for each family of the F -families, both its companion map and inverse map coincide with the map itself *i.e.* $\mathcal{R} = \mathcal{R}^{-1} = \overline{\mathcal{R}} = \overline{\mathcal{R}}^{-1}$.

Type	$f_{ab}(X, Y)$	$g_{ab}(X, Y)$	P
F_I	aYP	bXP	$\frac{(1-b)X + b - a + (a-1)Y}{b(1-a)X + (a-b)XY + a(b-1)Y}$
F_{II}	$\frac{Y}{a}P$	$\frac{X}{b}P$	$\frac{aX - bY + b - a}{X - Y}$
F_{III}	$\frac{Y}{a}P$	$\frac{X}{b}P$	$\frac{aX - bY}{X - Y}$
F_{IV}	YP	XP	$1 + \frac{b-a}{X-Y}$
F_V	$Y + P$	$X + P$	$\frac{a-b}{X-Y}$

Table 7.1: F -families of quadrirational maps

Interestingly, this classification can be obtained following a beautiful geometric construction [14]: consider a *pencil* of two nondegenerate conics \mathcal{Q}_1 and \mathcal{Q}_2 —a linear combination of \mathcal{Q}_1 and \mathcal{Q}_2 —on the plane \mathbb{CP}^2 , which are rational curves isomorphic

to \mathbb{CP}^1 . Take two points $\tilde{X} \in Q_1$ and $\tilde{Y} \in Q_2$, and let $\ell = \overline{\tilde{X}\tilde{Y}}$ be the line passing through \tilde{X}, \tilde{Y} . Generically the line ℓ intersects Q_1 and Q_2 respectively at two other points \tilde{U} and \tilde{V} (see Fig. 7.1). Indeed, there are five possible configurations $I - V$ of

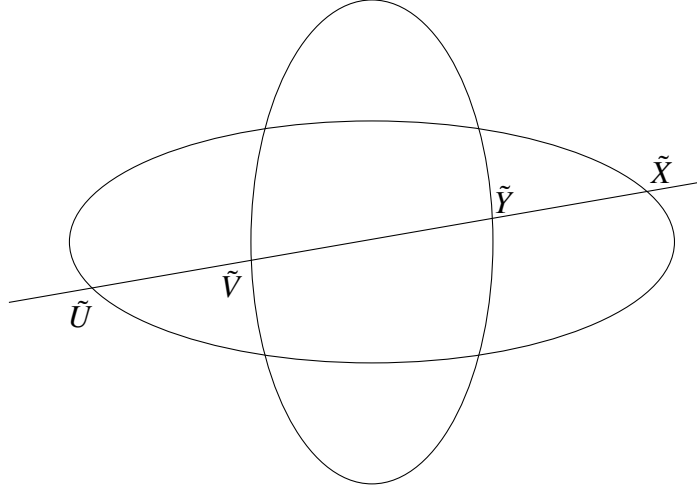


Fig. 7.1 : Pencil of conics, configuration I : four simple intersection points

a pencil of two conics (see *e.g.* [24]):

- I : four simple intersection points;
- II : two simple intersection points and one point of tangency;
- III : two points of tangency;
- IV : one simple intersection point and one point of the second order tangency;
- V : one point of the third order tangency.

By taking suitable *rational parametrizations* of the conics, one requires that the points $\tilde{X}, \tilde{Y}, \tilde{U}, \tilde{V}$ are parametrized by X, Y, U, V respectively. Then, equations governing the line $\ell = \overline{\tilde{X}\tilde{Y}\tilde{U}\tilde{V}}$ can be translated into a map from (X, Y) to (U, V) by using the parametrizations. The five maps constructed from the configurations $I - V$ of the pencil of conics are exactly equivalent to the maps $F_I - F_V$ listed in Table 7.1.

A further investigation of quadrirational maps was made in [97] following the observation that the action of $(\mathcal{M}\ddot{o}b)^4$ in general destroys the Yang-Baxter property, although the maps $F_I - F_V$ in their canonical forms (see Table 7.1) are Yang-Baxter maps. The following proposition specifies the Yang-Baxter equivalence which differs from the quadrirational equivalence *i.e.* $(\mathcal{M}\ddot{o}b)^4$ -equivalence.

Proposition 7.1.1 *Let $\psi(a)$ be a parameter-dependent bijection in the form*

$$\psi(a) : \mathbb{CP}^1 \rightarrow \mathbb{CP}^1, \quad X \mapsto \psi_a(X). \quad (7.5)$$

If $\mathcal{R}(a, b)$ is a parametric Yang-Baxter maps, then the map $\tilde{\mathcal{R}}(a, b)$, defined as

$$\tilde{\mathcal{R}}(a, b) = \psi^{-1}(a) \times \psi^{-1}(b) \mathcal{R}(a, b) \psi(a) \times \psi(b), \quad (7.6)$$

is also a Yang-Baxter map.

The relation (7.6) is precisely the Yang-Baxter equivalence. For the F -families of quadrirational maps, it is observed in the literature (see *e.g.* [98]) that certain sub-cases of $(\mathcal{M}\ddot{o}b)^4$ preserve the Yang-Baxter property. This feature is clarified in the following proposition [97].

Proposition 7.1.2 *Let $s(a)$ be an involutive symmetry of the parametric Yang-Baxter map $\mathcal{R}(a, b)$ satisfying*

$$s(a)^2 = Id \quad \text{and} \quad s(a) \times s(b) \mathcal{R}(a, b) = \mathcal{R}(a, b) s(a) \times s(b). \quad (7.7)$$

Then, the map $\mathcal{R}^s(a, b)$, defined as

$$\mathcal{R}^s(a, b) = (s(a) \times Id) \mathcal{R}(a, b) (Id \times s(b)), \quad (7.8)$$

is also a Yang-Baxter map.

The proofs of Prop. 7.1.1 and 7.1.2 can be easily obtained by direct computations at the level of the parametric set-theoretical Yang-Baxter equation (6.9). One can understand that \mathcal{R}^s defined in (7.8) is not equivalent to \mathcal{R} in the sense of (7.6).

For quadrirational maps, the symmetry map s corresponds to Möbius transformation. In [97], s was carefully considered for each family of $F_I - F_V$. This led to an additional classification of five families, up to the Yang-Baxter equivalence (7.6), called H -families. Therefore, each family of the H -families is related to that of the F -families through the use of certain s . Their explicit forms are listed in Table 7.2 [97].

Precisely, the family H_I is related to F_I by taking $s(a)(X) \equiv \frac{a}{X}$. The case of H_{II} is more complicated in the sense that it is an equivalent form of H_{II} (not the form of H_{II} in Table 7.2) that is related to another equivalent form of F_{II} (again not F_{II} in Table 7.1) by a certain $s(k)$. The link between F_{II} and H_{II} will be explicitly shown in Appendix E. There are two families H_{III}^A and H_{III}^B derived from F_{III} by using $s(a)(X) \equiv -X$ and $s(a)(X) \equiv -\frac{X}{a}$ respectively. No s exists for F_{IV} , thus no H_{IV} . The map H_V is the well-known Adler map [115, 10], here derived from F_V by taking $s(a)(X) \equiv -X$.

Type	$f_{ab}(X, Y)$	$g_{ab}(X, Y)$	P
H_I	YP^{-1}	XP	$\frac{(1-b)XY+(b-a)Y+b(a-1)}{(1-a)XY+(a-b)X+a(b-1)}$
H_{II}	YP^{-1}	XP	$\frac{a+(b-a)Y-bXY}{b+(a-b)X-aXY}$
H_{III}^A	$\frac{Y}{a}P$	$\frac{X}{b}P$	$\frac{aX+bY}{X+Y}$
H_{III}^B	YP^{-1}	XP	$\frac{aXY+1}{bXY+1}$
H_V	$Y - P$	$X + P$	$\frac{a-b}{X+Y}$

Table 7.2: H -families of quadrirational maps

Therefore, up to the Yang-Baxter equivalence (7.6), we have ten families of quadrirational Yang-Baxter maps $F_I - F_V$ and $H_I - H_V^1$, whose canonical forms are listed in Table 7.1 and 7.2.

7.2 Deriving reflection maps

In this section, we provide a method to classify reflection maps for the ten families of quadrirational Yang-Baxter maps $F_I - F_V$ and $H_I - H_V$.

Recall Prop. 7.1.2 in which a symmetry map s is used to derive $\mathcal{R}^s(a, b)$ from $\mathcal{R}(a, b)$. The following proposition states that $\mathcal{R}(a, b)$ and $\mathcal{R}^s(a, b)$ share the same reflection maps.

Proposition 7.2.1 *The map $\mathcal{B}(a)$ is a parametric reflection map for the parametric Yang-Baxter map $\mathcal{R}(a, b)$ if and only if it is a parametric reflection map for the parametric Yang-Baxter map $\mathcal{R}^s(a, b)$, defined in (7.8).*

Proof: The proof of this proposition consists in writing the set-theoretical reflection equation with $\mathcal{R}^s(a, b)$ expressed in (7.8). Then, remarking for example that $(Id \times s(b))K_1(a) = K_1(a)(Id \times s(b))$ and using $s(a)^2 = Id$, one proves that this equation is equivalent to the set-theoretical reflection equation with $\mathcal{R}(a, b)$. ■

¹With the understanding that H_{IV} does not exist and there are two families H_{III}^A and H_{III}^B both related to F_{III} .

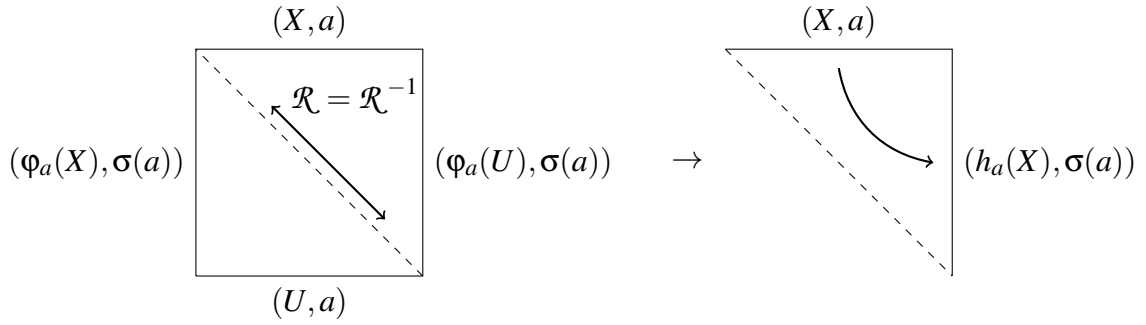


Fig. 7.2 : Folding

Following the arguments presented at the end of the previous section which relate the H -families to the F -families by the use of certain s , this proposition implies that the reflection maps for the families $F_I - F_V$ are the exactly same as the reflection maps for $H_I - H_V$ except for H_{II} . Therefore, in the following, we restrict our attention to the F -families. The particular case of H_{II} will be the subject of Appendix E.

To proceed, we propose an adaptation of the folding method. Roughly speaking, the idea is to see a reflection map as a Yang-Baxter map modulo some *folding* applied to the Yang-Baxter variables. Taking a quadrirational Yang-Baxter map in the form

$$\mathcal{R}(a, b) : (X, Y) \mapsto (U, V) \equiv (f_{ab}(X, Y), g_{ab}(X, Y)), \quad (7.9)$$

we impose the following *folding conditions*:

$$Y = \varphi_a(X), \quad V = \varphi_a(U), \quad b = \sigma(a), \quad (7.10)$$

where φ_a is a map depending on a . This can be viewed pictorially in Fig. 7.2 (remind that a Yang-Baxter map is represented by a square as depicted in Fig. 6.1). For convenience, we assume that σ is an involution as well as φ_a :

$$\sigma(\sigma(a)) = a, \quad \varphi_{\sigma(a)}(\varphi_a(X)) = X. \quad (7.11)$$

Considering the folding $Y = \varphi_a(X)$ and the form of $\mathcal{R}(a, b)$, we obtain two possibilities to express V in terms of X

$$V = \varphi_a(f_{a\sigma(a)}(X, \varphi_a(X))) = g_{a\sigma(a)}(X, \varphi_a(X)). \quad (7.12)$$

This provides a functional equation constraining admissible functions φ_a and σ . So, for each such admissible pair (φ_a, σ) , there is a well-defined map between V and X

which we denote h_a :

$$V = h_a(X), \tag{7.13}$$

and which can be computed using (7.12). The map h_a together with σ are the candidates for the reflection map \mathcal{K} .

To complete our set of functional equations, we can also look at the folding method from the point of view of the inverse map $\mathcal{R}^{-1}(a,b)$ which maps (U,V) to (X,Y) and the companion map $\overline{\mathcal{R}}(b,a)$ which maps (X,V) to (U,Y) . As stated in the previous section, for each F_τ , $\tau = I, II, \dots, V$, the companion map and inverse map coincide with the map itself:

$$\mathcal{R}^{-1}(a,b) : (U,V) \mapsto (X,Y) = (f_{ab}(U,V), g_{ab}(U,V)), \tag{7.14}$$

$$\overline{\mathcal{R}}(a,b) : (X,V) \mapsto (U,Y) = (f_{ab}(X,V), g_{ab}(X,V)), \tag{7.15}$$

where f_{ab} and g_{ab} are the same functions as those defined in (7.9).

Now taking the folding $V = \varphi_a(U)$ with the inverse map \mathcal{R}^{-1} results in

$$Y = \varphi_a(f_{a\sigma(a)}(U, \varphi_a(U))) = g_{a\sigma(a)}(U, \varphi_a(U)). \tag{7.16}$$

This gives an equivalent constraint to (7.12). Provided that admissible functions (φ_a, σ) and the related h_a are found, we deduce that $Y = h_a(U)$. In turn, given the folding conditions (7.10), one gets

$$Y = h_a(U), \quad V = h_a(X), \quad b = \sigma(a). \tag{7.17}$$

Comparing to (7.10), these relations are just folding conditions for the companion map $\overline{\mathcal{R}}$ (see Fig. 7.3). Due to the fact that $\mathcal{R} = \overline{\mathcal{R}}$, the folding maps φ_a and h_a play

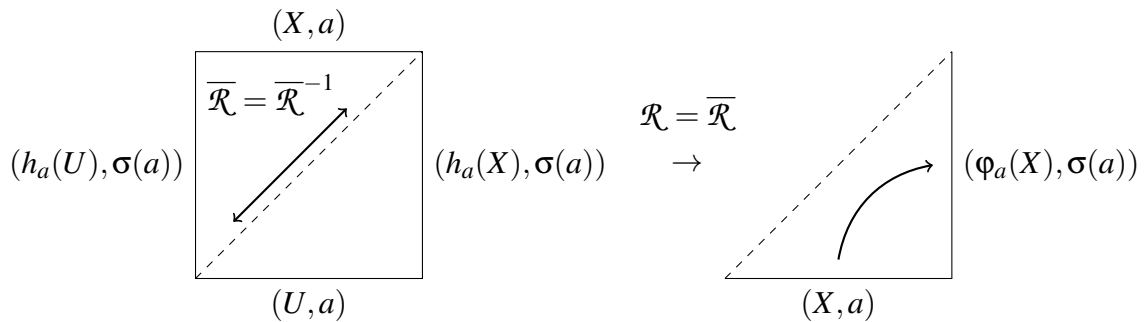


Fig. 7.3 : Duality

completely dual roles. Precisely, combining (7.17) and $\overline{\mathcal{R}}$ yields

$$Y = h_a(f_{a\sigma(a)}(X, h_a(X))) = g_{a\sigma(a)}(X, h_a(X)), \quad (7.18)$$

which is the dual form of (7.12).

Having clarified the duality of the folding conditions (7.10) and (7.17), we proceed to deriving reflection maps. First, the duality implies that given a σ there are two folding relations φ_a and h_a playing dual roles. If φ_a is chosen to be of a certain form, then h_a should be of the same form and vice versa. This is reminiscent of the properties derived in [14] concerning the quadrirationality—both the companion map and the map itself are birational. Also, the involution property (7.11) should hold for both φ_a and h_a . Therefore, it is natural to choose both φ_a and h_a to be Möbius transformations with the coefficients being polynomials of degree 1 in a :

$$\varphi_a(X) = \frac{p_1(a)X + p_2(a)}{p_3(a)X + p_4(a)}, \quad h_a(X) = \frac{q_1(a)X + q_2(a)}{q_3(a)X + q_4(a)}, \quad (7.19)$$

where $p_j(a) = p_j^0 + p_j^1 a$ and $q_j(a) = q_j^0 + q_j^1 a$, $j = 1, \dots, 4$. This corresponds to 16 free parameters a priori. We also choose σ to be an involutive Möbius transformation, which gives 3 additional parameters:

$$\sigma(a) = \frac{c_1 a + c_2}{c_3 a - c_1}. \quad (7.20)$$

Then, these 19 parameters are inserted into the following constraints as explained above:

$$h_a(X) = g_{a\sigma(a)}(X, \varphi_a(X)), \quad \varphi_{\sigma(a)}(\varphi_a(X)) = X, \quad h_{\sigma(a)}(h_a(X)) = X. \quad (7.21)$$

These operations have been performed with the help of symbolic computation software². The results lead to a complete characterization of φ_a , h_a and σ that will be reported in the following section.

We conclude this section by specifying the equivalence class for reflection maps.

Proposition 7.2.2 *Assume $\mathcal{R}(a, b)$ and $\tilde{\mathcal{R}}(a, b)$ are two equivalent Yang-Baxter maps up to the equivalence (7.6). They are related by the bijection $\psi(a)$. If $\mathcal{K}(a)$ and σ constitute a parametric reflection map for $\mathcal{R}(a, b)$, then the map $\tilde{\mathcal{K}}(a)$, defined as*

$$\tilde{\mathcal{K}}(a) = \psi^{-1}(\sigma(a)) \mathcal{K}(a) \psi(a), \quad (7.22)$$

²Here, we use *Mathematica*

together with σ constitute a reflection map for $\tilde{\mathcal{R}}(a, b)$.

The proof can be easily checked by taking both the forms (7.6) and (7.22) into the parametric set-theoretical reflection equation (6.17).

7.3 Classification of reflection maps

Solving the 19-parameter systems (7.19 - 7.21) for each family of $F_I - F_V$ by using the symbolic computation software gives classes of candidates for the reflection maps.

First, it is straightforward to check that the identity map, *i.e.* both h_a and σ are the identity map, is a solution for all families. In the following, we only present nontrivial solutions, *i.e.* either σ or h_a or both are not the identity maps. With the exception of one solution for the F_I family, all the maps satisfying (7.19 - 7.21) are reflection maps as we found by inspection. Therefore, in the context of quadrirational Yang-Baxter maps, a classification of involutive reflection maps is obtained.

Proposition 7.3.1 *Consider the quadrirational Yang-Baxter maps $F_I - F_V$ in their canonical forms. All the involutive reflection maps $(\varphi_a(X), \sigma(a))$ and $(h_a(X), \sigma(a))$, which are in the forms (7.19, 7.20) and satisfy the (duality and involution) constraints (7.21), are exhausted in Table 7.3, except for the identity map which is trivial. Moreover, we call these reflection maps quadrirational reflection maps.*

Proof: As we mentioned before, the results as well as the proof were obtained using the symbolic computation software. ■

Note that we did not find any solution for the F_V family other than the identity map. The duality property is explicitly shown in the table: the roles of h_a and φ_a can be swapped. All solutions depend on an arbitrary parameter μ . In view of discrete integrable systems, Yang-Baxter and reflection maps can be regarded as discrete systems defined on quadrilaterals and triangles respectively with the variables and parameters attached to the edges. Then, the free parameter μ represents an extra degree of freedom for the lattice parameters.

In the construction of the quadrirational maps $F_I - F_V$ in [14], singular analysis of the forms of f_{ab} and g_{ab} (see Eq. (7.3)) is another approach to classify quadrirational maps. It turns out that we can make use of these points in our construction to obtain other reflection maps which are referred to as *degenerate*. This is achieved by allowing $\varphi_a(X)$ in (7.12) to take the singular points of the corresponding family. For instance, in the most general case F_I , the singular points are $0, 1, \infty, \sigma(a)$. Each time a degenerate case is a solution, the set-theoretical reflection equation is satisfied for

Type	$\sigma(a)$	$h_a(X)$ (resp. $\varphi_a(X)$)	$\varphi_a(X)$ (resp. $h_a(X)$)
F_I	$\frac{\mu^2}{a}$	$\frac{\mu X}{a}$	$\frac{(X(1+\mu)-\mu-a)\mu}{X(a+\mu)-(1+\mu)a}$
	$\frac{a+\mu^2-1}{a-1}$	$\frac{(a+\mu^2-1)X}{X(a-\mu-1)+a\mu}$	$\frac{a+\mu-X\mu-1}{a-1}$
	$\frac{1-a}{a(\mu^2-1)+1}$	$\frac{(a-1)X}{X(a+\mu a-1)-a\mu}$	$\frac{\mu a+1-X\mu-a}{1+a(\mu^2-1)}$
F_{II}	$\frac{\mu^2}{a}$	$\frac{a}{\mu}(X-1)+1$	$-\frac{aX}{\mu}$
	$-a+2\mu$	$\frac{X}{2X-1}$	$\frac{a-\mu-aX}{a-2\mu}$
F_{III}	$\frac{\mu^2}{a}$	$\frac{aX}{\mu}$	$-\frac{aX}{\mu}$
F_{IV}	$-a+2\mu$	$-X$	$X-a+\mu$

Table 7.3: Reflection maps for quadrirational map $F_I - F_{IV}$

any map σ . Note that the duality property still holds for these degenerate cases. All the degenerate reflection maps are presented in Table 7.4.

According to Prop. 7.2.1, reflection maps for the H -families, except for H_{II} , are the same as those of F -families. Reflection maps for H_{II} will be shown in Appendix E. Note that, for each family of the H -families, the companion map does not coincide with the map itself due to the presence of the symmetry map s . This implies that the duality between h_a and φ_a is destroyed by s . However, thanks to Prop. 7.2.1, one can still conclude that for each σ , there are two reflection maps for each of the H -families.

Type	$h_a(X)$ (resp. $\varphi_a(X)$)	$\varphi_a(X)$ (resp. $h_a(X)$)
F_I	$\frac{\sigma(a)(a-1)X}{a(X-1)+\sigma(a)(a-X)}$	∞
	$\frac{a-X+\sigma(a)(X-1)}{a-1}$	0
	$\frac{\sigma(a)}{a}X$	1
	X	$\sigma(a)$
F_{II}	X	∞
	$\frac{a}{\sigma(a)}(X-1)+1$	0
	$\frac{a}{\sigma(a)}X$	1
F_{III}	X	∞
	$\frac{a}{\sigma(a)}X$	0
F_{IV}	X	∞
	$X-a+\sigma(a)$	0
F_V	X	∞

Table 7.4: Degenerate reflection maps

Quad-graph integrable systems with boundary

Recently, there has been considerable progress in the study of discrete integrable systems following various publications [28, 11, 29] in which discrete integrable systems were investigated on a more general framework called *quad-graphs*—planar graphs of cellular decompositions with quadrilateral faces—in contrast to the usual *regular square grid* \mathbb{Z}^2 . A significant step was made by Adler, Bobenko and Suris in [13] in which a classification of quad-graph integrable equations was obtained. The so-called *three-dimensional consistency* [91, 29] is at the heart of understanding the Adler-Bobenko-Suris (ABS) classification. Important notions such as discrete zero curvature representation and link to the discrete systems of Toda type were accordingly developed [29, 13]. This has laid the foundation for a vast number of interesting topics, and amongst them, we intend to ask the fundamental question of adding boundaries to quad-graph integrable systems.

The most striking feature of discrete integrable systems is probably that all the concepts and methods developed in the continuous theories have their deep roots in discrete systems. It is widely believed that, in many aspects, discrete systems are more fundamental than their continuous counterparts (see *e.g.* [92]). The generalization of discrete systems to quad-graphs has made the field more prominent, as integrable systems can now be defined on *arbitrary graphs* thanks to the quad-graph decompositions [29]. As yet the boundary problems for quad-graph systems have not been addressed, as only quad-graph configurations without boundary—decompositions of graphs with finite or infinite quadrilaterals—considered in the literature. Therefore, adding boundaries to quad-graph systems and understanding, in particular, the corresponding notions of integrability are problems of fundamental nature.

The introduction of reflection maps [38, 40] (see also Chapter 4 and 6) and, in particular, the classification of quadrirational reflection maps [40] (see also Chapter 7) represent another important motivation. This is because quadrirational Yang-Baxter maps can be considered as discrete systems with the Yang-Baxter variables assigned to the edges of quadrilaterals. Then, it turns out that quadrirational reflection maps are just integrable boundary conditions for such systems. Under the common concept of the $3D$ consistency, a link between quadrirational Yang-Baxter maps and quad-graph integrable systems have been unveiled from different angles [98, 72, 79]. This suggests that quadrirational reflection maps are also intimately linked to integrable boundary conditions for quad-graph integrable systems.

The objectives of this chapter are to discuss some exciting aspects of boundary problems for quad-graph integrable systems. First, the $3D$ consistency and the ABS classification [13] are briefly reviewed. Then, by adding boundaries to quad-graphs, we introduce carefully the notion of boundary conditions for quad-graph systems. Next, we propose a *three-dimensional boundary consistency* as a criterion for integrability. Integrable boundary conditions are incarnated in the so-call *boundary equations* that are also introduced. Following the ideas of [98] in which quadrirational Yang-Baxter maps are linked to quad-graph integrable equations by means of symmetry analysis, we show that quadrirational reflection maps can be used as a systematic tool to construct boundary equations that satisfy the $3D$ -boundary consistency. Finally, as an illustration, this construction of boundary equations is carried out for the equation $A1_{\delta}$ from the ABS classification. Boundary equations for other quad-graph equations will be presented in Appendix G

The results presented in this chapter were recently reported in [39]. It is worth noting that other interesting aspects of the problem such as Bäcklund transformations and zero curvature representations for the $3D$ -boundary consistency and link between boundary equations and the *three-leg forms* were also demonstrated in [39].

8.1 $3D$ -consistent equations on quad-graphs

This section reviews the $3D$ consistency [91, 29] and the ABS classification [13].

Equations of the ABS classification can be defined on an elementary quadrilateral in the form

$$Q(u_{00}, u_{10}, u_{01}, u_{11}, p, q) = 0, \quad (8.1)$$

where the fields $u_{00}, u_{10}, u_{01}, u_{11} \in \mathbb{CP}^1$ are assigned on the vertices and the lattice parameters $p, q \in \mathbb{C}$ on the edges (see Fig. 8.1). The equation $Q = 0$ satisfies the following properties:

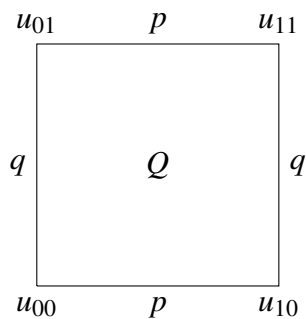


Fig. 8.1 : Equation Q on an elementary quadrilateral

- it is autonomous, *i.e.* the parameters p, q on the opposite edges of any quadrilateral face are equal.
- It is affine linear with respect to each variable, *i.e.*

$$\partial_{u_{kl}} Q(u_{00}, u_{10}, u_{01}, u_{11}, p, q) \neq 0, \quad \partial_{u_{kl}}^2 Q(u_{00}, u_{10}, u_{01}, u_{11}, p, q) = 0, \quad (8.2)$$

where k and $l = 0, 1$. As a result, Q can be solved with respect to each variable in a fractionally linear form of the other three.

- It is invariant under the group D_4 of the square symmetries, *i.e.*

$$\begin{aligned} Q(u_{00}, u_{10}, u_{01}, u_{11}, p, q) &= \varepsilon Q(u_{00}, u_{01}, u_{10}, u_{11}, q, p) \\ &= \sigma Q(u_{10}, u_{00}, u_{11}, u_{01}, p, q), \end{aligned} \quad (8.3)$$

where $\varepsilon, \sigma = \pm 1$.

The 3D consistency is the central criterion for integrability for the ABS classification. Precisely, it means that the equation (8.1) can be embedded into a 3D lattice in a consistent way so that each face of the 3D lattice represents the same equation Q (see Fig. 8.2). Given u_{000} , u_{100} , u_{001} and u_{010} , and p_1 , p_2 and p_3 , the equation (8.1) on three different faces gives three values u_{110} , u_{101} and u_{001} , *i.e.*

$$\begin{aligned} \{u_{000}, u_{100}, u_{010}, p_1, p_2\} &\rightarrow u_{110}, \\ \{u_{000}, u_{100}, u_{001}, p_1, p_3\} &\rightarrow u_{101}, \\ \{u_{000}, u_{010}, u_{001}, p_2, p_3\} &\rightarrow u_{001}. \end{aligned}$$

Then, repeat the process on the opposite faces, one gets

$$\begin{aligned} \{u_{001}, u_{101}, u_{011}, p_1, p_2\} &\rightarrow u_{111}, \\ \{u_{010}, u_{110}, u_{011}, p_1, p_3\} &\rightarrow \bar{u}_{111}, \\ \{u_{100}, u_{110}, u_{101}, p_2, p_3\} &\rightarrow \tilde{u}_{111}. \end{aligned}$$

The consistency means

$$u_{111} = \bar{u}_{111} = \tilde{u}_{111}. \quad (8.4)$$

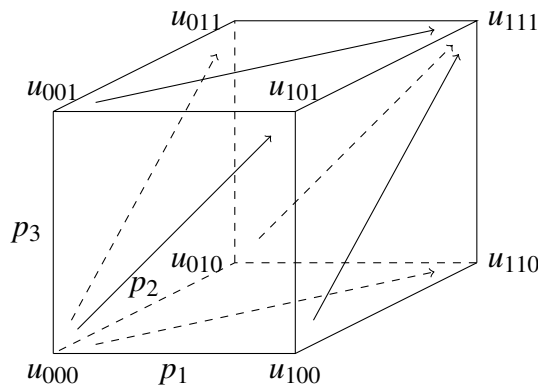


Fig. 8.2 : 3D consistency

For completeness, we list the equations of the ABS classification as follows:

$$\begin{aligned} (Q1) : & \quad p(u_{00} - u_{01})(u_{10} - u_{11}) - q(u_{00} - u_{10})(u_{01} - u_{11}) + \delta^2 pq(p - q) = 0, \\ (Q2) : & \quad p(u_{00} - u_{01})(u_{10} - u_{11}) - q(u_{00} - u_{10})(u_{01} - u_{11}) \\ & \quad + pq(p - q)(u_{00} + u_{10} + u_{01} + u_{11}) - pq(p - q)(p^2 - pq + q^2) = 0, \\ (Q3) : & \quad (q^2 - p^2)(u_{00}u_{11} + u_{10}u_{01}) + q(p^2 - 1)(u_{00}u_{10} + u_{01}u_{11}) \\ & \quad - p(q^2 - 1)(u_{00}u_{01} + u_{10}u_{11}) - \delta^2(p^2 - q^2)(p^2 - 1)(q^2 - 1)/(4pq) = 0, \\ (Q4) : & \quad \text{sn}(p)(u_{00}u_{10} + u_{01}u_{11}) - \text{sn}(q)(u_{00}u_{01} + u_{10}u_{11}) - \text{sn}(p - q)(u_{00}u_{11} + u_{10}u_{01}) \\ & \quad + \text{sn}(p - q)\text{sn}(p)\text{sn}(q)(1 + K^2 u_{00}u_{10}u_{01}u_{11}) = 0, \\ (H1) : & \quad (u_{00} - u_{11})(u_{10} - u_{01}) + q - p = 0, \\ (H2) : & \quad (u_{00} - u_{11})(u_{10} - u_{01}) + (q - p)(u_{00} + u_{10} + u_{01} + u_{11}) + q^2 - p^2 = 0, \\ (H3) : & \quad p(u_{00}u_{10} + u_{01}u_{11}) - q(u_{00}u_{01} + u_{10}u_{11}) + \delta^2(p^2 - q^2) = 0, \\ (A1) : & \quad p(u_{00} + u_{01})(u_{10} + u_{11}) - q(u_{00} + u_{10})(u_{01} + u_{11}) - \delta^2 pq(p - q) = 0, \end{aligned}$$

$$(A2) : \quad q(p^2 - 1)(u_{00}u_{01} + u_{01}u_{11}) - p(q^2 - 1)(u_{00}u_{10} + u_{01}u_{11}) \\ + (q^2 - p^2)(u_{00}u_{10}u_{01}u_{11} + 1) = 0.$$

We use the same titles (Q, H, A families) and forms as those used in [13] except for the equation Q4 which is in an equivalent form introduced in [71]. For Q4, $\text{sn}(p) \equiv \text{sn}(p; K)$ is the Jacobi elliptic function with modulus K . The free parameter δ appearing for equations Q1, Q3, H3 and A1 can be normalized either to 0 or either to ± 1 . Moreover, as proved in [13], the 3D consistency as well as the affinity and the D_4 -symmetry properties are preserved for each of the equations up to common Möbius transformations of the variables u_{00} , u_{10} , u_{01} and u_{11} .

8.2 Boundary conditions for quad-graph systems

In this section, the notion of quad-graph with boundary is clarified following standard procedure of discretizing surfaces. In particular, the notion of *boundary equations* is introduced that is used to represent boundary conditions of a quad-graph system with boundary.

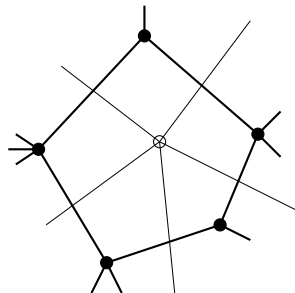


Fig. 8.3 : The vertex (white dot in the center) of $V(\mathcal{G}^*)$ dual to the face of $F(\mathcal{G})$

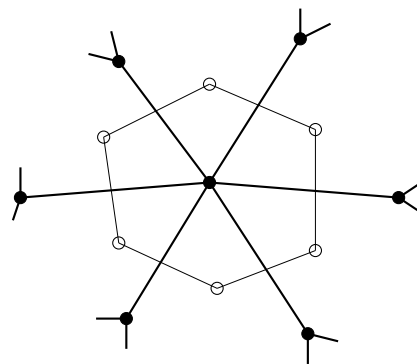


Fig. 8.4 : The face of $F(\mathcal{G}^*)$ dual to the vertex (black dot in the center) of $V(\mathcal{G})$

It is well-known that, in the case without boundary, an *arbitrary* cellular decomposition \mathcal{G} of a two-dimensional oriented surface can be "discretized" into quad-graphs [29]. The idea lies in the consideration of both the decomposition \mathcal{G} and its *dual decomposition* \mathcal{G}^* . Denote, respectively, by $F(\mathcal{G})$, $E(\mathcal{G})$ and $V(\mathcal{G})$ the set of faces, edges and vertices of \mathcal{G} . One can construct the dual cellular decomposition \mathcal{G}^* where $V(\mathcal{G})$, $E(\mathcal{G})$ and $F(\mathcal{G})$ of \mathcal{G} are in one-to-one correspondence to the faces $F(\mathcal{G}^*)$, edges $E(\mathcal{G}^*)$ and vertices $V(\mathcal{G}^*)$ of \mathcal{G}^* respectively. This correspondence is well illustrated in Fig. 8.3 and 8.4¹. The quad-graph decomposition of \mathcal{G} , called

¹These figures are borrowed from [29].

double \mathcal{D} , is obtained as follows:

- the set of the vertices of \mathcal{D} is the union of the set of the vertices of both \mathcal{G} and \mathcal{G}^* i.e. $V(\mathcal{D}) = V(\mathcal{G}) \cup V(\mathcal{G}^*)$;
- the set of the quad-tuples (v_1, f_1, v_2, f_2) , where (v_1, v_2) is an edge of \mathcal{G} and (f_1, f_2) is its dual edge, constitutes the faces of \mathcal{D} .

It is clear that all the faces of \mathcal{D} are quadrilateral.

This procedure can be easily generalized to the case with boundary (see e.g. [88]). Let \mathcal{S} be a two-dimensional oriented surface with a boundary. Consider a cellular decomposition \mathcal{G} of this surface with the only restriction that there is no edge on the boundary. A *quad-graph with boundary* is a cellular decomposition with the following additional properties:

- no edges are on the boundary of the surface;
- the faces which contain no points of the boundary are quadrilateral;
- the faces which contain points of the boundary are triangular.

An example of such cellular decomposition is given in Fig. 8.5. Besides the usual quad-graph decomposition of the *bulk* of \mathcal{S} , the boundary is now characterized by triangular blocks. A quad-graph with boundary is thus represented by elementary blocks of quadrilaterals and triangles.

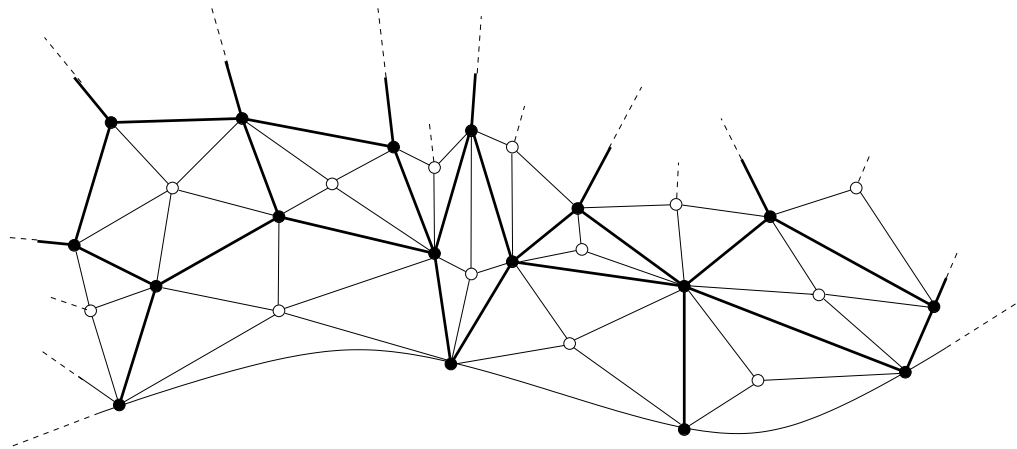


Fig. 8.5 : Example of a surface with a boundary and its quad-graph decomposition. The "horizontal" curved line is the boundary of \mathcal{S} . The black dots and the thick straight lines are, respectively, the vertices and edges of the initial cellular decomposition \mathcal{G} . The white dots are the vertices of the dual graph \mathcal{G}^* (the edges of \mathcal{G}^* are not presented). Black and white dots are the vertices of the quad-graph and the thin straight lines are its edges.

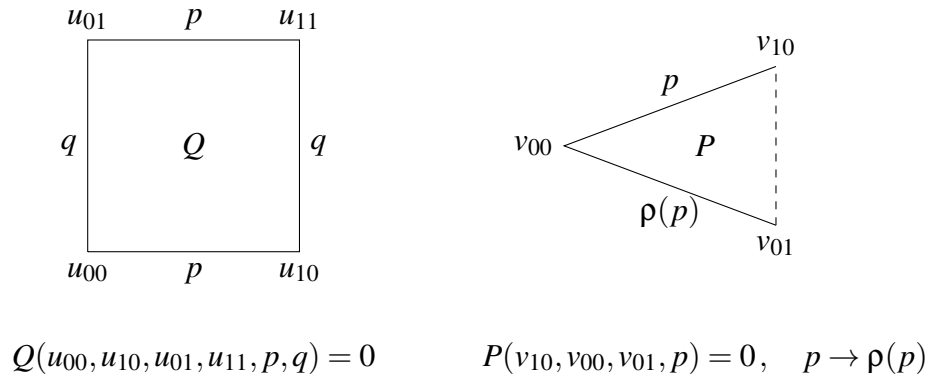


Fig. 8.6 : Elementary blocks to construct a quad-graph system with boundary

We are now in the position to define discrete systems on quad-graphs in the presence of boundaries. As presented in the previous section, a quad-graph equation—equation on the bulk—is represented by Eq. (8.1) with the fields and parameters assigned on the vertices and edges of a quadrilateral (see also the left-hand side of Fig. 8.6). The new elementary block needed to describe the boundary dynamics is the following equations defined on a triangle (see the right-hand side of Fig. 8.6):

$$P(v_{10}, v_{00}, v_{01}, p) = 0, \quad p \rightarrow \rho(p), \quad (8.5)$$

where v_{10}, v_{00}, v_{01} are fields assigned on the vertices and p is the lattice parameter assigned on one edge. We also require that the other edge of the triangle is associated to the lattice parameter $\rho(p)$ where ρ is a function of p . In Fig. 8.6, the following convention for P and ρ is taken: v_{10}, v_{01} in (8.5), namely the first and third variables of P , are vertices on the boundary—in Fig 8.6 the dashed line (v_{10}, v_{01}) represents the boundary—and the parameter p is assigned on the edge (v_{10}, v_{00}) formed by the first and second variables of P . We will call both P and ρ defined in (8.5) *boundary equation* that describe boundary dynamics of the system. Examples of boundary equations will be shown later in this chapter.

8.3 Integrability: the 3D-boundary consistency

The 3D consistency condition [91, 29] is widely considered to be a working definition of integrability for quad-graph equations [29, 13]. By analogy, we propose, in this section, a three-dimensional consistency condition, that takes account of the the presence of boundaries, to give a criterion for integrability for quad-graph systems with boundary. This consistency condition is referred to as *three-dimensional*

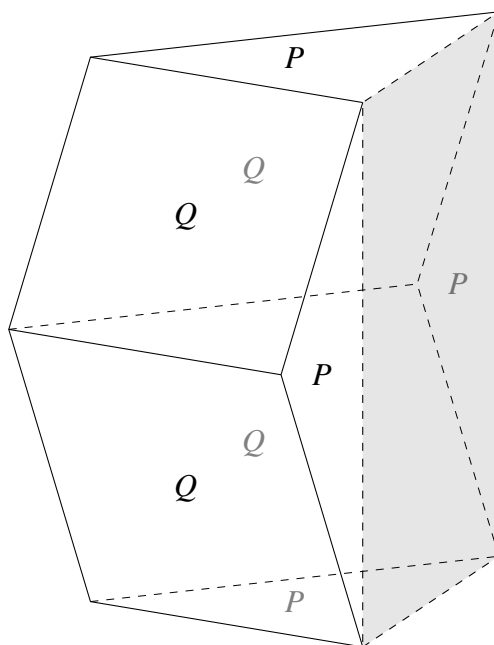


Fig. 8.7 : 3D-boundary consistency around a half of a rhombic dodecahedron

boundary consistency.

This condition is in fact a compatibility condition between the bulk equation Q defined on a quadrilateral and the boundary equation P and ρ defined on a triangle (see Fig. 8.6). Instead of a cube for the 3D consistency (see Fig. 8.2), the 3D-boundary consistency lies on a half of a rhombic dodecahedron as displayed in Fig. 8.7. The consistency is that the quadrilateral and triangular faces of Fig. 8.7 are represented by the same equations of motion on the quadrilateral and triangle.

More precisely, following the notations of Fig. 8.8, given u_{100} , u_{000} and u_{101} that are black dots in Fig. 8.8 and the lattice parameters p and q attached to the edges (u_{000}, u_{100}) and (u_{000}, u_{001}) respectively, first, one has the following three equations:

$$\begin{aligned} Q(u_{000}, u_{100}, u_{001}, u_{101}, p, q) &= 0, \\ P(u_{100}, u_{000}, u_{010}, p) &= 0, \quad p \rightarrow \rho(p), \\ P(u_{100}, u_{101}, u_{102}, q) &= 0, \quad q \rightarrow \rho(q), \end{aligned}$$

which give respectively the values of u_{001} , u_{010} and u_{102} that are white dots in Fig. 8.8. Then, taking account of the change of p and q through ρ , the equations

$$\begin{aligned} Q(u_{001}, u_{101}, u_{002}, u_{102}, p, \rho(q)) &= 0, \\ Q(u_{010}, u_{000}, u_{011}, u_{001}, \rho(p), q) &= 0, \end{aligned}$$

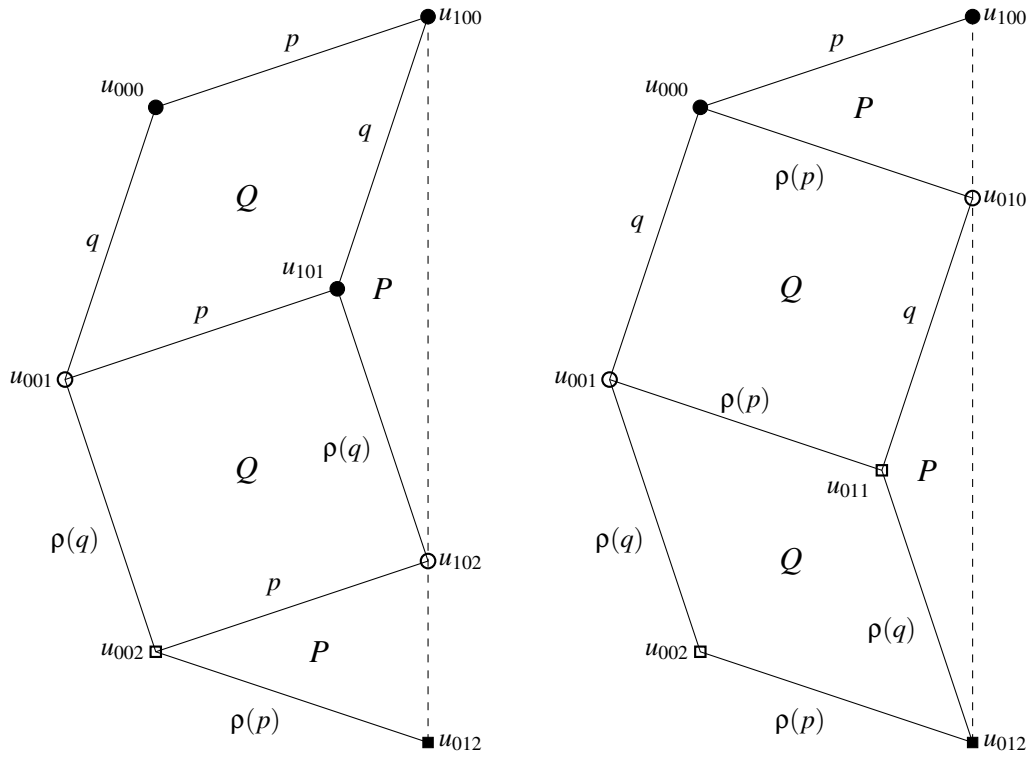


Fig. 8.8 : 3D-boundary consistency

give respectively the values of u_{002} and u_{011} (white squares in Fig. 8.8). Finally, the three equations

$$\begin{aligned} Q(u_{011}, u_{001}, u_{012}, u_{002}, \rho(p), \rho(q)) &= 0, \\ P(u_{102}, u_{002}, u_{012}, p) &= 0, \quad p \rightarrow \rho(p), \\ P(u_{010}, u_{011}, u_{012}, q) &= 0, \quad q \rightarrow \rho(q), \end{aligned}$$

provide three ways to compute u_{012} (black square in Fig. 8.8) which must be compatible.

For a given Q , to obtain a boundary equation P and ρ which preserves the integrability, one needs to solve the 3D-boundary consistency condition. We call quad-graph integrable systems with boundary the data of a quad-graph with boundary as well as the functions Q , P and ρ which satisfy the 3D consistency and the 3D-boundary consistency.

It is worth noting that Fig. 8.7 and 8.8 are closely related to Fig. 6.4 and 6.5 that are the pictorial representation of the set-theoretical reflection equation which also consists in certain consistency condition between Yang-Baxter maps and reflection maps. This link will be explored in the following section.

8.4 From reflection maps to boundary equations

In [98], a nice approach to connect $3D$ -consistent quad-graph equations to Yang-Baxter maps was established. The main idea of [98] is to explore the $3D$ consistency property of both integrable schemes—quad-graph equations on one hand and Yang-Baxter maps on the other—by considering a suitable change of variables from the vertex variables to edge variables. Technically, this connection was concretized by identifying certain lattice invariants of quad-graph equations through the use of the *Lie point symmetry* analysis [95, 96]. In [100], a complete list of Lie point symmetries for the equations from the ABS classification were obtained. Based on the results of [98] and [100], in this section, first, a list of Yang-Baxter maps is obtained by considering the equations of the ABS classification. For the sake of space, this list will be reported in Appendix F. Interestingly, all the Yang-Baxter maps obtained belong to the classification of quadrirational Yang-Baxter maps [14, 97] (see also Chapter 7). Then, motivated by the similarity between the $3D$ -boundary consistency and the set-theoretical reflection equation, we show that the quadrirational reflection maps classified in [40] (see also Chapter 7) can be used as a systematic tool to generate boundary equations. As a results, a number of boundary equations for the quad-graph equations of the ABS classification will be presented in Appendix G.

We start with a brief review of the method developed in [98] in which Yang-Baxter maps were derived from $3D$ -consistent equations. Given a quad-graph equation

$$Q(u_{00}, u_{10}, u_{01}, u_{11}, p, q) = 0, \quad (8.6)$$

let G_ε be a connected one-parameter group of transformations acting on the variables u_{00} , u_{10} , u_{01} and u_{11} :

$$G_\varepsilon : (u_{00}, u_{10}, u_{01}, u_{11}) \mapsto (\hat{u}_{00}, \hat{u}_{10}, \hat{u}_{01}, \hat{u}_{11}). \quad (8.7)$$

This transformation is said to be a symmetry of (8.6), if

$$Q(\hat{u}_{00}, \hat{u}_{10}, \hat{u}_{01}, \hat{u}_{11}, p, q) = 0, \quad (8.8)$$

whenever (8.6) holds. The corresponding infinitesimal action reads

$$\mathbf{v}Q = 0, \quad (8.9)$$

where \mathbf{v} is the infinitesimal generator of G_ε in the form

$$\mathbf{v} = \eta_{00} \frac{\partial}{\partial u_{00}} + \eta_{10} \frac{\partial}{\partial u_{10}} + \eta_{01} \frac{\partial}{\partial u_{01}} + \eta_{11} \frac{\partial}{\partial u_{11}}. \quad (8.10)$$

Clearly here G_ε is a Lie group whose group structure can be obtained using the exponential map. The quantity η_{kl} , k and $l = 0, 1$, that is *characteristic* of G_ε , depends precisely on the vertex (kl) :

$$\eta_{kl} = \frac{d}{d\varepsilon} G_\varepsilon(u_{kl}). \quad (8.11)$$

This justifies the use of the term "one-point Lie symmetry" for G_ε and \mathbf{v} . Methods to obtain the one-point characteristic η^2 for quad-graph equations can be seen in [82, 83]. Knowing η , the following step is to identify a *lattice invariant* I satisfying

$$\mathbf{v}I = 0, \quad (8.12)$$

and use the lattice invariant to define the edge variables (X, Y, U, V) from the vertex variables $(u_{00}, u_{10}, u_{01}, u_{11})$ (see Fig. 8.9) by

$$X = I(u_{00}, u_{10}), \quad Y = I(u_{10}, u_{11}), \quad U = I(u_{01}, u_{11}), \quad V = I(u_{00}, u_{01}). \quad (8.13)$$

Here, the form of I can be easily obtained using the *method of characteristics*. Having the $3D$ -consistent equation Q (8.6) and the change of variables (8.13), one can obtain two relations relating the four edge variables X, Y, U and V . Solving this two relations gives a map $\mathcal{R} : (X, Y) \mapsto (U, V)$. In [97], it was shown that if such map is unique, then it is a Yang-Baxter map. The proof is well illustrated in Fig. F.1 in which the $3D$ consistency of Q guarantees the Yang-Baxter property of \mathcal{R} .

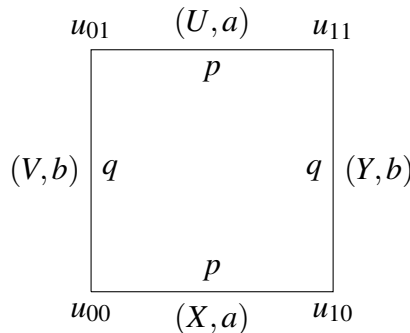


Fig. 8.9 : Link between quad-equation and Yang-Baxter map

²We drop the subscript kl with the understanding that η depends on its lattice coordinate kl .

Therefore, in order to derive Yang-Baxter maps from the 3D-consistent quad-graph equations, it is crucial to have the symmetries of the latter. Study of the symmetries of the quad-graph equations from the ABS classification was made in [100]. In contrast to the one-point symmetry (8.11), the authors considered a more general symmetry called *five-point symmetry* in which the characteristic η depends on five points. A complete list of the five-point symmetries for the ABS classification was also obtained [100]. For the purpose of linking quad-graph equations to Yang-Baxter maps, we restrict ourselves to the class of one-point symmetries (8.11) that is indeed a subclass of the five-point symmetries. Using the corresponding results exhausted in [100], it is straightforward to obtain the Yang-Baxter maps corresponding to the ABS classification. They are reported in Table F.1 in Appendix F. Interestingly, all the Yang-Baxter maps obtained here belong to the quadrirational yang-Baxter maps classified in [14, 97] (see also Chapter 7).

Remark 8.4.1 *The importance of Table F.1 is that a correspondence between the two classified integrable schemes: the ABS classification on one hand and the quadrirational Yang-Baxter maps on the other, is established. However, the correspondence is not "complete" due to the fact that for families $Q2$, $Q3_{\delta=1}$ and $Q4$ ($K \neq \pm 1$) there is no one-point symmetry [100]³. Similar correspondence was also obtained in [79, 78]⁴ using an "inverse" approach that derives 3D-consistent equations from quadrirational Yang-Baxter maps.*

Remark 8.4.2 *Several technical difficulties take place here to establish such quad-graph equation-Yang-Baxter map correspondence. First, the quadrirational Yang-Baxter maps obtained using the symmetries of the quad-graph equations are in general not in their canonical forms as that listed in the Table 7.1 and 7.2. Up to the Yang-Baxter equivalence (7.6), one needs to find suitable transformations transforming them into their canonical forms in order to identify them with the maps in Table 7.1 and 7.2. Second, the parameters a, b of the quadrirational Yang-Baxter maps are expressed in terms of the lattice parameters p, q of quad-graph equations. A transformation $\phi : (p, q) \rightarrow (a, b)$ is also needed to recognize the maps with their canonical forms. These two features will be discussed in the following section and also in Appendix F when going through the examples.*

³In [100], a one-point symmetry was given in the case of $Q4$ ($K = \pm 1$) which would generate a Yang-Baxter map. However, due to the equivalence between $Q3_{\delta=0}$ and $Q4$ ($K = \pm 1$) (here we thank A.P. Veselov for showing us such correspondence), $Q4$ ($K = \pm 1$) will give the same Yang-Baxter map, that is H_1 , as $Q3_{\delta=0}$ does. Indeed, $Q4$ ($K = \pm 1$) can be obtained from $Q3_{\delta=0}$ by performing $x \mapsto \frac{x-1}{x+1}$ to the vertice variables and $p \rightarrow e^{2p}$, $q \rightarrow e^{2q}$ to the paramters.

⁴We thank P. Kassotakis and M. Nieszporski for providing us their unpublished paper [78].

Having established the quad-graph equation-Yang-Baxter map correspondence (see Table F.1), we now proceed to deriving boundary equations—equations in the form (8.5) together with a $3D$ -consistent quad-graph equation satisfying the $3D$ -boundary consistency—from the quadrirational reflection maps [40] (see Chapter 7). Let a quad-graph equation from the ABS classification be in the form

$$Q(u_{00}, u_{10}, u_{01}, u_{11}, p, q) = 0. \quad (8.14)$$

Assume that it possesses some one-point symmetries so that certain quadrirational Yang-Baxter maps denoted by $\mathcal{R}(p, q)$ can be accordingly obtained. Here the parameters p, q of \mathcal{R} are those of Q . Let the reflection maps for \mathcal{R} be in the form

$$\mathcal{K}: (X, a) \mapsto (h_a(X), \sigma(a)), \quad X \in \mathcal{S}, \quad a \in \Sigma. \quad (8.15)$$

Then, for each Q in the form (8.14), its boundary equations can be written as

$$P(u_{10}, u_{00}, u_{01}, p) \equiv I(u_{00}, u_{01}) - h_p(I(u_{00}, u_{10})) = 0, \quad p \rightarrow \rho(p) \equiv \sigma(p). \quad (8.16)$$

The formula (8.16) is the main result of this section. This states that, for a given Q , once its associated Yang-Baxter maps \mathcal{R} are known, reflection maps \mathcal{K} of \mathcal{R} give boundary equations, *i.e.* P and ρ , which along with Q satisfy the $3D$ -boundary consistency. Indeed, the origin of this formula comes from the folding method explained in Chapter 7 in the aim of constructing reflection maps. When folding a square in half (see Fig. 7.2), through the corresponding change of variables (8.13), one gets (8.16). Our construction also ensures that Q and P satisfy the $3D$ -boundary consistency property since the corresponding Yang-Baxter and reflection maps satisfy the set-theoretical reflection equation. In other word, besides the quad-graph equation-Yang-Baxter map correspondence, the formula (8.16) gives rise to the underlying correspondence between boundary equations and reflection maps. Next, we can put the quadrirational reflection maps classified in Chapter 7 into use. As a result, a number of boundary equations for various quad-graph equations from the ABS classification will be shown in Appendix G. Note that we make no claim of completeness, and a method for a complete classification is in fact an interesting open problem.

8.5 Boundary equations for $A1_{\delta=0}$ as an example

In this section, boundary equations for the quad-graph equation $A1_{\delta=0}$ from the ABS classification are explicitly constructed using the method introduced in the previous section, in order to illustrate certain technical subtleties.

In order to use the formula (8.16), the main technical obstacle is to find the corresponding reflection maps for the quadrirational Yang-Baxter maps derived from the quad-graph equation. To fix notation, we denote a quad-graph equation by

$$\mathcal{Q}(u_{00}, u_{10}, u_{01}, u_{11}, p, q) = 0, \quad (8.17)$$

with p, q being the lattice parameters and a (parametric) quadrirational Yang-Baxter map by

$$\mathcal{R}(a, b) : (X, Y) \mapsto (U = f_{ab}(X, Y), V = g_{ab}(X, Y)), \quad (8.18)$$

with a, b being the map parameters. Then, the aim is to use the classification of the quadrirational reflection maps that were presented in Table 7.3. However, as mentioned in Remark 8.4.2, the quadrirational Yang-Baxter maps obtained from a quad-graph equation are in general not in their canonical forms, which implies that the reflection maps from Table 7.3 cannot be directly used. Recall the Yang-Baxter equivalence (7.6) and the "reflection equivalence" (7.22). For both of them, a certain bijection $\psi(a) : \mathbb{CP}^1 \rightarrow \mathbb{CP}^1$ is evolved. Now, to have correct reflection maps for (8.16), one needs to find such $\psi(a)$. Moreover, as pointed out in Remark 8.4.2, a transformation ϕ transforming parameters p, q to a, b is also required.

Precisely, the equation $A1_{\delta=0}$ is in the form

$$\mathcal{Q}(u_{00}, u_{10}, u_{01}, u_{11}, p, q) = p(u_{00} + u_{01})(u_{10} + u_{11}) - q(u_{00} + u_{10})(u_{01} + u_{11}). \quad (8.19)$$

For $A1_{\delta=0}$, three one-point symmetry generators were given in [100]:

$$\eta_1 = (-1)^{k+l}, \quad \eta_2 = u_{00}, \quad \eta_3 = (-1)^{k+l} u_{00}^2. \quad (8.20)$$

Using the method of characteristics, the corresponding invariants I_1 , I_2 and I_3 read

$$I_1(s, t) = s + t, \quad I_2(s, t) = \frac{s}{t}, \quad I_3(s, t) = \frac{1}{s} + \frac{1}{t}. \quad (8.21)$$

Note that all these invariants can be defined up to a certain constant which represents apparently an additional parameter for the associated Yang-Baxter maps. However, this extra parameter can be easily removed by taking account of the Yang-Baxter

equivalence (7.6). Thus, without loss of generality, we choose I_i , $i = 1, 2, 3$ to be in its simplest form (8.21).

For I_1 , the lattice invariants—Yang-Baxter variables—read

$$X = u_{00} + u_{10}, \quad Y = u_{10} + u_{11}, \quad U = u_{01} + u_{11}, \quad V = u_{00} + u_{01}, \quad (8.22)$$

which satisfy

$$X - Y = V - U, \quad pVY - qXU = 0. \quad (8.23)$$

This yields the relations

$$f_{pq}(X, Y) = pY \left(\frac{X - Y}{qX - pY} \right), \quad g_{pq}(X, Y) = f_{qp}(Y, X), \quad (8.24)$$

which represent a quadrirational Yang-Baxter map. To recognize the family to which this map belongs, one takes the transformation in the sense of the Yang-Baxter equivalence (7.6) with $\psi(p) : X \mapsto pX$ and also a transformation $\phi : p \rightarrow a, q \rightarrow b$ acting on the parameters. It is straightforward to check that (8.24) is equivalent to the F_{III} quadrirational Yang-Baxter map (see Table 7.1). For this family, we have the following nontrivial reflection maps (see also Table 7.3):

$$\sigma(a) = \frac{\mu^2}{a}, \quad h_a(X) = \frac{aX}{\mu} \quad \text{or} \quad h_a(X) = -\frac{aX}{\mu}, \quad (8.25)$$

where μ is a free parameter. Performing the transformation in the sense of the "reflection equivalence" (7.22) with $\tilde{\psi}(a) \equiv \psi^{-1}(a) : X \rightarrow \frac{X}{a}$ and also $\tilde{\phi} : a \rightarrow p, b \rightarrow q$, one obtains the reflection maps for (8.24). They read

$$\sigma(p) = \frac{\mu^2}{p}, \quad h_p(X) = \frac{\mu X}{p} \quad \text{or} \quad h_p(X) = -\frac{\mu X}{p}. \quad (8.26)$$

Inserting this into the formula (8.16) yields the boundary equations for $A1_{\delta=0}$:

$$P(x, y, z, p) = \mu(x + y) - p(y + z), \quad \text{or} \quad P(x, y, z, p) = \mu(x + y) + p(y + z), \quad (8.27)$$

both valid with $\rho(p) \equiv \sigma(p) = \frac{\mu^2}{p}$. Note that in this case, the two possibilities for $P = 0$ are related by the transformation $\mu \rightarrow -\mu$ which leaves $\rho(p)$ invariant so that we only have one boundary equation here.

Let us perform the same analysis for I_2 . The Yang-Baxter variables are

$$X = u_{00}/u_{10}, \quad Y = u_{10}/u_{11}, \quad U = u_{01}/u_{11}, \quad V = u_{00}/u_{01}, \quad (8.28)$$

and they satisfy

$$XY = UV, \quad pX(Y+U)(Y+1) - qY(X+1)(U+1) = 0, \quad (8.29)$$

which yields

$$f_{pq}(X, Y) = \frac{qY - pXY + qXY - pXY^2}{p + pY - qY - qXY}, \quad g_{pq}(X, Y) = f_{qp}(Y, X). \quad (8.30)$$

Now, letting $\psi : X \mapsto -X$ and $\phi : p \rightarrow a, q \rightarrow b$, and performing the transformation (7.6) with ψ , one obtains from (8.30) the H_{II} quadrirational Yang-Baxter map (see Table 7.2). For this family, we have the following reflection maps (see Appendix E):

$$\sigma(a) = \frac{\mu^2}{a}, \quad h_a(X) = \frac{a + \mu - X\mu}{a}, \quad \text{or} \quad h_a(X) = \frac{aX}{aX + \mu - X\mu}, \quad (8.31)$$

$$\sigma(a) = -a + 2\mu, \quad h_a(X) = -X, \quad \text{or} \quad h_a(X) = \frac{a + (X-1)\mu}{aX + \mu - X\mu}, \quad (8.32)$$

where μ is a free parameter. Performing the transformation (7.22) with $\tilde{\psi} \equiv \psi^{-1} = \psi$ and $\tilde{\phi} : a \rightarrow p, b \rightarrow q$, one gets the following reflection maps for (8.30):

$$\sigma(p) = \frac{\mu^2}{p}, \quad h_p(X) = -\frac{p + \mu + X\mu}{p}, \quad \text{or} \quad h_p(X) = \frac{pX}{-pX + \mu + X\mu}, \quad (8.33)$$

$$\sigma(p) = -p + 2\mu, \quad h_p(X) = -X, \quad \text{or} \quad h_p(X) = \frac{p - (1+X)\mu}{pX - (1+X)\mu}. \quad (8.34)$$

Inserting them into the formula (8.16) yields the boundary equations

$$P(x, y, z, p) = px(y+z) + (x+y)z\mu, \quad \text{or} \quad P(x, y, z, p) = y(p(y+z) - (x+y)\mu), \quad (8.35)$$

both valid with $\rho(p) \equiv \sigma(p) = \frac{\mu^2}{p}$, and,

$$P(x, y, z, p) = y(x+z), \quad \text{or} \quad P(x, y, z, p) = p(y^2 - xz) - (x+y)(y-z)\mu, \quad (8.36)$$

both valid for $\rho(p) \equiv \sigma(p) = -p + 2\mu$. Here the two relations in (8.35) are equivalent, if we consider $P = 0$ and the transformation $\mu \rightarrow -\mu$.

Finally, using I_3 gives again the relations (8.23) so that we obtain the F_{III} quadrirational Yang-Baxter map. Therefore, we can use the same reflection maps (8.26)

here. Expressions of boundary equations are in the form

$$P(x, y, z, a) = ax(y + z) + (x + y)z\mu, \quad \text{or} \quad P(x, y, z, a) = ax(y + z) - (x + y)z\mu, \quad (8.37)$$

both valid with $\rho(a) = \frac{\mu^2}{a}$. These are in fact the same solutions under the transformation $\mu \rightarrow -\mu$ and coincide with the first solutions (8.35) already obtained from the use of I_2 .

All boundary equations obtained here for the equation $A1_{\delta=0}$ are summarized in Table G.3 in Appendix G. One can show by direct computation that all P and ρ found here together with $A1_{\delta=0}$ satisfy the $3D$ -boundary consistency. Example of boundary equations for other equations from the ABS classification will also be shown in Appendix G.

Conclusion

This thesis has investigated the fundamental problem of adding boundaries to integrable systems for various integrable schemes. The key contributions are as follows:

- in Chapter 3, classes of integrable BCs for the vector NLS equation on the half-line were derived. N -soliton reflections in the presence of an integrable boundary were constructed. An interesting phenomenon of transmission between different components of vector solitons before and after interacting with the boundary was demonstrated.
- In Chapter 4, the factorization property of the soliton-soliton and soliton-boundary interactions, in the context of the vector NLS equation on the half-line, were fully understood by virtue of the set-theoretical Yang-Baxter and set-theoretical reflection equations.
- In Chapter 5, N -soliton reflections for the vector NLS equation on the half-line were constructed using a space-evolution method that we also introduced.
- In Chapter 6, we introduced various aspects of reflection maps, that are solutions of the set-theoretical reflection equation.
- In Chapter 7, a classification of quadrirational reflection maps was obtained.
- In Chapter 8, boundaries were added to quad-graph integrable systems and BCs were encoded into boundary equations. A criterion for integrability was established using a three-dimensional boundary consistency. Integrable boundary equations were found for a number of quad-graph equations.

These results can be naturally extended to the following open questions. First, as to soliton models on the half-line, the method developed for solving the vector

NLS equation on the half-line can be adapted to other soliton models which also possess the folding symmetry in space variable *i.e.* transforming the variable x to $-x$. As remarked in the end of Chapter 5, the space-evolution method seems to be of particular interest to treat half-line problems. It provides a physical way to transform the nonlinearly coupled system (3.55) to the linearly coupled system (5.26), although the precise transformation is unknown. It would be interesting to unveil such a linearization process. In the context of quadrirational reflection maps, one can also seek their geometric interpretations in terms of pencil of conics as the constructions of quadrirational Yang-Baxter maps. Also, following the introduction of the zero curvatures conditions for the $3D$ -boundary consistency in [39], one can also look for similar structure for the set-theoretical reflection equation. Finally, the folding technique presented in various places in this thesis shows how relevant it is in the integrable theories with boundaries. Again using folding technique seems to be a good tool to classify boundary equations for quad-graph equations.

We stress that the notions of reflection maps and integrable boundaries for quad-graph systems consist of *novel* aspects in the discipline. With the introduction of the $3D$ -boundary consistency [39] (see also Chapter 8), we believe that a vast amount of interesting topics has been open, amongst which are: finding a method for classifying boundary equations for quad-graph equations; tackling the problem of posing the initial-boundary value problem for a quad-graph system with a boundary; finding soliton solutions on quad-graphs with boundary; implementing the discrete inverse scattering method with boundaries in light of Fokas method; taking the continuous limits of boundary equations, etc.

Appendices

Unified transform method and linearizable boundary conditions

The purposes of this chapter are 1) to adapt the unified transform method to the vector NLS equation on the half-line; 2) to derive the linearizable boundary conditions that are equivalent to the integrable boundary conditions obtained in Sec. 3.1.

The unified transform method was developed by Fokas (see *e.g.* [51, 52, 54]) aiming at solving two-dimensional partial differential equations with generic initial-boundary conditions. The main idea lies in the simultaneous treatments of both the x and t -part of the Lax pair. It turns out that the initial and boundary conditions can be encoded into two scattering systems through the direct scattering processes of both the x -part and t -part of the Lax pair. Then the solutions of the original system with generic boundary conditions are nicely translated into a Riemann-Hilbert (RH) problem in which the jump matrix contains all the information of the initial-boundary conditions. Indeed, the unified transform method can be regarded as a generalization of the usual ISM. It provides an ideal and powerful framework to study soliton equations on the half-line [52, 53, 32, 57]. In particular, a class of boundary conditions that are called *linearizable boundary conditions* are shown to be of particular interest [52, 53, 54] and consists of the main issues of this chapter.

We follow the standard presentation of the unified transform method to collect main results needed in this chapter. Details and proofs are referred to [57] in which the scalar NLS equation on the half-line was investigated in detail.

A.1 From Lax pair to global relation

To be concrete, let the commutator operator $\hat{\Sigma}_3$ act as

$$\hat{\Sigma}_3 A = [\Sigma_3, A], \quad e^{A\hat{\Sigma}_3} B = e^{A\Sigma_3} B e^{-A\Sigma_3}, \quad (\text{A.1})$$

with Σ_3 being defined in (2.6). Define an exact one-form \mathcal{F} as

$$\mathcal{F}(x, t, k) = e^{i\phi(x, t, k)\hat{\Sigma}_3} (Q\Phi(x, t, k)dx + Q_T\Phi(x, t, k)dt), \quad (\text{A.2})$$

where Q , Q_T and ϕ are respectively defined in (2.3), (2.6) and (2.17), then the Lax pair (2.4, 2.5) can be equivalently formulated as

$$d(e^{i\phi(x, t, k)\hat{\Sigma}_3}\Phi(x, t, k)) = \mathcal{F}(x, t, k). \quad (\text{A.3})$$

For the domain of the space and time variables being

$$0 \leq x < \infty, \quad 0 \leq t < \infty, \quad (\text{A.4})$$

solutions of (A.3) are in the following form:

$$\Phi(x, t, k) = I_{n+1} + \int_{(x_0, t_0)}^{(x, t)} e^{-i\phi(x, t, k)\hat{\Sigma}_3} \mathcal{F}(\xi, \tau, k), \quad (\text{A.5})$$

where the two points (x_0, t_0) and (x, t) identify a path on the domain (A.4). One can

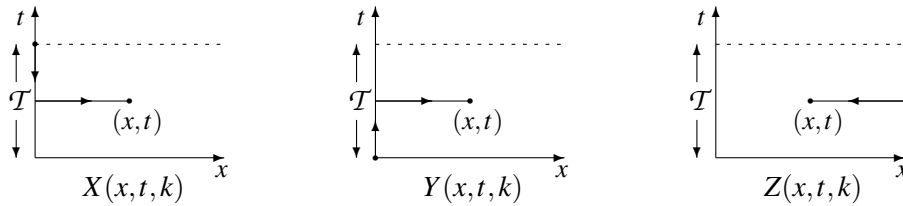


Fig. A.1 : Paths of $X(x, t, k)$, $Y(x, t, k)$ and $Z(x, t, k)$ on $0 \leq x < \infty$, $0 \leq t < \mathcal{T}$

define three Jost solutions $X(x, t, k)$, $Y(x, t, k)$ and $Z(x, t, k)$ following three different paths represented in Fig. A.1. Precisely, they correspond to

$$X(x, t, k) : (x_0, t_0) = (0, \mathcal{T}), \quad (\text{A.6a})$$

$$Y(x, t, k) : (x_0, t_0) = (0, 0), \quad (\text{A.6b})$$

$$Z(x, t, k) : (x_0, t_0) = (\infty, t_0). \quad (\text{A.6c})$$

It follows from the standard theory of (Volterra) integral equations that X , Y and Z can be split into two block-column forms as

$$X = (X^{(2)}, X^{(3)}), \quad Y = (Y^{(1)}, Y^{(4)}), \quad Z = (Z^{(-)}, Z^{(+)}), \quad (\text{A.7})$$

where the superscripts (1), (2), (3) and (4) denote respectively the four quadrants of the k -complex planes (see Fig. A.2), whilst (+), (-) denote the upper and lower half k -complex planes. The block-column functions are understood to be analytic and bounded in the domains corresponding to their superscript. Next, we seek the

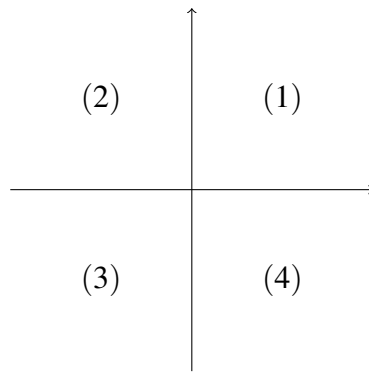


Fig. A.2 : Four quadrants of the k -complex plane

following matrices $S(k)$, $T(k)$ relating the Jost solution X , Y and Z as

$$Z(x, t, k) = Y(x, t, k) e^{-i\phi(x, t, k) \hat{\Sigma}_3} S(k), \quad (\text{A.8})$$

$$X(x, t, k) = Y(x, t, k) e^{-i\phi(x, t, k) \hat{\Sigma}_3} T(k). \quad (\text{A.9})$$

As a direct consequence of the forms of X , Y and Z , one has

$$\det S(k) = \det T(k) = 1, \quad (\text{A.10})$$

and

$$S(k) = Z(0, 0, k), \quad T(k) = X(0, 0, k). \quad (\text{A.11})$$

In contrast to the usual ISM, one needs two scattering systems (A.8) and (A.9) due to the presence of the three Jost solutions. They complete the direct scattering processes of a half-line system. In component, $S(k)$ and $T(k)$, and their inverse matrices can be written in 2×2 block-matrix forms as

$$S(k) = \begin{pmatrix} \mathbf{a}^{(-)}(k) & \mathbf{b}^{(+)}(k) \\ \mathbf{b}^{(-)}(k) & \mathbf{a}^{(+)}(k) \end{pmatrix}, \quad S^{-1}(k) = \begin{pmatrix} \mathbf{c}^{(+)}(k) & \mathbf{d}^{(+)}(k) \\ \mathbf{d}^{(-)}(k) & \mathbf{c}^{(-)}(k) \end{pmatrix}, \quad (\text{A.12})$$

where $\mathbf{a}^{(+)}$ and $\mathbf{c}^{(+)}$ (resp. $\mathbf{a}^{(-)}$ and $\mathbf{c}^{(-)}$) are analytic and bounded in the upper (resp. lower) half k -complex plane, and

$$T(k) = \begin{pmatrix} \mathbf{A}^{(24)}(k) & \mathbf{B}^{(13)}(k) \\ \mathbf{B}^{(24)}(k) & \mathbf{A}^{(13)}(k) \end{pmatrix}, \quad T^{-1}(k) = \begin{pmatrix} \mathbf{C}^{(13)}(k) & \mathbf{D}^{(13)}(k) \\ \mathbf{D}^{(24)}(k) & \mathbf{C}^{(24)}(k) \end{pmatrix}. \quad (\text{A.13})$$

where $\mathbf{A}^{(24)}$ and $\mathbf{C}^{(24)}$ (resp. $\mathbf{A}^{(13)}$ and $\mathbf{C}^{(13)}$) are analytic and bounded in the union of the quadrants (2) and (4) (resp. (1) and (3)).

Based on (A.8, A.9), we are ready to construct the RH problem. Define the following matrix quantities:

$$G_1(x, t, k) = (Y^{(1)}(\mathbf{c}^{(+)})^{-1}, Z^{(+)})(x, t, k), \quad (\text{A.14})$$

$$G_2(x, t, k) = (X^{(2)}(\Lambda^{(+)})^{-1}, Z^{(+)})(x, t, k), \quad (\text{A.15})$$

$$G_3(x, t, k) = (Z^{(-)}, X^{(3)}(\Lambda^{(-)})^{-1})(x, t, k), \quad (\text{A.16})$$

$$G_4(x, t, k) = (Z^{(-)}, Y^{(4)}(\mathbf{c}^{(-)})^{-1})(x, t, k), \quad (\text{A.17})$$

where

$$\Lambda^{(+)} = \mathbf{c}^{(+)}\mathbf{A}^{(24)} + \mathbf{d}^{(+)}\mathbf{B}^{(24)}, \quad \Lambda^{(-)} = \mathbf{c}^{(-)}\mathbf{A}^{(13)} + \mathbf{d}^{(-)}\mathbf{B}^{(13)}. \quad (\text{A.18})$$

Apparently G_j , $j = 1, \dots, 4$ is analytic in the j th quadrant of the k -complex plane. Let $\rho^{(\pm)} \equiv (\mathbf{a}^{(\mp)})^{-1}\mathbf{b}^{(\pm)}$, then, G_1 , G_2 , G_3 and G_4 satisfy the following RH problem (see Fig. A.3):

$$G_4(x, t, k) = G_1(x, t, k) e^{-i\phi(x, t, k)\hat{\Sigma}_3} J_4(k), \quad J_4 = \begin{pmatrix} I & -\rho^+ \\ \rho^- & I - \rho^- \rho^+ \end{pmatrix}, \quad k \in \mathbb{R}^+, \quad (\text{A.19})$$

$$G_2(x, t, k) = G_1(x, t, k) e^{-i\phi(x, t, k)\hat{\Sigma}_3} J_1(k), \quad J_1 = \begin{pmatrix} I & 0 \\ \Xi^+ & I \end{pmatrix}, \quad k \in i\mathbb{R}^+, \quad (\text{A.20})$$

$$G_2(x, t, k) = G_3(x, t, k) e^{-i\phi(x, t, k)\hat{\Sigma}_3} J_2(k), \quad J_2 = J_3 J_4^{-1} J_1, \quad k \in \mathbb{R}^-, \quad (\text{A.21})$$

$$G_4(x, t, k) = G_3(x, t, k) e^{-i\phi(x, t, k)\hat{\Sigma}_3} J_3(k), \quad J_3 = \begin{pmatrix} I & -\Xi^- \\ 0 & I \end{pmatrix}, \quad k \in i\mathbb{R}^-, \quad (\text{A.22})$$

where \mathbb{R}^+ (resp. \mathbb{R}^-) represents the positive (resp. negative) real axis and

$$\Xi^{(+)} = (\mathbf{a}^{(+)})^{-1}\mathbf{B}^{(24)}(\Lambda^{(+)})^{-1}, \quad \Xi^{(-)} = (\mathbf{a}^{(-)})^{-1}\mathbf{B}^{(13)}(\Lambda^{(-)})^{-1}. \quad (\text{A.23})$$

One can state that the solutions of the RH problem are solutions of the Lax pair (2.4, 2.5). This gives rise to solutions of the half-line problem through certain re-

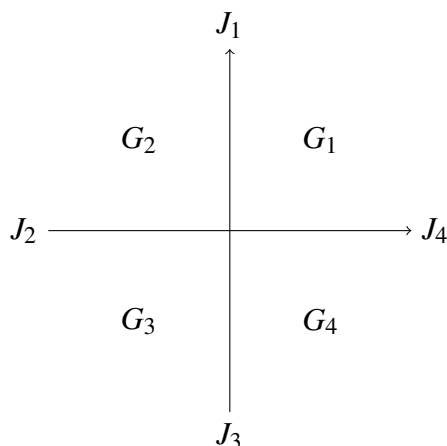


Fig. A.3 : A RH problem with four jump matrices J_1 , J_2 , J_3 and J_4

construction formula [57].

A crucial observation is the following: the matrices $S(k)$ and $T(k)$ containing scattering data are not independently, indeed they are related by a so-called *global relation*. Precisely, from (A.8, A.9), one has

$$Z(0, t, k) = X(0, t, k) e^{-i\phi(0, t, k)\hat{\Sigma}_3} (T^{-1} S)(k). \quad (\text{A.24})$$

In addition, from its definition, Z can also be written as

$$Z(0, t, k) = I + \int_{\infty}^0 e^{-i\phi(\xi, t, k)\hat{\Sigma}_3} (QZ)(\xi, t, k) d\xi. \quad (\text{A.25})$$

Combining this two relations together and taking $t \rightarrow \mathcal{T} = \infty$ yield

$$-I + (T^{-1} S)(k) = \lim_{t \rightarrow \infty} e^{-i\phi(0, t, k)\hat{\Sigma}_3} \int_{\infty}^0 e^{-i\phi(\xi, t, k)\hat{\Sigma}_3} (QZ)(\xi, t, k) d\xi. \quad (\text{A.26})$$

This is the global relation that is a functional constraint relating the elements of $S(k)$ to those of $T(k)$. Study of this relation is beyond the scope of this presentation. In [31] global relation for the scalar NLS case was treated. Although in general one cannot solve this relation, *i.e.* express the elements of $T(k)$ in terms of those of $S(k)$, a particular reduction using the inner symmetry of the system can be used. This reduction leads to the important concept of linearizable boundary conditions.

A.2 Linearizable boundary conditions

The argument is the following [57]: under the transformations $k \rightarrow -k$ and $x \rightarrow -x$, the domains of analyticity of G_j , $j = 1, \dots, 4$ are unchanged. This implies that the system of $G_j(-x, t, -k)$, $j = 1, \dots, 4$ may also satisfy certain RH problem which gives solutions to the half-line problem. To extract this information, one introduces a nonsingular matrix $N(k)$ satisfying

$$V(t, -k)N(k) = N(k)V(t, k), \quad (\text{A.27})$$

where the matrix $V(t, k)$ is defined as

$$V(t, k) \equiv -i2k^2\Sigma_3 + Q_T(0, t, k). \quad (\text{A.28})$$

Note that (A.27) is defined at $x = 0$ due to the form of $V(t, k)$. If such $N(k)$ exists, then (A.27) leads to an extra reduction relation for the scattering matrix $T(k)$ because of the definition of $T(k)$ (A.9, A.11). Therefore, a particular class of boundary conditions, that is referred to as *linearizable* in Fokas' language, can be obtained by solving (A.27).

Precisely, one has

$$V(t, k) = \begin{pmatrix} -2ik^2I_n + iRR^\dagger(0, t) & 2kR(0, t) + iR_x(0, t) \\ -2kR^\dagger(0, t) + iR_x^\dagger(0, t) & 2ik^2 - iR^\dagger R(0, t) \end{pmatrix}. \quad (\text{A.29})$$

Following the condition

$$\det V(t, k) = \det V(t, -k), \quad (\text{A.30})$$

one gets either

$$\begin{aligned} & \det \left((2ik^2I_n - iR^\dagger R) - (-2kR^\dagger + iR_x^\dagger)(-2ik^2 + iRR^\dagger)^{-1}(2kR + iR_x) \right) \\ &= \det \left((2ik^2I_n - iR^\dagger R) - (2kR^\dagger + iR_x^\dagger)(-2ik^2 + iRR^\dagger)^{-1}(-2kR + iR_x) \right), \end{aligned} \quad (\text{A.31})$$

or

$$\begin{aligned} & 2kiR_x^\dagger(-2ik^2 + iRR^\dagger)^{-1}R - 2ikR^\dagger(-2ik^2 + iRR^\dagger)^{-1}R_x \\ &= 2ikR^\dagger(-2ik^2 + iRR^\dagger)^{-1}R_x - 2kiR_x^\dagger(-2ik^2 + iRR^\dagger)^{-1}R, \end{aligned} \quad (\text{A.32})$$

where both R and R_x are evaluated at $x = 0$. By direct computations, both (A.31)

and (A.32) can be reduced to

$$RR_x^\dagger = R_x R^\dagger. \quad (\text{A.33})$$

The quantity RR_x^\dagger is clearly hermitian. Now, suppose that $R_x = HR$ and H is time-independent, then H is a hermitian matrix. Hence H is diagonalizable. Inserting $R_x = HR$ into (A.33) yields

$$HRR^\dagger = RR^\dagger H, \quad (\text{A.34})$$

which is the same relation as what we obtained in Sec. 3.1. This justifies our early claim in Remark 3.1.1 that the linearizable boundary conditions for the vector NLS equation on the half-line is equivalent to the integrable boundary conditions (3.22, 3.23).

To obtain the form of $N(k)$, it follows from (A.27) that

$$2ik^2[\Sigma_3, N(k)] = Q_T(0, t, -k)N(k) - N(k)Q_T(0, t, k). \quad (\text{A.35})$$

Recall Eq. (3.5) which is in the form

$$2ik^2[\Sigma_3, L(k)] = \tilde{Q}_T(0, t, k)L(k) - L(k)Q_T(0, t, k). \quad (\text{A.36})$$

Here both $N(k)$ and $L(k)$ are time-independent. Observing that

$$Q_T(0, t, -k) = \Sigma_3 \tilde{Q}_T(0, t, k) \Sigma_3, \quad (\text{A.37})$$

then this relation together with (A.35) and (A.36) yield

$$\Sigma_3 L(0, t, k) = N(k), \quad (\text{A.38})$$

which was already pointed out in Remark 3.1.1. From the results obtained in Sec. 3.1 for the form of $L(k)$, one can state that $N(k)$ can be written as

$$N(k) = \begin{pmatrix} \frac{k-i\alpha}{k+i\alpha} I_n & \\ & -1 \end{pmatrix}, \quad \text{or } N(k) = \begin{pmatrix} \sigma_1 & & & \\ & \ddots & & \\ & & \sigma_n & \\ & & & -1 \end{pmatrix}, \quad (\text{A.39})$$

where $\sigma_j = -1$, $j \in M$ and $\sigma_j = 1$, $j \in \{1, \dots, n\} \setminus M$, M being a nonempty subset of $\{1, \dots, n\}$.

Proof of Eq. (3.25)

Assume, without loss of generality, that all the quantities involved in this chapter are evaluated at $t = 0$. Indeed, the time-dependence can be easily added for time here acts only as a parameter. To proceed, one needs to clarify the following notions.

1. We work with the x -part of the Lax pair which is in the form

$$\Phi_x(x, k) + ik[\Sigma_3, \Phi(x, k)] = Q(x) \Phi(x, k). \quad (\text{B.1})$$

where Φ is an $(n + 1 \times n + 1)$ matrix function and Σ_3 and $Q(x)$ are the same objects as defined in Sec. 2.1. In Sec. 3.1, the symmetry relation

$$\tilde{Q}(x) = Q(-x) \quad (\text{B.2})$$

was imposed, which led to the following Bäcklund transformation

$$\tilde{\Phi}(x, k) = L(x, k) \Phi(x, k), \quad (\text{B.3})$$

with the Bäcklund matrix $L(0, k)$ being in the form (3.24). Here $\tilde{\Phi}(x, k)$ is understood to satisfy the relation (B.1) with $Q(x)$ being replaced by $\tilde{Q}(x)$.

2. Considering the relations (B.1) and (B.2), one can show that $\Phi(x, t)$ and $\tilde{\Phi}(x, k)$ are related by

$$\Sigma_3 \Phi(x, k) = \tilde{\Phi}(-x, -k) \left(e^{-ikx\Sigma_3} M(k) e^{ikx\Sigma_3} \right), \quad (\text{B.4})$$

where $M(k)$ is an invertible matrix depending only on k . The simple way to get (B.4) is to show that $\Sigma_3 \Phi(x, t) e^{-ikx\Sigma_3}$ and $\tilde{\Phi}(-x, -k) e^{-ikx\Sigma_3}$ satisfy the same auxiliary problem. Then, they must be related by a k -dependent invertible

matrix function that is denoted by $M(k)$ in (B.4).

3. The matrix $S(k)$ involved in the scattering system (2.24) can be in general defined as

$$S(k) = \lim_{x \rightarrow \infty} \left(e^{ikx\Sigma_3} \Phi(x, k) e^{-ikx\Sigma_3} \right) \left(e^{-ikx\Sigma_3} \Phi^{-1}(-x, k) e^{ikx\Sigma_3} \right), \quad k \in \mathbb{R}, \quad (\text{B.5})$$

for all Φ satisfying (B.1).

4. From the points 1 - 3, one can show that for the quantity $\tilde{S}(k)$ defined as

$$\tilde{S}(k) = \lim_{x \rightarrow \infty} \left(e^{ikx\Sigma_3} \tilde{\Phi}(x, k) e^{-ikx\Sigma_3} \right) \left(e^{-ikx\Sigma_3} \tilde{\Phi}^{-1}(-x, k) e^{ikx\Sigma_3} \right), \quad k \in \mathbb{R}, \quad (\text{B.6})$$

on one hand, through the use of (B.3), one gets

$$\tilde{S}(k) = \lim_{x \rightarrow \infty} \left(e^{ikx\Sigma_3} (L\Phi)(x, k) e^{-ikx\Sigma_3} \right) \left(e^{-ikx\Sigma_3} (\Phi^{-1}L^{-1})(-x, k) e^{ikx\Sigma_3} \right), \quad k \in \mathbb{R}, \quad (\text{B.7})$$

on the other, through the use of (B.4), one gets

$$\tilde{S}(k) = \Sigma_3 S^{-1}(-k) \Sigma_3, \quad (\text{B.8})$$

with $S(k)$ defined in (B.5).

To prove Eq. (3.25), one needs to compare (B.7) with (B.8). This consists in having the form of the Bäcklund matrix $L(x, k)$ evaluated as $x \rightarrow \pm\infty$, *i.e.* to obtained $L_+(k)$ and $L_-(k)$ defined as

$$L_+(k) \equiv \lim_{x \rightarrow \infty} L(x, k), \quad L_-(k) \equiv \lim_{x \rightarrow -\infty} L(x, k). \quad (\text{B.9})$$

One can observe from the the form of $L(0, k)$ (defined in (3.24)) that $L(0, k)$ can be written up to a scalar factor either as

$$L(0, k) = \left(I_{n+1} + \left(\frac{k - i\alpha}{k + i\alpha} - 1 \right) \mathcal{P}_0 \right), \quad (\text{B.10})$$

or as

$$L(0, k) = \left(I_{n+1} + \left(\frac{k + i\alpha}{k - i\alpha} - 1 \right) \mathcal{Q}_0 \right). \quad (\text{B.11})$$

The forms of the matrices \mathcal{P}_0 and \mathcal{Q}_0 depend on the boundary condition that one put at $x = 0$. Precisely, taking the Robin boundary condition (3.22), one has

$$\mathcal{P}_0 = \begin{pmatrix} I_n & 0 \\ 0 & 0 \end{pmatrix}, \quad \mathcal{Q}_0 = \begin{pmatrix} 0 & 0 \\ 0 & 1 \end{pmatrix}. \quad (\text{B.12})$$

Taking the mixed Neumann and Dirichlet boundary condition (3.23), the forms of $L(0, k)$ (B.18, B.19) are understood with the limit $a \rightarrow -\infty$. Thus, in this case

$$\frac{k + i\alpha}{k - i\alpha} = \frac{k - i\alpha}{k + i\alpha} = -1, \quad a \rightarrow -\infty. \quad (\text{B.13})$$

Then, one has

$$\mathcal{P}_0 = \begin{pmatrix} D_n & 0 \\ 0 & 0 \end{pmatrix}, \quad \mathcal{Q}_0 = \begin{pmatrix} I_n - D_n & 0 \\ 0 & 1 \end{pmatrix}, \quad (\text{B.14})$$

where D_n is a diagonal matrix with the entries being either 0 or 1 on its diagonal. It follows from (B.12) and (B.14) that \mathcal{P}_0 and \mathcal{Q}_0 can be considered to be projectors satisfying

$$\mathcal{P}_0 + \mathcal{Q}_0 = I_{n+1}. \quad (\text{B.15})$$

One can thus put \mathcal{P}_0 and \mathcal{Q}_0 in the following forms:

$$\mathcal{P}_0 = \beta_0(\beta_0^\dagger \beta_0)^{-1} \beta_0^\dagger, \quad \mathcal{Q}_0 = \gamma_0(\gamma_0^\dagger \gamma_0)^{-1} \gamma_0^\dagger, \quad (\text{B.16})$$

where β_0 and γ_0 are matrices determined by the forms of \mathcal{P}_0 and \mathcal{Q}_0 respectively.

The Bäcklund matrix L depends in general on x . Its x -dependence can be obtained by inserting (B.3) into (B.1):

$$L_x + ik[\Sigma_3, L] = \tilde{Q}L - LQ. \quad (\text{B.17})$$

Indeed, $L(x, k)$ is a dressing factor of degree 1. It can be written either as

$$L(x, k) = \left(I_{n+1} + \left(\frac{k - i\alpha}{k + i\alpha} - 1 \right) \mathcal{P}(x) \right), \quad (\text{B.18})$$

or as

$$L(x, k) = \left(I_{n+1} + \left(\frac{k + i\alpha}{k - i\alpha} - 1 \right) \mathcal{Q}(x) \right), \quad (\text{B.19})$$

with the matrices $\mathcal{P}(x)$ and $\mathcal{Q}(x)$ being projectors defined as

$$\mathcal{P}(x) = \beta(\beta^\dagger \beta)^{-1} \beta^\dagger(x), \quad \mathcal{Q}(x) = \gamma(\gamma^\dagger \gamma)^{-1} \gamma^\dagger(x). \quad (\text{B.20})$$

Here the matrices $\beta(x)$ and $\gamma(x)$ are well defined at $x = 0$ with

$$\beta(0) \equiv \beta_0, \quad \gamma(0) \equiv \gamma_0. \quad (\text{B.21})$$

Evaluating (B.17) at $k = \pm i\alpha$, one can show that $\beta(x)$ and $\gamma(x)$ satisfy

$$U(x, i\alpha)\beta(x) = \beta_x(x), \quad U(x, -i\alpha)\gamma(x) = \gamma_x(x), \quad (\text{B.22})$$

where

$$U(x, k) \equiv -ik\Sigma_3 + Q(x). \quad (\text{B.23})$$

Then, using standard method [47, 62] to evaluate the projectors $\mathcal{P}(x)$ and $\mathcal{Q}(x)$ as $x \rightarrow \infty$ and $x \rightarrow -\infty$ respectively, one has

$$\lim_{x \rightarrow \infty} \mathcal{P}(x) = \mathcal{P}_0, \quad \lim_{x \rightarrow -\infty} \mathcal{Q}(x) = \mathcal{Q}_0. \quad (\text{B.24})$$

This reveals that up to a certain scalar factor

$$L_+(k) = L_-(k) = L(0, k). \quad (\text{B.25})$$

Substituting this relation into (B.7) and comparing the resulting formula with (B.8), one has

$$\Sigma_3 S^{-1}(-k) \Sigma_3 = L(0, k) S(k) L^{-1}(0, k). \quad (\text{B.26})$$

With the following identification:

$$W S^{-1}(k) W^{-1} = S^\dagger(k^*), \quad \mathcal{B}(k) = \Sigma_3 L(0, k), \quad (\text{B.27})$$

one can prove Eq. (3.25).

Algorithm for constructing paired norming constants

We provide an algorithm to solve recursively the nonlinearly coupled system (3.48) of β_j and β_{j+N} , $j = 1, \dots, N$. The key observation is relying on Theorem 2.2.7. Let

$$d_{1\dots 2N}(k) = d_1 d_{2,\{1\}} \dots d_{2N,\{1\dots 2N-1\}}(k), \quad (\text{C.1})$$

$d_{1\dots 2N}(k)$ is defined in (2.67 - 2.69). Recall also the definition of \mathcal{A}_{j+N} in (2.71). The dressing factor defined in (C.1) leads to the following expression:

$$\mathcal{A}_{j+N} = \prod_{i=1, i \neq j+N}^{2N} \left(\frac{k_{j+N} - k_i}{k_{j+N} - k_i^*} \right) \left(d_{2N,\{1\dots 2N-1\}}^{-1} \dots d_{j+N+1,\{1\dots j+N\}}^{-1} \pi_{j+N,\{1\dots j+N-1\}} \right. \\ \left. d_{j+N-1,\{1\dots j+N-2\}}^{-1} \dots d_1^{-1} \right) (k_{j+N}), \quad (\text{C.2})$$

where

$$d_{j,\{1\dots j-1\}}(k) = I_n + \left(\frac{k_j^* - k_j}{k - k_j^*} \right) \pi_{j,\{1\dots j-1\}}, \quad (\text{C.3})$$

$$\pi_{j,\{1\dots j-1\}} = \frac{\xi_{j,\{1\dots j-1\}} \xi_{j,\{1\dots j-1\}}^\dagger}{\xi_{j,\{1\dots j-1\}}^\dagger \xi_{j,\{1\dots j-1\}}}, \quad \xi_{j,\{1\dots j-1\}} = d_{1\dots j-1}^\dagger(k_j) \beta_j. \quad (\text{C.4})$$

First, take $j = N$. Inserting (C.2, C.3) into (3.48) implies

$$\beta_N \xi_{2N,\{1\dots 2N-1\}}^\dagger = B(k_N^*) \prod_{i=1}^{2N-1} \left(\frac{k_{2N} - k_i}{k_{2N} - k_i^*} \right) \pi_{2N,\{1\dots 2N-1\}}. \quad (\text{C.5})$$

Define an n -vector \mathbf{v}_{2N} as

$$\mathbf{v}_{2N} = \frac{\xi_{2N, \{1 \dots 2N-1\}}}{|\xi_{2N, \{1 \dots 2N-1\}}|^2} = \left(M(k_N^*) \prod_{i=1}^{2N-1} \left(\frac{k_{2N} - k_i}{k_{2N} - k_i^*} \right) \right)^{-1} \beta_N. \quad (\text{C.6})$$

Combining (C.5) and (C.6) together gives

$$\xi_{2N, \{1 \dots 2N-1\}} = \frac{\mathbf{v}_{2N}}{|\mathbf{v}_{2N}|^2}. \quad (\text{C.7})$$

With the knowledge of $\xi_{2N, \{1 \dots 2N-1\}}$, we can thus compute $d_{2N, \{1 \dots 2N-1\}}(k)$. Next, take $j = N - 1$. From (3.48) and (C.2), one gets

$$\begin{aligned} \beta_{N-1} \xi_{2N-1, \{1 \dots 2N-2\}}^\dagger &= M(k_{N-1}^*) \prod_{i=1, i \neq 2N-1}^{2N} \left(\frac{k_{2N-1} - k_i}{k_{2N-1} - k_i^*} \right) \times \\ & d_{2N, \{1 \dots 2N-1\}}^{-1}(k_{2N-1}) \pi_{2N-1, \{1 \dots 2N-2\}}. \end{aligned} \quad (\text{C.8})$$

Since the form of $d_{2N, \{1 \dots 2N-1\}}(k)$ is known, define \mathbf{v}_{2N-1} as

$$\begin{aligned} \mathbf{v}_{2N-1} &= \frac{\xi_{2N-1, \{1 \dots 2N-2\}}}{|\xi_{2N-1, \{1 \dots 2N-2\}}|^2} \\ &= \left(M(k_{N-1}^*) d_{2N, \{1 \dots 2N-1\}}^{-1}(k_{2N-1}) \prod_{i=1, i \neq 2N-1}^{2N} \left(\frac{k_{2N-1} - k_i}{k_{2N-1} - k_i^*} \right) \right)^{-1} \beta_{N-1}. \end{aligned} \quad (\text{C.9})$$

Combining (C.8) and (C.9) gives

$$\xi_{2N-1, \{1 \dots 2N-2\}} = \frac{\mathbf{v}_{2N-1}}{|\mathbf{v}_{2N-1}|^2}. \quad (\text{C.10})$$

This implies that the dressing factor $d_{2N-1, \{1 \dots 2N-2\}}(k)$ is known. Recursively, taking $j = N - 2, N - 3$ up to 1, we are able to derive $\xi_{j+N, \{1 \dots j+N-1\}}$ and $d_{j+N, \{1 \dots j+N-1\}}$ step by step from $j = N - 2$ to $j = 1$. Since $\{k_j; \beta_j\}$, $j = 1, \dots, N$ are known quantities, we have thus the access of $d_{j, \{1 \dots j-1\}}(k)$, $j = 1, \dots, N$ as well. Therefore, β_{j+N} can be derived thanks to (C.4).

Proof of Prop. 4.2.1

To prove (4.26), we need the mirror symmetry relations (4.25) and the permutability property of dressing transformations (Theorem 2.2.7). To avoid tedious notations, we choose to work with $\{1\dots N\}$ instead of $\{i_1\dots i_N\}$. We need to keep in mind that $\{1\dots N\}$ can be indeed replaced by any permutation of itself but indexed by the ordered number from 1 to N by taking $j \rightarrow i_j$. Regardless of any particular permutation, the relations (4.25) always hold with respect to the index j . Write $d_{1\dots 2N}$ in the following form:

$$d_{1\dots 2N} = d_1 \dots d_{N,\{1\dots N-1\}} d_{N+1,\{1\dots N\}} \dots d_{2N,\{1\dots 2N-1\}}. \quad (\text{D.1})$$

First, taking $j = N$ in (4.25), then \mathcal{A}_{2N} (see Eq. (2.67 - 2.69) and (2.71)) can be written as

$$\mathcal{A}_{2N} = \prod_{i=1}^{2N-1} \left(\frac{k_{2N} - k_i}{k_{2N} - k_i^*} \right) \pi_{2N,\{1\dots 2N-1\}} d_{1\dots 2N-1}^{-1}(k_{2N}). \quad (\text{D.2})$$

Substituting this into (4.25) gives

$$\beta_N \xi_{2N,\{1\dots 2N-1\}} = B(k_N^*) \prod_{i=1}^{2N-1} \left(\frac{k_{2N} - k_i}{k_{2N} - k_i^*} \right) \pi_{2N,\{1\dots 2N-1\}}, \quad (\text{D.3})$$

where $\xi_{2N,\{1\dots 2N-1\}}^\dagger$ is defined in (2.69). Taking the definitions (4.9, 4.10) and the mirror symmetry $k_{j+N} = -k_j^*$, we come to the following identification:

$$\gamma_{2N,\{1\dots 2N-1\}} = \xi_{2N,\{1\dots 2N-1\}}, \quad (\text{D.4})$$

$$\gamma_N = \prod_{i=1}^{2N-1} \left(\frac{k_{2N} - k_i}{k_{2N} - k_i^*} \right)^{-1} \beta_N, \quad (\text{D.5})$$

Define an n -vector \mathbf{u}_{2N} as

$$\mathbf{u}_{2N} = \frac{\xi_{2N, \{1 \dots 2N-1\}}}{|\xi_{2N, \{1 \dots 2N-1\}}|^2} = \mathbf{B}^{-1}(k_N^*) \gamma_N. \quad (\text{D.6})$$

Inserting (D.4 - D.6) into D.3 gives

$$\mathbf{p}_{2N, \{1 \dots 2N-1\}} = \frac{\mathbf{u}_{2N}}{|\mathbf{u}_{2N}|} = \bar{\mathbf{B}}(k_N) \mathbf{p}_N. \quad (\text{D.7})$$

This relation proves (4.26) with $j = N$. Next, taking $j = N - 1$, one has

$$\mathcal{A}_{2N-1} = \prod_{i=1, i \neq 2N-1}^{2N} \left(\frac{k_{2N} - k_i}{k_{2N} - k_i^*} \right) d_{2N, \{1 \dots 2N-1\}}^{-1} \pi_{2N-1, \{1 \dots 2N-2\}} d_{1 \dots 2N-2}^{-1}(k_{2N-1}). \quad (\text{D.8})$$

Substituting this into (4.25) implies

$$d_{2N, \{1 \dots 2N-1\}}(k_{2N-1}) \mathbf{B}^{-1}(k_{N-1}^*) \beta_{N-1} \xi_{2N-1, \{1 \dots 2N-2\}}^\dagger = \prod_{i=1, i \neq 2N-1}^{2N} \left(\frac{k_{2N-1} - k_i}{k_{2N-1} - k_i^*} \right) \pi_{2N-1, \{1 \dots 2N-2\}}. \quad (\text{D.9})$$

With (D.7) and $k_{j+N} = -k_j^*$, one gets

$$\begin{aligned} d_{2N, \{1 \dots 2N-1\}}(k_{2N-1}) \mathbf{B}^{-1}(k_{N-1}^*) &= \left(I_n + \left(\frac{k_{2N}^* - k_{2N}}{k_{2N-1} - k_{2N}^*} \right) \mathbf{p}_{2N, \{1 \dots 2N-1\}} \mathbf{p}_{2N, \{1 \dots 2N-1\}}^\dagger \right) \mathbf{B}^{-1}(k_{N-1}^*) \\ &= \mathbf{B}^{-1}(k_{N-1}^*) \left(I_n + \frac{k_N - k_N^*}{k_{N-1}^* - k_N} \mathbf{p}_N \mathbf{p}_N^\dagger \right) \\ &= \mathbf{B}^{-1}(k_{N-1}^*) d_N^\dagger(k_{N-1}). \end{aligned} \quad (\text{D.10})$$

According to (4.9), it comes to the following identification:

$$\gamma_{N-1, \{N\}} = \prod_{\substack{p=1, p \neq N \\ p \neq N-1}}^{2N} \left(\frac{k_{N-1}^* - k_p}{k_{N-1}^* - k_p^*} \right) d_N^\dagger(k_{N-1}) \beta_{N-1}, \quad (\text{D.11})$$

$$\gamma_{2N-1, \{1 \dots 2N-2\}} = \left(\frac{k_{2N-1}^* - k_{2N}}{k_{2N-1}^* - k_{2N}^*} \right) \xi_{2N-1, \{1 \dots 2N-2\}}. \quad (\text{D.12})$$

Define now \mathbf{u}_{2N-1} as

$$\mathbf{u}_{2N-1} = \frac{\gamma_{2N-1, \{1 \dots 2N-2\}}}{|\gamma_{2N-1, \{1 \dots 2N-2\}}|} = \mathbf{B}^{-1}(k_{N-1}^*) \gamma_{N-1, \{N\}}. \quad (\text{D.13})$$

Combining (D.9 - D.13) together gives

$$\mathbf{p}_{2N-1, \{1 \dots 2N-2\}} = \frac{\mathbf{u}_{2N-1}}{|\mathbf{u}_{2N-1}|} = \bar{B}(k_{N-1}) \mathbf{p}_{N-1, \{N\}}. \quad (\text{D.14})$$

Recursively, taking $j = N - 2, N - 3$ up to 1, the following relation always holds

$$d_{q+N, \{1 \dots q-1+N\}}(k_{j+N}) B^{-1}(k_j^*) = B^{-1}(k_j^*) d_{q, \{q+1 \dots N\}}^\dagger(k_j), \quad j \leq q. \quad (\text{D.15})$$

Then, in the same way, by inserting $k_{j+N} = -k_j^*$, $\gamma_{j, \{j+1 \dots N\}}$ and $\gamma_{j+N, \{1 \dots j+N\}}$ into (4.25), it follows from direct computations that

$$\mathbf{p}_{j+N, \{j \dots j-1+N\}} = \bar{B}(k_j) \mathbf{p}_{j, \{j+1 \dots N\}}. \quad (\text{D.16})$$

Now we can add an order to the system by replacing $\{1, \dots, N\}$ with $\{i_1, \dots, i_N\}$, *i.e.* $j \rightarrow i_j$. Because of Theorem 2.2.7, the order is indeed irrelevant, we thus come to prove Eq. (4.26). Note that Eq. (4.28) can be obtained by following the same reasoning by taking account of the following dressing factor

$$\begin{aligned} d_{1 \dots 2N} &= d_1 \dots d_{j-1, \{1 \dots j-2\}} d_{j+1, \{1 \dots j-1\}} \dots d_{N, \{1 \dots \hat{j} \dots N-1\}} d_{j, \{1 \dots \hat{j} \dots N\}} d_{j+N, \{1 \dots N\}} \\ &\dots d_{j+N-1, \{1 \dots j+N-2\}} d_{j+N+1, \{1 \dots j+N-1\}} \dots d_{2N, \{1 \dots \widehat{j+N} \dots 2N-1\}} d_{j+N, \{1 \dots \widehat{j+N} \dots 2N\}}. \end{aligned} \quad (\text{D.17})$$

This means that $d_{j, \{1 \dots \hat{j} \dots N\}}$ is the last dressing factor added in the product of the first N dressing factors, and $d_{j+N, \{1 \dots \widehat{j+N} \dots 2N\}}$ is the last dressing factor added in the product of the total $2N$ dressing factors. Then applying (4.26) yields directly (4.28).

Reflection maps for H_{II}

Both F_{II} and H_{II} , given in Table 7.1 and 7.2, are in their canonical forms up to the Yang-Baxter equivalence (7.6). Define the bijections Ψ and $\tilde{\Psi}$ and the symmetry map s as

$$\Psi(X) : X \mapsto \frac{1}{X}, \quad \tilde{\Psi}(X) : X \mapsto 1 - X, \quad s(X) : X \mapsto \frac{X}{1 - X}. \quad (\text{E.1})$$

Thanks to Prop. 7.1.1 and 7.1.2, one can show that F_{II} is related to H_{II} by

$$\mathcal{R}_{F_{II}} \xleftrightarrow{\Psi} \tilde{\mathcal{R}}_{F_{II}} \xrightarrow{s} \tilde{\mathcal{R}}_{H_{II}} \xleftrightarrow{\tilde{\Psi}} \mathcal{R}_{H_{II}}. \quad (\text{E.2})$$

As to the reflection maps for H_{II} , since reflection maps for \tilde{F}_{II} and \tilde{H}_{II} are the same according to Prop. 7.2.1, reflection maps for H_{II} can be obtained using Prop. 7.2.2 in which equivalence class for reflection maps is specified. Precisely, one has

$$\mathcal{K}_{F_{II}} \xleftrightarrow{\Psi} \tilde{\mathcal{K}}_{F_{II}} = \tilde{\mathcal{K}}_{H_{II}} \xleftrightarrow{\tilde{\Psi}} \mathcal{K}_{H_{II}}. \quad (\text{E.3})$$

The explicit forms of $\mathcal{K}_{H_{II}}$ are shown in Table E.1.

Type	$\sigma(a)$	$h_a(X)$	$\phi_a(X)$
H_{II}	$\frac{\mu^2}{a}$	$\frac{aX}{aX - \mu X + \mu}$	$\frac{a - \mu X + \mu}{a}$
	$-a + 2\mu$	$-X$	$\frac{a + \mu X - \mu}{aX - \mu X + \mu}$

Table E.1: Reflection maps for H_{II}

Quad-graph equation-Yang-Baxter map correspondence

The main idea, presented in [98], which underlies the correspondence between $3D$ -consistent equations and Yang-Baxter maps, is the $3D$ consistency property for both integrable schemes. This idea can be well illustrated in Fig. F.1.

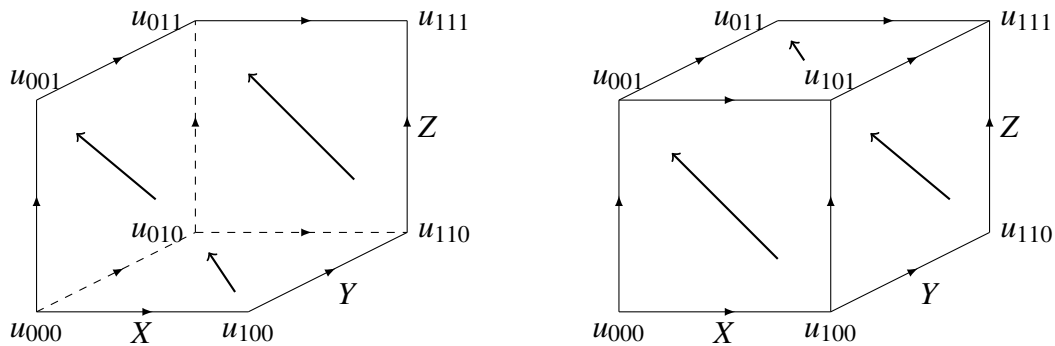


Fig. F.1 : $3D$ consistency of Yang-Baxter maps and quad-graph equations around a cube

Here, we list the Yang-Baxter maps derived from the ABS classification in Table F.1. Interestingly, they are all quadrirational maps (see Table 7.1 and 7.2). As a follow-up to the discussion made in Remark 8.4.2, we present explicitly here the construction of the quadrirational Yang-Baxter maps for the equations $Q3_{\delta=0}$.

To proceed, recall the Yang-Baxter equivalence (7.6) and the "reflection equivalence" (7.22). We also fix the convention that the quad-graph equations are parametrized by p, q whilst the quadrirational Yang-Baxter maps in their canonical forms are parametrized by a, b .

For $Q3_{\delta=0}$, through the invariant

$$I(s, t) = s/t, \tag{F.1}$$

one gets a map $\mathcal{R}(p, q) : (X, Y) \mapsto (U = f_{pq}(X, Y), V = g_{pq}(X, Y))$ with

$$f_{pq}(X, Y) = \frac{Y(p - pq^2 + qX(q - Y) + p^2X(-1 + qY))}{q - p^2q + p(p - X)Y + q^2(-1 + pX)Y}, \quad g_{pq}(X, Y) = f_{qp}(Y, X). \quad (\text{F.2})$$

Then performing the transformation (7.6) with $\psi(p) : X \mapsto \frac{X}{p}$ and also $\phi : p^2 \rightarrow a, q^2 \rightarrow b$ transforming parameters p, q to a, b , one can get the H_I quadrirational Yang-Baxter map.

In contrast to the case $A1_{\delta=0}$ in which the transformation ϕ , transforming the lattice parameters p, q to the map parameters a, b , is trivial— $\phi : p \rightarrow a, q \rightarrow b$ —for $Q3_{\delta=0}$, such ϕ are in more complicated forms, and will affect the search for reflection maps and boundary equations (see Appendix G).

Quad-graph Equation	Characteristic	Invariant	Yang-Baxter map
Q1 $_{\delta=0}$	$\eta_1 = 1$	$I(s, t) = s - t$	H_{III}^A
	$\eta_2 = u_{00}$	$I(s, t) = s/t$	H_{II}
	$\eta_3 = u_{00}^2$	$I(s, t) = 1/s - 1/t$	H_{III}^A
Q1 $_{\delta=1}$	$\eta_1 = 1$	$I(s, t) = s - t$	H_{II}
Q3 $_{\delta=0}$	$\eta_1 = u_{00}$	$I(s, t) = s/t$	H_I
H1	$\eta_1 = 1$	$I(s, t) = s - t$	H_V
	$\eta_2 = (-1)^{k+l}$	$I(s, t) = s + t$	F_V
	$\eta_3 = (-1)^{k+l} u_{00}$	$I(s, t) = st$	F_{IV}
H2	$\eta_1 = (-1)^{k+l}$	$I(s, t) = s + t$	F_{IV}
H3 $_{\delta=0}$	$\eta_1 = u_{00}$	$I(s, t) = s/t$	H_{III}^B
	$\eta_2 = (-1)^{k+l} u_{00}$	$I(s, t) = st$	F_{III}
H3 $_{\delta=1}$	$\eta_1 = (-1)^{k+l} u_{00}$	$I(s, t) = st$	F_{II}
A1 $_{\delta=0}$	$\eta_1 = (-1)^{k+l}$	$I(s, t) = s + t$	F_{III}
	$\eta_2 = u_{00}$	$I(s, t) = s/t$	H_{II}
	$\eta_3 = (-1)^{k+l} u_{00}^2$	$I(s, t) = 1/s + 1/t$	F_{III}
A1 $_{\delta=1}$	$\eta_1 = (-1)^{k+l}$	$I(s, t) = s + t$	F_{II}
A2	$\eta_1 = (-1)^{k+l} u_{00}$	$I(s, t) = st$	F_I

Table F.1: Correspondence between the ABS classification and the quadrirational Yang-Baxter maps

Boundary equations for the ABS classification

Following the construction of boundary equations, presented in Sec. 8.4, for the $3D$ -consistent equations from the ABS classification, we list some results of boundary equations in the following tables (Table G.1, G.2 and G.3). Indeed, the reason the construction formula (8.16) is valid is that the $3D$ -boundary consistency is underlying both schemes as depicted in Fig. G.1 and G.2. In addition, the equation $Q3_{\delta} = 0$ is treated in the following to illustrate some technical subtleties.

For $Q3_{\delta} = 0$, as pointed out in Appendix F, its correspondence to the H_I quadri-rational Yang-Baxter map is established by taking the invariant (F.1), which leads to (F.2). It was also understood in Appendix F that (F.2) is equivalent to H_I by taking the transformation (7.6) with certain bijection ψ . In addition, one needs to perform a non trivial transformation $\phi : p^2 \rightarrow a, q^2 \rightarrow b$ transforming the lattice parameters p, q of $Q3_{\delta} = 0$ to the parameters a, b of H_I . This affects the forms of reflections maps for the map (F.2), as now one needs to solve the equation

$$\sigma(p^2) = q^2, \quad (\text{G.1})$$

for q with σ being defined in Table 7.3 for the F_I thus H_I families. Solutions of (G.1) are double-valued. For $\sigma(a) = \frac{\mu^2}{a}$, one has

$$q = \rho(p) = \frac{\mu}{p}, \quad \text{or} \quad q = \rho(p) = -\frac{\mu}{p}, \quad (\text{G.2})$$

which is in a "nice" fractional form and can be used to construct reflection maps for

(F.2) and then boundary equations for $Q3_{\delta=0}$. For $\sigma(a) = \frac{a+\mu^2-1}{a-1}$, one has

$$q = \rho(p) = -\sqrt{1 + \frac{\mu^2}{-1+p^2}}, \quad \text{or} \quad q = \rho(p) = \sqrt{1 + \frac{\mu^2}{-1+p^2}}, \quad (\text{G.3})$$

which is in a "ugly" form. "Ugly" expressions are also obtained for the reflection maps for (F.2) and boundary equations for $Q3_{\delta=0}$.

Note that this multi-valued situation happens also for the equations $H3_{\delta=1}$ and A2. For sake of simplicity and conciseness, in Table G.1, G.2 and G.3, we only list the results that are in "nice" forms *i.e.* excluding the expressions involving square root or logarithm functions. However, one has to keep in mind that, by construction, the "ugly" expressions of boundary equations together with their corresponding quad-graph equations satisfy also the 3D-boundary consistency.

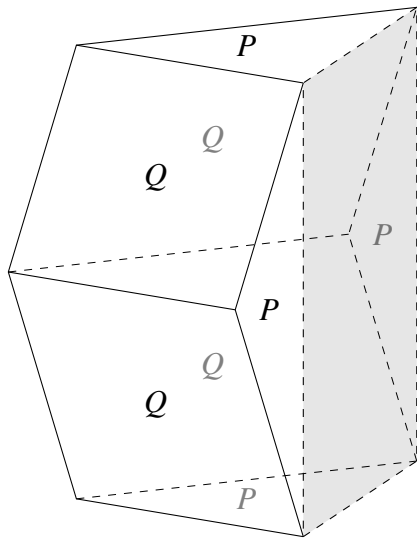


Fig. G.1 : 3D-boundary consistency

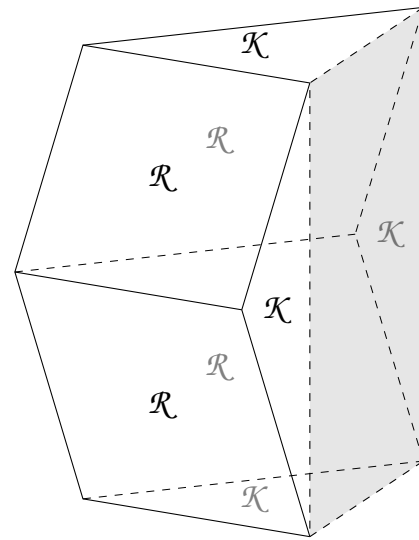


Fig. G.2 : 3D consistency for the set-theoretical reflection equation

Equations	$\rho(p)$	$P(x, y, z, p)$
$Q1_{\delta=0}$	$\frac{\mu^2}{p}$ $-p + 2\mu$	$p(y - z) + (x - y)\mu$ $px(y - z) + (-x + y)z\mu$ $y(x + z)$ $p(y^2 - xz) + (x - y)(y + z)\mu$
$Q1_{\delta=1}$	$\frac{\mu^2}{p}$ $-p + 2\mu$	$p(y - z - \mu) - \mu(x - y + \mu)$ $p(y - z - \mu) + \mu(x - y + \mu)$ $x - z$ $p(p - 2\mu) - (x - y)(y - z)$
$Q3_{\delta=0}$	$\frac{\mu}{p}$	$y(x + z)$ $y(x - z)$ $p^2(y^2 + xz) + (y^2 + xz)\mu - py(x + z)(1 + \mu)$ $p^2(y^2 - xz) - (y^2 - xz)\mu - py(x - z)(1 - \mu)$

Table G.1: Results for boundary equations (Q family)

Equations	$\rho(p)$	$P(x, y, z, p)$
H1	$-p + 2\mu$	$\frac{y(x+z)}{y(z-x) + p - \mu}$
H2	$-p + \mu$	$\frac{x + 2y + z + \mu}{z - x}$
H3 $_{\delta=0}$	$\frac{\mu}{p}$	$\frac{y(p^2x - \mu z)}{y(x+z)}$
H3 $_{\delta=1}$	$\frac{\mu}{p}$	$\frac{y(x+z)}{p^2 + py(x+z) + \mu}$ $\frac{p^2 - py(-x+z) - \mu}{y(z-x)}$

Table G.2: Results for boundary equations (H family)

Equations	$\rho(p)$	$P(x, y, z, p)$
$A1_{\delta=0}$	$\frac{\mu^2}{p}$ $-p + 2\mu$	$\mu(x+y) + p(y+z)$ $px(y+z) + (x+y)z\mu$ $y(x+z)$ $p(y^2 - xz) - (x+y)(y-z)\mu$
$A1_{\delta=1}$	$\frac{\mu^2}{p}$ $-p + 2\mu$	$p(y+z-\mu) + (x+y-\mu)\mu$ $p(y+z-\mu) - (x+y-\mu)\mu$ $p(p-2\mu) + (x+y)(y+z)$ $z-x$
$A2$	$\frac{\mu}{p}$	$y(z-x)$ $y(x+z)$ $(p^2 + \mu)(xy^2z + 1) - py(x+z)(1+\mu)$ $(p^2 - \mu)(xy^2z - 1) + py(x-z)(1-\mu)$

Table G.3: Results for boundary equations (A family)

Bibliography

- [1] Ablowitz, M.J. and Fokas, A.S. *Complex variables: introduction and applications*. Cambridge University Press, 2003.
- [2] Ablowitz, M.J. and Ladik, J.F. Nonlinear differential- difference equations. *Journal of Mathematical Physics*, 16:598, 1975.
- [3] Ablowitz, M.J. and Ladik, J.F. Nonlinear differential–difference equations and fourier analysis. *Journal of Mathematical Physics*, 17:1011, 1976.
- [4] Ablowitz, M.J. and Segur, H. The inverse scattering transform: Semi-infinite interval. *Journal of Mathematical Physics*, 16:1054, 1975.
- [5] Ablowitz, M.J. and Segur, H. *Solitons and the Inverse Scattering Transform*. Studies in Applied Mathematics, 1981.
- [6] Ablowitz, M.J. and Segur, H. *Solitons, Nonlinear Evolution Equations and Inverse Scattering.*, volume 244. Cambridge Univ Press, 1992.
- [7] Ablowitz, M.J. Kaup, D.J. Newell, A.C. and Segur, H. *The Inverse Scattering Transform-Fourier Analysis for Nonlinear Problems*. Studies in Applied Mathematics, 1974.
- [8] Ablowitz, M.J. Prinari, B. and Trubatch, A.D. *Discrete and continuous nonlinear Schrödinger systems*, volume 302. Cambridge University Press, 2003.
- [9] Ablowitz, M.J. Prinari, B. and Trubatch, A.D. Soliton interactions in the vector NLS equation. *Inverse Problems*, 20(4):1217, 2004.
- [10] Adler, V.E. Recuttings of polygons. *Functional Analysis and Its Applications*, 27(2):141–143, 1993.

- [11] Adler, V.E. Discrete equations on planar graphs. *Journal of Physics A: Mathematical and General*, 34(48):10453, 2001.
- [12] Adler, V.E. and Veselov, A.P. Cauchy problem for integrable discrete equations on quad-graphs. *Acta Applicandae Mathematicae*, 84(2):237–262, 2004.
- [13] Adler, V.E. Bobenko, A.I. and Suris, Y.B. Classification of integrable equations on quad-graphs. The consistency approach. *Communications in Mathematical Physics*, 233(3):513–543, 2003.
- [14] Adler, V.E. Bobenko, A.I. and Suris, Y.B. Geometry of Yang–Baxter maps: pencils of conics and quadrirational mappings. *Commun. Anal. Geom.*, 12(033):967–1007, 2004.
- [15] Ahn, C. and Koo, W.M. Boundary Yang-Baxter equation in the RSOS/SOS representation. *Nuclear Physics B*, 468(3):461–486, 1996.
- [16] Babelon, O. Bernard, D. and Talon, M. *Introduction to Classical Integrable Systems*. Cambridge University Press, 2003.
- [17] Baxter, R.J. Partition function of the eight-vertex lattice model. *Annals of Physics*, 70(1):193–228, 1972.
- [18] Baxter, R.J. *Exactly solvable models in statistical mechanics*, 1982.
- [19] Baxter, R.J. The Yang-Baxter equations and the Zamolodchikov model. *Physica D: Nonlinear Phenomena*, 18(1):321–347, 1986.
- [20] Bazhanov, V.V. Mangazeev, V.V. and Sergeev, S.M. Quantum geometry of three-dimensional lattices. *Journal of Statistical Mechanics: Theory and Experiment*, 2008(07):P07004, 2008.
- [21] Beals, R. and Coifman, R.R. Scattering and inverse scattering for first order systems. *Communications on Pure and Applied Mathematics*, 37(1):39–90, 1984.
- [22] Behrend, R.E. Pearce, P.A. and O’Brien, D.L. Interaction-round-a-face models with fixed boundary conditions: the ABF fusion hierarchy. *Journal of statistical physics*, 84(1-2):1–48, 1996.
- [23] Bellon, M.P. and Viallet, C. Algebraic entropy. *Communications in mathematical physics*, 204(2):425–437, 1999.

- [24] Berger, M. *Geometry: Vol.: 2*. Springer-Verlag, 1987.
- [25] Bibikov, P.N. and Tarasov, V.O. Boundary-value problem for nonlinear Schrödinger equation. *Teoreticheskaya i Matematicheskaya Fizika*, 79(3):334–346, 1989.
- [26] Bikbaev, R.F. and Tarasov, V.O. Initial boundary value problem for the nonlinear Schrödinger equation. *Journal of Physics A: Mathematical and General*, 24(11):2507, 1991.
- [27] Biondini, G. and Hwang, G. Solitons, boundary value problems and a nonlinear method of images. *Journal of Physics A: Mathematical and Theoretical*, 42(20):205207, 2009.
- [28] Bobenko, A.I. and Pinkall, U. Discretization of surfaces and integrable systems. *OXFORD LECTURE SERIES IN MATHEMATICS AND ITS APPLICATIONS*, 16:3–58, 1999.
- [29] Bobenko, A.I. and Suris, Y.B. Integrable systems on quad-graphs. *International Mathematics Research Notices*, 2002(11):573–611, 2002.
- [30] Boussinesq, J. Essai sur la théorie des eaux courantes. *Mémoires présentés par divers Savants à l'Académie des Sciences*, 23:1–680, 1877.
- [31] Boutet De Monvel, A. Fokas, A.S. and Shepelsky, D. Analysis of the global relation for the nonlinear Schrödinger equation on the half-line. *Letters in Mathematical Physics*, 65(3):199–212, 2003.
- [32] Boutet De Monvel, A. Fokas, A.S. and Shepelsky, D. The mKdV equation on the half-line. *JOURNAL-INSTITUTE OF MATHEMATICS OF JUSSIEU*, 3(2):139–164, 2004.
- [33] Boutet De Monvel, A. Fokas, A.S. and Shepelsky, D. Integrable nonlinear evolution equations on a finite interval. *Communications in mathematical physics*, 263(1):133–172, 2006.
- [34] Butler, S. and Joshi, N. An inverse scattering transform for the lattice potential KdV equation. *Inverse Problems*, 26(11):115012, 2010.
- [35] Carillo, S. and Schiebold, C. Matrix kdv and mkdv hierarchies: Noncommutative soliton solutions and explicit formulae. Technical report, Mid Sweden University, Department of Natural Sciences, Engineering and Mathematics, 2009.

- [36] Caudrelier, V. On a Systematic Approach to Defects in Classical Integrable Field Theories. *International Journal of Geometric Methods in Modern Physics*, 5:1085–+, 2008.
- [37] Caudrelier, V. and Zhang, C. Vector nonlinear Schrödinger equation on the half-line. *Journal of Physics A: Mathematical and Theoretical*, 45(10):105201, 2012.
- [38] Caudrelier, V. and Zhang, C. Yang-Baxter and reflection maps from vector solitons with a boundary. *arXiv preprint arXiv:1205.1133*, 2012.
- [39] Caudrelier, V. Crampé, N. and Zhang, C. Integrable boundary for quad-graph systems: Three-dimensional boundary consistency. *ArXiv e-prints*, July 2013.
- [40] Caudrelier, V. Crampé, N. and Zhang, C. Set-theoretical reflection equation: Classification of reflection maps. *Journal of Physics A: Mathematical and Theoretical*, 46:095203, 2013.
- [41] Caudrey, P.J. The inverse problem for a general $N \times N$ spectral equation. *Physica D: Nonlinear Phenomena*, 6(1):51–66, 1982.
- [42] Cherednik, I.V. Factorizing particles on a half-line and root systems. *Theoretical and Mathematical Physics*, 61(1):977–983, 1984.
- [43] Drinfeld, V.G. Quantum groups. *Zapiski Nauchnykh Seminarov POMI*, 155:18–49, 1986.
- [44] Drinfeld, V.G. On some unsolved problems in quantum group theory. *Quantum groups*, pages 1–8, 1992.
- [45] Etingof, P. Geometric crystals and set-theoretical solutions to the quantum Yang-Baxter equation. 2003.
- [46] Etingof, P. Schedler, T. and Soloviev, A. Set-theoretical solutions to the quantum Yang-Baxter equation. *Duke mathematical journal*, 100(2):169–210, 1999.
- [47] Faddeev, L.D. and Takhtajan, L.A. *Hamiltonian Methods in the Theory of Solitons*. Springer, 2007.
- [48] Fan, H. Hou, B.Y. and Shi, K.J. General solution of reflection equation for eight-vertex SOS model. *Journal of Physics A: Mathematical and General*, 28(17):4743, 1995.

- [49] Fermi, E. Pasta, J. and Ulam, S. Studies of nonlinear problems. Technical report, I, Los Alamos Scientific Laboratory Report No. LA-1940, 1955.
- [50] Fokas, A.S. An initial-boundary value problem for the nonlinear Schrödinger equation. *Physica D: Nonlinear Phenomena*, 35(1):167–185, 1989.
- [51] Fokas, A.S. A unified transform method for solving linear and certain nonlinear PDEs. *Proceedings of the Royal Society of London. Series A: Mathematical, Physical and Engineering Sciences*, 453(1962):1411–1443, 1997.
- [52] Fokas, A.S. Integrable nonlinear evolution equations on the half-line. *Communications in mathematical physics*, 230(1):1–39, 2002.
- [53] Fokas, A.S. Linearizable initial boundary value problems for the sine-Gordon equation on the half-line. *Nonlinearity*, 17(4):1521, 2004.
- [54] Fokas, A.S. *A unified approach to boundary value problems*, volume 78. Society for Industrial Mathematics, 2008.
- [55] Fokas, A.S. and Its, A.R. The linearization of the initial-boundary value problem of the nonlinear Schrödinger equation. *SIAM Journal on Mathematical Analysis*, 27(3):738–764, 1996.
- [56] Fokas, A.S. and Pelloni, B. A transform method for linear evolution PDEs on a finite interval. *IMA journal of applied mathematics*, 70(4):564–587, 2005.
- [57] Fokas, A.S. Its, A.R. and Sung, L.Y. The nonlinear Schrödinger equation on the half-line. *Nonlinearity*, 18(4):1771, 2005.
- [58] Fukuda, K. Yamada, Y. and Okado, M. Energy functions in box ball systems. *International Journal of Modern Physics A*, 15(09):1379–1392, 2000.
- [59] Gakhov, F.D. *Boundary value problems*. Dover Publications, 1966.
- [60] Gardner, C.S. Korteweg-de Vries Equation and Generalizations. IV. The Korteweg-de Vries Equation as a Hamiltonian System. *Journal of Mathematical Physics*, 12, Dec. 1970.
- [61] Gardner, C.S. Greene, J.M. Kruskal, M.D. and Miura, R.M. Method for Solving the Korteweg-De Vries Equation. *Phys. Rev. Lett.*, 19(19):1095–1097, Nov. 1967.
- [62] Gerdjikov, V.S. Basic aspects of soliton theory. *arXiv preprint nlin/0604004*, 2006.

- [63] Goncharenko, V.M. Multisoliton solutions of the matrix kdv equation. *Theoretical and Mathematical Physics*, 126(1):81–91, 2001.
- [64] Goncharenko, V.M. and Veselov, A.P. Yang-Baxter maps and matrix solitons. *New Trends in Integrability and Partial Solvability*, pages 191–197, 2004.
- [65] Grammaticos, B. Ramani, A. and Papageorgiou, V. Do integrable mappings have the Painlevé property? *Physical Review Letters*, 67(14):1825, 1991.
- [66] Habibullin, I.T. The Bäcklund transformation and integrable initial boundary value problems. *Matematicheskie Zametki*, 49(4):130–137, 1991.
- [67] Habibullin, I.T. and Svinolupov, S.I. Integrable boundary value problems for the multicomponent Schrödinger equations. *Physica D: Nonlinear Phenomena*, 87(1):134–139, 1995.
- [68] Hasegawa, A. and Tappert, F. Transmission of stationary nonlinear optical pulses in dispersive dielectric fibers. I. Anomalous dispersion. *Applied Physics Letters*, 23(3):142–144, 1973.
- [69] Hatayama, G. Kuniba, A. and Takagi, T. Soliton cellular automata associated with crystal bases. *Nuclear Physics B*, 577(3):619–645, 2000.
- [70] Hietarinta, J. Permutation-type solutions to the Yang-Baxter and other n-simplex equations. *Journal of Physics A: Mathematical and General*, 30(13):4757, 1997.
- [71] Hietarinta, J. Searching for CAC-maps. *Journal of Nonlinear Mathematical Physics*, 12(sup2):223–230, 2005.
- [72] Hietarinta, J. and Viallet, C. Integrable lattice equations with vertex and bond variables. *Journal of Physics A: Mathematical and Theoretical*, 44(38):385201, 2011.
- [73] Hirota, R. Nonlinear partial difference equations. I. A difference analogue of the Korteweg-de Vries equation. *J. Phys. Soc. Japan*, 43:1424–1433, 1977.
- [74] Hirota, R. Nonlinear partial difference equations. III. Discrete sine-Gordon equation. *J. Phys. Soc. Japan*, 43(6):2079–2086, 1977.
- [75] Jimbo, M. Aq-difference analogue of U (g) and the Yang-Baxter equation. *Letters in Mathematical Physics*, 10(1):63–69, 1985.

- [76] Jimbo, M. A q -analogue of $U(\mathfrak{gl}(N+1))$, Hecke algebra and the Yang-Baxter equation. *Lett. Math. Phys.*, 11:247–252, 1986.
- [77] Kac, V.G. *Infinite-dimensional Lie algebras*, volume 44. Cambridge University Press, 1994.
- [78] Kassotakis, P. and Nieszporski, M. Systems of difference equations on a vector valued function that admit 3D space of scalar potentials. *In preparation*.
- [79] Kassotakis, P. and Nieszporski, M. On non-multiaffine consistent-around-the-cube lattice equations. *Physics Letters A*, 2012.
- [80] Korteweg, D.J. and de Vries, G. On the Change of Form of Long Waves Advancing in a Rectangular Channel and on a New Type of Long Stationary Waves. *Phil. Mag*, 39:422–443, 1895.
- [81] Lax, P.D. Integrals of Nonlinear Equations of Evolution and Solitary Waves. *Commun. Pure Appl. Math*, 21:467–490, 1968.
- [82] Levi, D. and Winternitz, P. Continuous symmetries of difference equations. *Journal of Physics A: Mathematical and General*, 39(2):R1, 2006.
- [83] Levi, D. Petrera, M. and Scimiterna, C. The lattice Schwarzian KdV equation and its symmetries. *Journal of Physics A: Mathematical and Theoretical*, 40(42):12753, 2007.
- [84] Lieb, E.H. and Liniger, W. Exact analysis of an interacting Bose gas. I. The general solution and the ground state. *Physical Review*, 130(4):1605, 1963.
- [85] Lobb, S. and Nijhoff, F. Lagrangian multiforms and multidimensional consistency. *Journal of Physics A: Mathematical and Theoretical*, 42(45):454013, 2009.
- [86] Lu, J.H. Yan, M. and Zhu, Y.C. On the set-theoretical Yang-Baxter equation. *Duke Mathematical Journal*, 104(1):1–18, 2000.
- [87] Manakov, S.V. On the theory of two-dimensional stationary self-focusing electro-magnetic waves. *JETPh*, 65:505–516, 1973.
- [88] Mercat, C. *Holomorphie discrète et modèle d’Ising*. PhD thesis, Université Louis Pasteur-Strasbourg I, 1998.
- [89] Mikhailov, A.V. The reduction problem and the inverse scattering method. *Physica D: Nonlinear Phenomena*, 3(1):73–117, 1981.

- [90] Miura, R.M. Gardner, C.S. and Kruskal, M.D. Korteweg-de Vries Equation and Generalizations. II. Existence of Conservation Laws and Constants of Motion. *Journal of Mathematical physics*, 9:1204, 1968.
- [91] Nijhoff, F. Lax pair for the Adler (lattice Krichever–Novikov) system. *Physics Letters A*, 297(1):49–58, 2002.
- [92] Nijhoff, F. and Capel, H. The discrete korteweg-de vries equation. *Acta Applicandae Mathematicae*, 39(1):133–158, 1995.
- [93] Nijhoff, F. Atkinson, J. and Hietarinta, J. Soliton solutions for ABS lattice equations: I. Cauchy matrix approach. *Journal of Physics A: Mathematical and Theoretical*, 42(40):404005, 2009.
- [94] Nijhoff, F.W. Quispel, G.R.W. and Capel, H.W. Direct linearization of nonlinear difference-difference equations. *Physics Letters A*, 97(4):125–128, 1983.
- [95] Olver, P.J. *Equivalence, invariants and symmetry*. Cambridge University Press, 1995.
- [96] Olver, P.J. *Applications of Lie groups to differential equations*, volume 107. Springer verlag, 2000.
- [97] Papageorgiou, V.G. Suris, Y.B. Tongas, A.G. Veselov, A.P. On Quadrirational Yang-Baxter Maps. *Sigma*, 6(033):9, 2010.
- [98] Papageorgiou, V.G. Tongas, A.G. and Veselov, A.P. Yang-Baxter maps and symmetries of integrable equations on quad-graphs. *arXiv preprint math/0605206*, 2006.
- [99] Quispel, G.R.W. Nijhoff, F.W. Capel, H.W. and Van der Linden, J. Linear integral equations and nonlinear difference-difference equations. *Physica A: Statistical Mechanics and its Applications*, 125(2):344–380, 1984.
- [100] Rasin, O.G. and Hydon, P.E. Symmetries of Integrable Difference Equations on the Quad-Graph. *Studies in Applied Mathematics*, 119(3):253–269, 2007.
- [101] Reshetikhin, N. and Veselov, A. Poisson Lie groups and Hamiltonian theory of the Yang-Baxter maps. *arXiv preprint math/0512328*, 2005.
- [102] Russell, J.S. Report on waves. In *14th meeting of the British Association for the Advancement of Science*, pages 311–390, 1844.

- [103] Sklyanin, E.K. Boundary conditions for integrable equations. *Functional Analysis and its Applications*, 21(2):164–166, 1987.
- [104] Sklyanin, E.K. Boundary conditions for integrable quantum systems. *Journal of Physics A: Mathematical and General*, 21(10):2375, 1988.
- [105] Sklyanin, E.K. Classical limits of the SU (2)-invariant solutions of the Yang-Baxter equation. *Journal of Soviet Mathematics*, 40(1):93–107, 1988.
- [106] Suris, Y.B. and Veselov A.P. Lax matrices for Yang-Baxter maps. *Journal of Nonlinear Mathematical Physics*, 10(sup2):223–230, 2003.
- [107] Takahashi, D. and Satsuma, J. A soliton cellular automaton. *J. Phys. Soc. Japan*, 59(10):3514–3519, 1990.
- [108] Takhtadzhian, L.A. and Faddeev, L.D. The quantum method of the inverse problem and the Heisenberg XYZ model. *Russian Mathematical Surveys*, 34(5):11–68, 1979.
- [109] Tarasov, V.O. The integrable initial-boundary value problem on a semiline: nonlinear Schrödinger and sine-Gordon equations. *Inverse Problems*, 7(3):435, 1991.
- [110] Tsuchida, T. Study of multi-Component Soliton Equations Based on the Inverse Scattering Method. *Ph.D thesis*, 2000.
- [111] Tsuchida, T. N-soliton collision in the Manakov model. *arXiv preprint nlin/0302059*, 2003.
- [112] Veselov, A.P. Integrable maps. *Russian Mathematical Surveys*, 46(5):1–51, 1991.
- [113] Veselov, A.P. Yang-Baxter maps and integrable dynamics. *Physics Letters A*, 314(3):214–221, 2003.
- [114] Veselov, A.P. Yang-Baxter maps: dynamical point of view. *arXiv preprint math/0612814*, 2006.
- [115] Veselov, A.P. and Shabat, A.B. Dressing Chains and Spectral Theory of the Schrödinger Operator. *Funktsional'nyi Analiz i ego prilozheniya*, 27(2):1–21, 1993.
- [116] Wadati, M. The modified Korteweg–de Vries equation. *J. Phys. Soc. Japan*, 34(1):289–1, 1973.

-
- [117] Wahlquist, H.D. and Estabrook, F.B. Bäcklund transformation for solutions of the Korteweg-de Vries equation. *Physical review letters*, 31(23):1386, 1973.
- [118] Weinstein, A. and Xu, P. Classical solutions of the quantum Yang-Baxter equation. *Communications in mathematical physics*, 148(2):309–343, 1992.
- [119] Yang, C.N. Some exact results for the many-body problem in one dimension with repulsive delta-function interaction. *Physical Review Letters*, 19(23):1312–1315, 1967.
- [120] Zabusky, N.J. and Kruskal, M.D. Interaction of "solitons" in a collisionless plasma and the recurrence of initial states. *Physical Review Letters*, 15(6):240–243, 1965.
- [121] Zakharov, V.E. and Calogero, F. *What is integrability?* Springer-Verlag, 1991.
- [122] Zakharov, V.E. and Faddeev, L.D. Korteweg-de Vries equation: A completely integrable Hamiltonian system. *Journal Functional Analysis and Its Applications*, 5:422–443, Oct. 1971.
- [123] Zakharov, V.E. and Shabat, A.B. Exact Theory of Two-Dimensional Self-Focusing and One-Dimensional Self-Modulation of Waves in Nonlinear media. *Soviet Physics*, 34:62–69, Jan. 1972.
- [124] Zakharov, V.E. and Shabat, A.B. A scheme for integrating the nonlinear equations of mathematical physics by the method of the inverse scattering problem. I. *Functional Analysis and Its Applications*, 8:226–235, 1974. 10.1007/BF01075696.
- [125] Zakharov, V.E. and Shabat, A.B. Integration of nonlinear equations of mathematical physics by the method of inverse scattering. II. *Functional Analysis and Its Applications*, 13(3):166–174, 1979.
- [126] Zamolodchikov, A.B. and Zamolodchikov, A.B. Factorized S -matrices in two dimensions as the exact solutions of certain relativistic quantum field theory models. *Annals of Physics*, 120(2):253–291, 1979.